Improved Dual-Loop Detection System for Collecting Real-Time Truck Data

by

Nancy Nihan
Professor/Director
Transportation Northwest

Yinhai Wang
Assistant Professor

Xiaoping Zhang
Graduate Research Assistant

Civil and Environmental Engineerin
University of Washington
Seattle, WA 98195-2700

TECHNICAL REPORT STANDARD TITLE PAGE

1. REPORT NO. TNW2005-02	2. GOVERNMENT ACCESSION NO.	3. RECIPIENT'S CATALOG NO.
4. TITLE AND SUBTITLE Improved Dual-Loop Detection System for Collecting Real-Time Truck Data		5. REPORT DATE February 2005
		6. PERFORMING ORGANIZATION CODE
7. AUTHOR(S) Xiaoping Zhang, Nancy Nihan, and Yinhai Wang		8. PERFORMING ORGANIZATION REPORT NO. TNW2005-02
9. PERFORMING ORGANIZATION NAME AND ADDRESS Transportation Northwest Regional Center X (TransNow) Box 352700, 123 More Hall University of Washington Seattle, WA 98195-2700		10. WORK UNIT NO.
		11. CONTRACT GRANT NO.
12. SPONSORING AGENCY NAME AND ADDRESS		13. TYPE OF REPORT AND PERIOD COVERED Final Report
		14. SPONSORING AGENCY CODE
15. SUPPLEMENTARY NOTES This study was conducted in cooperation with the University of Washington and the US Department of Transportation		

16. ABSTRACT

The WSDOT's dual-loop detector's capability of measuring vehicle lengths makes the dual-loop detection system a potential real-time truck data source for freight movement study. However, a previous study found the WSDOT dual-loop detection system was not consistently reporting accurate truck volumes. (Truck volumes estimates by basic length category are developed from the vehicle length measurements produced by the dual-loop detectors.) The problems include undercount, over-count, and misclassification.

As an extension of the previous study, this research project investigated and identified possible causes of dual-loop miscount and misclassification under un-congested traffic conditions. A quick remedy method was proposed to improve the performance of the dual-loop detection system without replacing any part of the current system hardware or software. A new dual-loop algorithm that can tolerate erroneous loop actuation signals was also developed to improve the performance of the WSDOT loop detection system.

The improved dual-loop detection system will provide reliable timely truck volume data. WSDOT will benefit from this work by gaining more reliable volume and vehicle classification data without having to resort to any other traffic detection technologies.

17. KEY WORDS Real-Time Truck Data, Dual-Loop Detectors		18. DISTRIBUTION STATEMENT	
19. SECURITY CLASSIF. (OF THIS REPORT) None	20. SECURITY CLASSIF. (OF THIS PAGE) None	21. NO. OF PAGES 194	22. PRICE $24.75

DISCLAIMER

The contents of this report reflect the views of the authors, who are responsible for the facts and the accuracy of the data presented herein. This document is disseminated through Transportation Northwest (TransNow) Regional Center under the sponsorship of the Department of Transportation UTC Grant Program in the interest of information exchange. The U.S. Government assumes no liability for the contents or use thereof. The contents do not necessarily reflect the views or policies of the U.S. Department of Transportation or any of the local sponsors.

TABLE OF CONTENTS

LIST OF FIGURES

LIST OF TABLES

EXECUTIVE SUMMARY

Inductive loop detectors have been widely deployed on freeways in this nation to provide real-time traffic data. Inductive loop detectors are frequently deployed as single-loop detectors, i.e., one loop per lane, or as dual-loop detectors formed by two consecutive single-loop detectors placed several meters apart in each lane. Single-loop detectors are used to measure volume and lane occupancy; while dual-loop detectors provide two independent sets of volume and occupancy measurements and also measure speed and vehicle length. The dual-loop detector's capability of measuring vehicle length makes the dual-loop detection system a potential real-time truck data source for freight movement studies in that truck volume estimates by basic length category can be developed from the vehicle length measurements produced by the dual-loop detectors.

The Washington State Department of Transportation (WSDOT) has a network of loop detectors on its Greater Seattle freeway network that provides real-time traffic data to its Advanced Traffic Management System (ATMS) and its Advanced Traveler Information System (ATIS). If working properly, the WSDOT's dual-loop detection system could be a good real-time truck data source. However, a pilot study found that the dual-loop detectors were consistently underreporting truck volumes, whereas the single-loop detectors were consistently over counting vehicle volumes. Therefore, as an extension of the previous study, this research, sponsored by Transportation Northwest (TransNow), the USDOT University Transportation Center for Federal Region 10, attempted to address the WSDOT loop detection system's miscount and misclassification problems to improve the system's performance. The improved loop detection system is expected to provide reliable truck volume data for freight movement study.

This research determined possible causes of loop errors under non-forced-flow traffic conditions by examining the loop detector detecting process. A new dual-loop algorithm that can address these error causes was developed to improve the performance of the WSDOT loop detection system. The new dual-loop algorithm is much more flexible than the current WSDOT dual-loop algorithm in that it is capable of including and correcting erroneous raw loop actuation signals and outputting acceptable volume and

vehicle classification data. A quick remedy method was also recommended to improve the performance of the dual-loop detection system without replacing any part of the existing system hardware or software. In addition, a laptop-based detector event data collection system (DEDAC) that can collect loop detector event data without interrupting a loop detection system's normal operation was developed in this research. The DEDAC system enables various kinds of transportation research and applications that could not otherwise be possible. The DEDAC software is available to the public from the TransNow website (www.transnow.org).

CHAPTER 1   INTRODUCTION

1.1   RESEARCH BACKGROUND

Over the past years the freight transportation industry in the United States has evolved to serve a changing and growing economy. Freight transportation has proven to be vital to economic growth [1]. The importance of freight transportation is explicitly recognized in the Transportation Equity Act for the 21st Century (TEA-21). As demand for freight service grows, freight transportation system continues to evolve in response to increasing needs and changing patterns of freight movements.

A 1998 Bureau of Transportation Statistics (BTS) report stated that "The effectiveness and efficiency of the freight transportation system are heavily dependent on reliable data to inform a range of decisions at all levels of government and in the private sector about economic and infrastructure investments and policy issues. Data on goods movements are needed to identify and evaluate options for mitigating congestion, improve regional and global economic competitiveness, enable effective land use planning, inform investment and policy decisions about modal optimization, enhance transportation safety and security, identify transportation marketing opportunities, and reduce fuel consumption and improve air quality. While data alone cannot guarantee good decisions, informed choices are not possible without good data [2]. "

Gathering data on freight and traffic flows at the federal, state or local level is a costly and time-consuming process [3]. Surveys, including carrier surveys, distribution surveys, shipper surveys, and receiver surveys are the conventional and the primary freight data collection methods [4]. Since such surveys have accuracy issues, are frequently

expensive and a burden on respondents, it will be important to identify and exploit additional data sources to populate the freight database. Intelligent Transportation System (ITS) data collected by traffic sensors have already been identified as a promising source to enrich the freight database [5, 6].

1.1.1 Freeway ITS Data Collection Sensors

Truck movement data can be collected by a variety of ITS data sensors, such as videos, Remote Traffic Microwave Sensors (RTMS), infrared sensors, acoustic sensors, Global Positioning System (GPS)/Wireless devices, Automatic Vehicle Identification (AVI) transponders, and inductive loop detectors, etc.

Video imaging systems have interested transportation researchers in the past decade [7-13]. However, due to their limitations under unfavorable weather conditions, such as bad lighting conditions, they cannot collect reliable traffic data continuously. Even under favorable lighting conditions, the video imaging technology has not advanced enough to accurately collect vehicle-classification and speed data, especially extracting information from images collected by un-calibrated CCTV cameras.

RTMS is a relatively new technology for collecting traffic data [14-16]. But since it is still in the testing stage, only a limited number of RTMS have been installed. Therefore, it cannot be used for wide-area data collection. Infrared and acoustic sensors are also used to provide traffic data [17-19]. But due to their limitations in collecting traffic data, they are not widely used for freeway traffic data collection.

GPS/Wireless devices are attracting more and more attention. But based on the study [20] conducted by The Washington State Transportation Center (TRAC), the

GPS/Wireless In-Truck system to support freight transportation planning efforts should not be deployed yet. The costs of the technology are too high, and the suite of analysis tools that would allow for successful management and manipulation of the data are not mature.

AVI Transponders are short-range communication devices. They can be mounted on the inside of the vehicle's windshield and used to identify trucks electronically. The transponder reader antennas are placed on poles over the roadway or at elevation at facility entrances. The reader antennas communicate electronically to verify a truck's transponder identification (ID) number, and then to correlate this number with a records database for state enforcement data for Commercial Vehicle Information Systems and Networks (CVISN) for the TransCorridor system. Based on the same study conducted by TRAC [20], the transponder data are effective for calculating travel times if data are available, however, the data accuracy was limited by the size and density of the deployed Transponder network.

Inductive loop detector technology, one of the most popular automated traffic data collection methods, was first introduced for detection of vehicles in the early 1960's [21], and today, after a 40-year evolution, it has become a ubiquitous means for collecting traffic data from freeways in the United States. Inductive loop detectors are frequently deployed as single-loop detectors, i.e., one loop per lane, or as dual-loop detectors formed by two consecutive single-loop detectors placed several meters apart in each lane. Single-loop detectors are used to measure volume and lane occupancy; while dual-loop detectors provide two independent sets of volume and occupancy measurements and also measure speed and vehicle length.

The Washington State Department of Transportation (WSDOT) has a network of loop detectors on its Greater Seattle freeway network that provides real-time traffic data to its Advanced Traffic Management System (ATMS) and its Advanced Traveler Information System (ATIS). There are 620 loop stations installed along the freeway network. In total, there are 4800 single-loop detectors and 1020 dual-loop detectors (also called speed traps, dual loops, or T loops in the state of Washington) embedded in the pavement for traffic data collection. Most of the loop detectors deployed on the Greater Seattle freeway network are square-shaped detectors with a dimension of 6 feet in length and 6 feet in width. In recent years, some damaged square-shaped loop detectors were replaced by circle-shaped detectors.

1.1.2   Current WSDOT Single-Loop and Dual-Loop Algorithm

As shown in Figure 1-1, the principle components of an inductive loop detector system include one or more turns of insulated loop wire wound in a shallow slot sawed in the pavement, a lead-in cable from the curbside pull box to the roadside controller cabinet, and a detector electronics unit housed in cabinet. Simply stated, the loop system forms a tuned electrical circuit for which the loop wire is the inductive element. When a vehicle passes over the loop, it decreases the inductance of the loop. This decrease in inductance then actuates the detector electronics output relay or solid state circuit, which, in turn, sends an impulse to the controller unit signifying that it has detected the passage or presence of a vehicle. After the vehicle leaves the loop, the inductance goes back to its normal level, i.e., when there is no vehicle present on a single-loop detector, the detector rests in the "off" state. The detector changes its state from "off" to "on" when a vehicle arrives at the leading edge of the detector and from "on" to "off" when the vehicle

departs from the rear edge of the detector. This change of state from "off" to "on" and then back to "off" represents the passage of a vehicle. The duration during which a vehicle occupies a single-loop detector is called the detector on-time, which can be aggregated to calculate lane occupancy for a particular interval. This is how a single-loop detector collects volume and lane occupancy data.

When a vehicle passes two single-loop detectors spaced a few meters apart (a dual-loop detector), it first activates the upstream detector (designated as the M loop by WSDOT) and then the downstream detector (designated as the S loop by WSDOT). The time it takes for the vehicle to travel from the M loop to the S loop is called the elapsed time. If the distance from the leading edge of the M loop to that of the S loop is known, the speed at which the vehicle traverses the dual-loop detector can be calculated by dividing this distance by the elapsed time. The calculated speed can then be used to calculate vehicle length using the detector on-time collected from either of the two single-loop detectors (M or S loop) and the known length of the loop. In the current WSDOT system, vehicles are classified according to their lengths by assigning each identified vehicle to one of four bins: (a) Bin 1 - PCs and smaller vehicles (length 26 ft or less); (b) Bin 2 - small trucks, etc. (26 ft to 39 ft); (c) Bin 3 - larger trucks and buses (39 ft to 65 ft); and (d) Bin 4 - largest trucks and articulated buses (length greater than 65 ft). Vehicles that fall inside Bins 2, 3, and 4 are considered recreational vehicles, trucks, or buses. This is how a dual-loop detector collects speed and vehicle length data. To save disk space, the collected individual vehicle data are aggregated into 20-second averages of flow, occupancy, velocity, and vehicle length data.

Eight validity checks were implemented in the WSDOT dual-loop algorithm to filter out erroneous individual vehicle data. These eight types of errors are represented by a byte, which contains 8 bits; each of them corresponds to a type of error. If the bit is set with value 1, the corresponding error has occurred. The digits and their corresponding errors are:

Bit 8 – Operator disabled a loop in the dual-loop detector.

Bit 7 – Two vehicles in the dual-loop detector. Calculation aborted, data were not collected for these two vehicles.

Bit 6 – Lost vehicle (vehicle hits only one loop). Calculation aborted, data were not collected for these two vehicles.

Bit 5 – Bad occupancy ratio between two single-loop detectors that form a dual-loop detector. If the measured on-time difference between the two single-loop detectors is greater than 10% for a vehicle, this bit will be set. Calculation aborted, data were not collected for this vehicle.

Bit 4 – Measured vehicle speed is less than the minimum speed, 5 mi/hr. Data were collected for this vehicle.

Bit 3 – Vehicle speed is greater than the maximum speed, 100 mi/hr. Data were collected for this vehicle.

Bit 2 – Vehicle length is less than the minimum length, 5 feet. Data were collected for this vehicle.

Bit 1 – Vehicle length is greater than the maximum length, 150 feet. Data were collected for this vehicle.

If two types of errors occur in a 20-second interval, two bits of the 8-bit binary number should be set with value 1. For instance, if a binary number is 01010000, the two "1" digits represent two different types of errors. Counting from right to left, the first "1" digit represents a bad occupancy ratio between two single-loop detectors that form a dual-loop detector and the second "1" digit represents that there were two vehicles in the dual-loop detector.

1.2   PROBLEM STATEMENT

Since the majority of vehicles in Bins 2 through 4 represent trucks, correct vehicle counts and bin assignment would yield a ubiquitous means of obtaining truck flow data along the freeway network. However, a preliminary study [22] conducted in 2001 on Interstate 5 (I-5) found the WSDOT dual-loop detection system was not consistently reporting accurate truck volumes. In that study, the accuracy of dual-loop vehicle classification data was evaluated using video ground-truth data, and the major findings are:

- o Dual-loop detectors undercount vehicle volumes. This is a very common problem in the dual-loop detection system. More than 80% of the dual-loop detectors have significant and substantial under-count errors.

- o Dual-loop detectors misclassify vehicles across bins, especially between Bin1 and Bin2, and Bin3 and Bin4. For the data collected during the off-peak hour period, observed errors in truck misclassifications ranged from 30% to 41% and, for the data collected during peak-hour period, observed errors in bin assignment for trucks ranged from 33% to 55%.

Admittedly, dual-loop detectors were primarily deployed for measuring vehicle speeds rather than classification and bin volume data; nonetheless, if the capability of measuring vehicle length could be improved and fully utilized, they would become a widespread and cost-efficient truck data source for freeway freight movement study and economic analysis for the Seattle Metropolitan Region. This then raised the issue of the need for more accurate dual-loop bin volume data. Therefore, this research was attempted to address the WSDOT loop detections system's miscount and misclassification problems. The expected outcome of this research was an improved loop detection system that provides accurate single-loop count data and dual-loop bin volume data.

1.3   RESEARCH OBJECTIVE

The inductive loop detection system is subject to errors, which can be caused by the system hardware and software. If the errors go undetected prior to their use in traffic management and information system applications, the integrity of the systems is compromised by inaccurate data. Therefore, as an extension of the previous study, this research, sponsored by Transportation Northwest (TransNow), the USDOT University Transportation Center for Federal Region 10, aimed at providing a solution to improve the performance of the current WSDOT loop detection system so that it collects accurate real-time volume and vehicle classification data. The improved system would then provide reliable truck volume data for freight movement study.
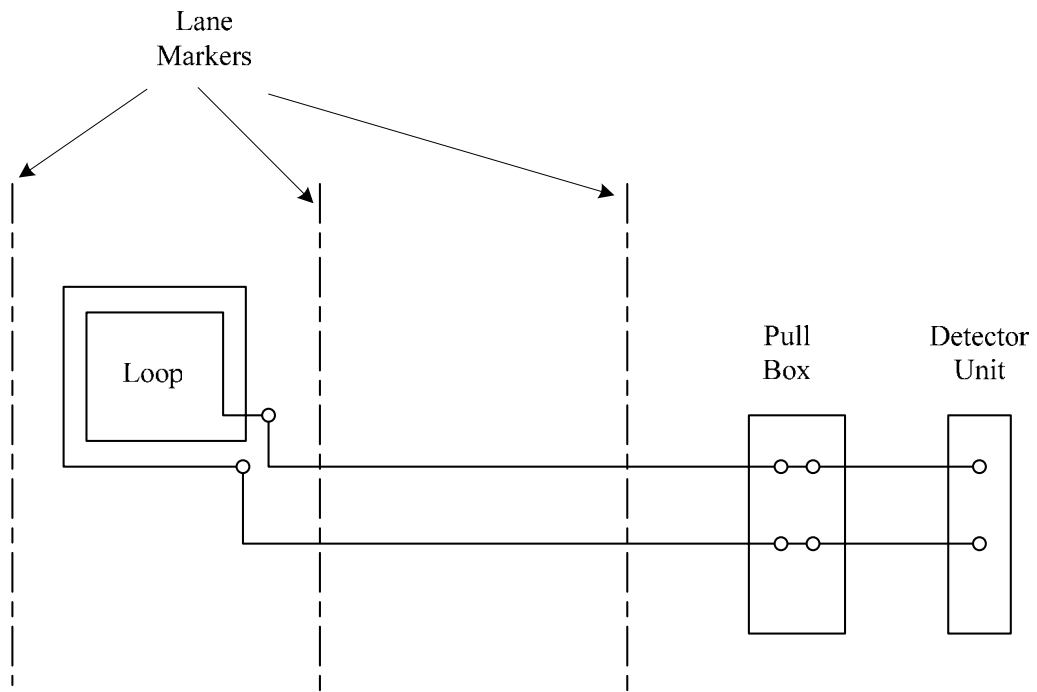
Figure 1-1. Diagram of A Single-Loop Detector

Reference: Traffic Detector Handbook (Second Edition). Institute of Transportation
Engineers. Washington, D.C., 1997.

CHAPTER 2   STATE OF THE ART

Because of the vulnerability of the loop detectors, how to timely identify loop errors, investigate causes of malfunction, and apply remedial methods has been of a great interest to transportation professionals. Consequently, error detection and correction techniques have continued to evolve in the past three decades.

2.1   LOOP ERROR DETECTION TECHNIQUES

The loops operate in presence mode (that is, they turn on and stay on as long as a vehicle is occupying the loop). At each station, the field microprocessor checks or scans the loop actuations 60 times each second. Typical freeway loop detection systems, under normal operation, aggregate individual-loop detector actuations sampled at 60 Hz into 20-second or 30-second averages of flow, occupancy, velocity, and length measurements. So, there are two types of loop data, raw loop actuation signals and aggregated loop data, available for malfunction inspection. Accordingly, based on the type of data being inspected, two approaches have been explored for inductive loop erroneous data detection and malfunction identification. One of the approaches is aggregated-data-based malfunction detection, and the other is raw-actuations-based malfunction detection.

2.1.1   Aggregated-Data-Based Malfunction Detection

Aggregated-data-based malfunction detection applies reliability checks to the aggregated traffic measurements prior to their use in traffic management and information system applications. Some commonly used tests establish certain thresholds, such as maximum and minimum acceptable values, beyond which the data cannot be said to reflect actual traffic

operations. This type of checks is fairly primitive and crude and can hardly be trusted to meet the data needs of the advanced traffic management and control systems [23, 24]. More sophisticated tests use the inherent relationships among traffic parameters such as speed, volume, and occupancy by applying traffic flow theory principles to ensure the validity of the data.

Cleghorn et al [25] suggested a few screening methods with both single and paired loops. Their approaches provided some interesting insights into the upper limits beyond which the data are considered erroneous. The first approach developed a theoretical upper bound for part of the flow-occupancy data and was useful for single-loop detector systems. The other approaches were developed for paired-loop systems and involve comparisons of loop data as well as the development of boundaries defining acceptable combinations of speed, flow, and occupancy data.

Payne and Thompson [26] addressed malfunction characteristics of inductive loop detectors with freeway surveillance applications. A malfunction detection algorithm was developed and tested using recorded loop data at various aggregation levels from the I-880 database [27]. The algorithm utilized 14 distinct validity tests to identify faulty sensor data. If a sensor failed any of these tests, a malfunction would be declared. These tests were intended to identify obviously faulty data. The objective was to apply conservative validity tests to the I-880 data set and thereby obtain a conservative estimate of the malfunction rates associated with inductive loops. In many instances, both 30-second and 5-minute aggregated measurement values were employed.

Nihan and Jacobson [28, 29] at the University of Washington detected erroneous loop detector data in a freeway traffic management system according to an "acceptable region" in the volume-occupancy plane and declared that samples are good only if they fall inside the region. The boundaries of the acceptable region were defined by a set of parameters, which were calibrated from historical data or derived from traffic theory.

Turochy and Smith [30] went one-step further by combining both threshold-value-based and traffic-flow-theory-based tests to introduce a new procedure for detector data screening in traffic management systems. The data screening procedure was applied to data from the entire Hampton Road system for one day, and the results showed that their procedure is a powerful and thorough method.

Recent research conducted by Park, et al. [31], involved developing more sophisticated empirical approaches to detect outliers from archived ITS data under the presumption that suspicious observations would not be consistent with the main traffic pattern, but would rather exhibit an abnormal pattern and could be categorized as outliers. The methods used current data and classified data as outliers based on comparisons to empirical cutoff points derived from extensive archived data rather than from standard statistical tables. In addition to the ideas of classical Hotelling's T^2 statistic, modern statistical trend removal and blocking were also incorporated. The methods were applied to ITS data collected in San Antonio and Austin, Texas to show how the suggested methods performed on high quality traffic data and apparently lesser quality traffic data.

2.1.2   Raw-Actuations-Based Malfunction Detection

The raw-actuations-based malfunction detection method processes the raw signals from a loop directly. Individual vehicle information, such as vehicle arrival, departure, and presence times, can be calculated from the detector's "on" and "off" indications.

This approach was first pursued by the Institute of Transportation Studies at the University of California, Berkeley, and the resulting algorithms were described by Chen and May [23]. Their methodology examines the distribution of vehicles' on-time, i.e., the time the detector is occupied by a vehicle. Of primary interest is the development of a diagnostics scheme in which the average vehicle on-time is examined as a test statistic. By comparing this value against the average on-times for a station of detectors, the validity of detector operation can be checked. This scheme was tested at the San Francisco-Oakland Bay Bridge and was found to yield good results. The false-alarm rate was low compared with that for the occupancy diagnostic method. Sensitivity to true detector failures was improved.

Coifman [32] compared the measured on-times from each loop in a dual-loop detector on a vehicle-by-vehicle basis. At free flow velocities the on-times from the two loops should be virtually identical, even allowing for hard decelerations, regardless of vehicle length. At lower velocities, vehicle acceleration can cause the two on-times to differ even though both loops are functioning properly; therefore, congested periods were excluded from the analysis. He also presented eight new detector validation tests that employ event data to identify detector errors [33]. Five of these tests can be applied to single-loop detectors or non-invasive sensors that aggregate data using similar techniques, while all of the tests can be applied to dual-loop detectors.

2.2   ERRONEOUS DATA CORRECTION TECHNIQUES

Various erroneous data correction techniques have been proposed to correct loop errors. Daily and Wall [34] developed an algorithm for correcting errors in freeway traffic management system archived loop data that are the result of poorly calibrated sensors. These errors pose a significant difficulty when trying to use archived data in offline analysis because the calibration errors are difficult to detect using traditional methods. In their work, consistency of vehicle counts was used to judge the validity of the data; if vehicle counts were balanced the data were valid, if vehicle counts were not balanced the data were not valid. The method could also determine a correction factor. This correction factor was used to create a time series that could be combined with the original data to adjust the volume to create a consistent data set.

Payne and Thompson [26], after examining the malfunction rates of I-880 data by applying 14 validity tests, developed a repairing algorithm from the I-880 database utilizing historical traffic distributions as well as current measurements from surrounding sensors. The resulting measurement estimates were shown to be unbiased for short-term malfunctions. This data-repair algorithm is suitable for applications that do not rely on the absolute accuracy of individual measurement data.

Chen, et al. [35], developed a diagnostics algorithm to detect malfunctioning single-loop detectors from their volume and occupancy measurements. Unlike previous approaches, the algorithm employed a time series of many samples, rather than basing decisions on a single sample. They then developed a linear regression imputation algorithm using the linear relationship between neighboring loops to estimate the value of missing or bad samples.

Previous research has been focused on checking the validity of loop data and correcting errors in the data, and little has been done to identify where the errors occur in the loop detecting process. Therefore, in this research the loop detecting process was examined to identify possible causes of loop errors so that the error source could be eliminated.

CHAPTER 3   RESEARCH APPROACH

According to the stated research objectives, the research approach can be divided into the following three parts: 1) investigating the causes of loop errors by examining the loop detecting process up to but not including the communication part, 2) developing a new dual-loop algorithm by taking into account the identified error causes that led to the unsatisfactory performance of the   current algorithm, and 3) proposing an easy-to-implement quick-fix method to tune up the system hardware (loop detectors) to improve the accuracy of the raw loop data.

3.1   DETERMINATION OF ERROR CAUSES

As stated in Section 1.2, a tremendous portion of the dual-loop detectors have miscount and misclassification errors, which can be caused by any problematic step involved in the dual-loop detecting process. Therefore, a systematic examination of the whole process through which dual-loop detectors detect vehicles and produce measurements is able to identify possible causes of dual-loop data errors. The WSDOT loop detecting process is simplified in Figure 3-1.

As shown in Figure 3-1, the Model 170 controller samples individual loop detector actuation signals at 60 Hz to get loop event data, which are then processed by applying the WSDOT dual-loop algorithm to get individual vehicle information, such as length and speed. The individual vehicle information is aggregated into 20-second average velocity and length measurements and then sent to the Traffic System Management Center (TSMC). If any step of the process fails, the data collected will be erroneous.

The examination focuses on factors such as hardware malfunction, defects in the dual-loop algorithm, bugs in the code implementing the dual-loop algorithm, insufficient computing power of the cabinet controller, and any combination of these factors. The procedure to identify loop error causes is illustrated in Figure 3-2.

In order to identify where the errors occur in the dual-loop detecting process, a modified version of the current WSDOT dual-loop algorithm that runs on an independent Windows computer needed to be developed to process loop detector event data to produce individual vehicle data such as presence time, speed, and length. The modified algorithm still implemented the same validity checks as the current WSDOT dual-loop algorithm, but unlike the current algorithm, the modified algorithm did not discard the vehicles detected with error flags. The individual vehicle presence data were then compared to ground-truth vehicle presence data. If they did not agree, the event data would be problematic indicating the hardware was not functioning properly. If they agreed, it could be concluded that (1) the collected event data were sound in terms of detecting the presence of passing vehicles; (2) the current WSDOT dual-loop algorithm, or the 170 controller, or both had problems. If the latter case were true, more tests would be required to determine whether the current dual-loop algorithm or the 170 controller had problems.

Since the modified WSDOT algorithm does not discard the vehicles detected with error flags, the volume it collects should be higher than that collected by the current algorithm. If the difference between the two sets of volume data were approximately equal to the number of vehicles detected with flag signaled in Bit 5, Bit 6, or Bit 7, then the validity checks that cause the current algorithm to discard vehicles would be the cause of dual-loop

undercount problems. If this were not the case, more tests would need to be conducted to determine whether the problems were caused by the insufficiency of computing power of the current 170 controller, given that the controller has too many instructions to execute in a finite amount of time, or by any hidden bugs in the code that implements the current dual-loop algorithm.

To test whether the current 170 controller has insufficient computing power, the detector event data would need to be input to a new Model 170-compatible controller programmed with the current WSDOT dual-loop algorithm to get 20-second aggregated data. Since the new controller has much stronger computing power than the current one, it should successfully execute all the instructions requested by the current WSDOT algorithm. The collected volume data would then be compared to the volumes collected by applying the modified loop algorithm. If the difference were small, it could be concluded that the current 170 controller is insufficient in computing power. If not, the conclusion would be that the code that implements the current WSDOT algorithm is inadequate.

Typical freeway inductive loop detection systems, under normal operations, aggregate individual loop detector actuations sampled at 60 Hz into 20- or 30-second averages of traffic measurements. While such aggregations are appropriate for serving as inputs to control system algorithms and save disk space for archiving loop data, useful data regarding individual vehicles, such as arrival and departure times, speed, and length are lost. Yet this information is very desirable for in-depth investigation of loop error causes. Therefore, a detector event data collection (DEDAC) system, which provides loop event

data for subsequent data analysis, needed to be developed before the error cause investigation could happen.

3.2   DEVELOPMENT OF A NEW DUAL-LOOP ALGORITHM

The WSDOT current loop cabinet uses a Model 170 controller. The Central Processing Unit (CPU), an 8-bit 6808-based machine, was a product first released in 1975 by Motorola, Inc. The current WSDOT dual-loop algorithm was coded in Assembly (a low-level programming language that is not currently in common use) in order to efficiently utilize the limited hardware resources (memory, CPU, etc.). Since the software was coded in Assembly, it is difficult to understand and update. Also perhaps because of the limited computing power of the 170 controllers, erroneous loop actuation signals were simply screened out rather than corrected by the current WSDOT dual-loop algorithm. This screening process filtered out a tremendous amount of erroneous loop actuation signals that could otherwise be corrected to give acceptable speed and vehicle length information.

The new dual-loop algorithm is designed to filter out all the noise and keep as much individual vehicle information as possible despite the unreliability of the raw loop actuation signals. The new dual-loop algorithm employs a thorough noise filtering scheme and an intensive validity checking process. All possible errors that may occur when raw loop actuation signals are being processed will be caught and flagged with unique error codes. All in all, the new dual-loop algorithm is expected to produce more individual vehicle data and have much more tolerability for errors than the current WSDOT dual-loop algorithm.

3.3   RECOMMENDATION OF A QUICK-FIX METHOD

Despite the availability of a new dual-loop algorithm, it may take a while for the new dual-loop algorithm to be put into effect because upgrading the current 170 controller to the new generation controller involves both technical and non-technical issues, such as project funding. Therefore, an easy-to-implement quick-fix method is also proposed in this research so that the quality of the loop data can be improved in a timely manner. The quick-fix method involves adjusting the sensitivity settings of the loop detectors so that the two single loops that form a dual-loop detector generate similar on-time pulses for the same vehicle under non-forced-flow traffic conditions.
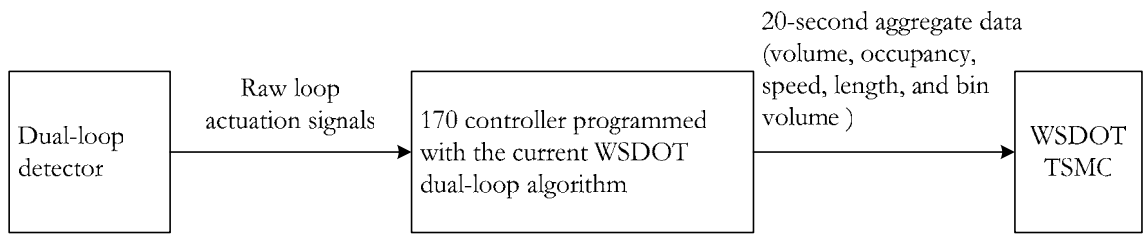
Figure 3-1. Diagram of The Dual-Loop Detecting Process
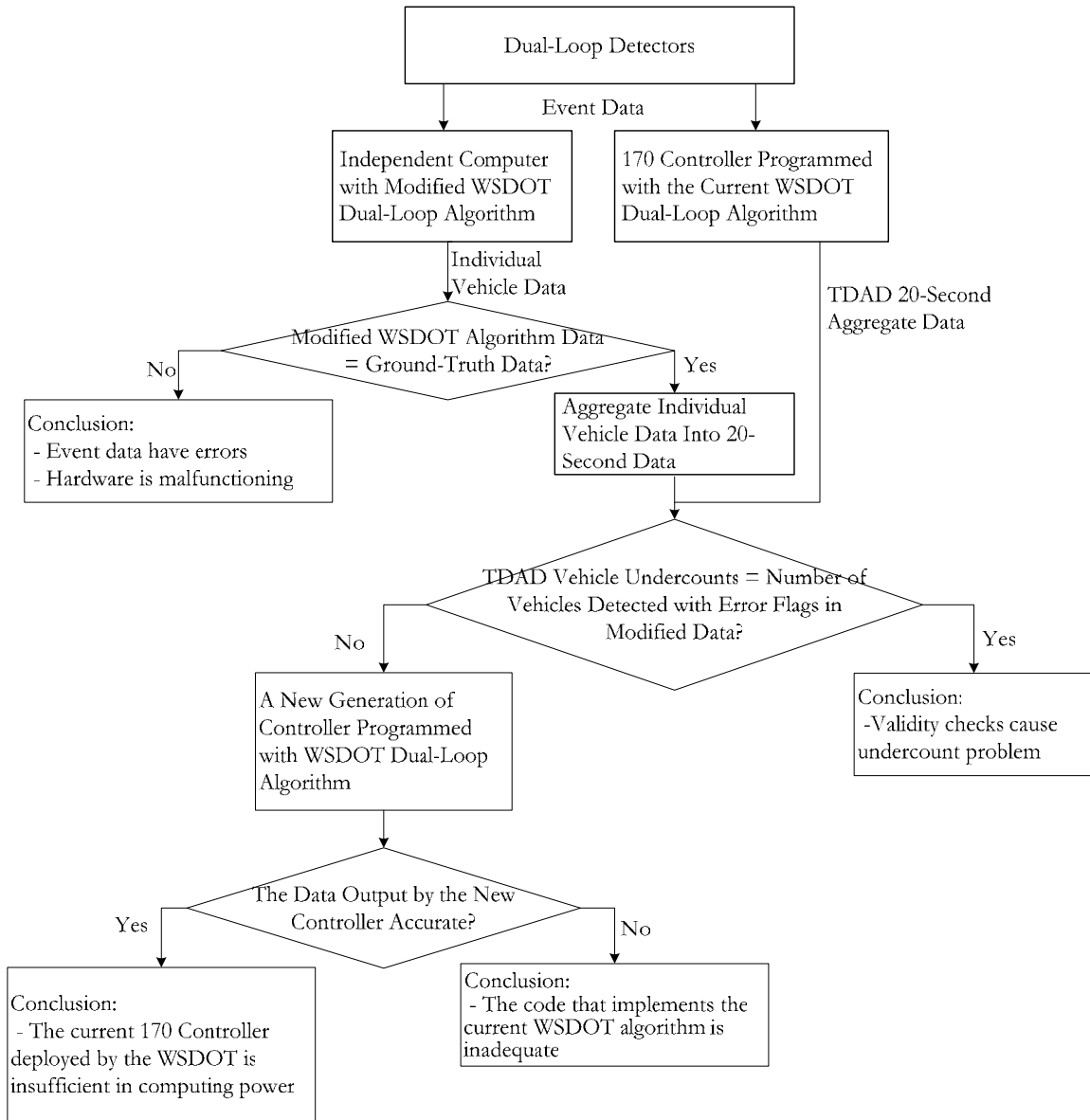
Figure 3-2. Flow Chart of The Error Detecting Process

CHAPTER 4   DEVELOPMENT OF A DEDAC SYSTEM

4.1   THE NEED FOR A DEDAC SYSTEM

Aggregating individual loop detector actuation signals sampled at 60 Hz into 20-second or 30-second averages of traffic measurements makes unavailable the individual vehicle data that are very desirable for transportation researchers and planners. For instance, members of the Berkeley Highway Laboratory (BHL) group collected an extensive amount of 60 Hz loop event data from 19 detector stations during the I-880 Field Experiment in 1993 [36]. The availability and the richness of this 60 Hz loop data set made in-depth and improved speed, link travel time, and error identification studies [37, 38, 39] possible.

As one of the leading resources for traffic research around the world, the collection of the BHL group's 60 Hz loop event data was labor-extensive. The standard California Department of Transportation's (Caltrans) detector station uses a Model 170 controller. Since the 60 Hz event data are internal to the controller, Caltrans had to develop new controller software for the I-880 Field Experiment that preserved the 60 Hz event data. The I-880 Field Experiment used a laptop computer, in conjunction with each controller, to collect and store this data stream in the field. Because of the limited capability of a Model 170 controller, simply outputting this event data stream through the controller would exhaust its processing power, and seriously obstruct its normal operation. Therefore, the type of individual vehicle (event) data set collected by the BHL group in the field cannot be easily reproduced by existing freeway data collection systems. To perform this type of detector event data collection, an additional, complementary system that can be introduced at the controller site is needed.

In this research a DEDAC system that collects event data without interrupting a controller's normal operation was developed. The development of the system consists of two phases. The first phase was to develop a desktop-based DEDAC system to investigate the feasibility of collecting loop detector event data from loop cabinet. The second phase was the upgrade from the desktop-based DEDAC to laptop-based DEDAC to improve the DEDAC system's portability and usability. The user manual of the laptop-based DEDAC is included in Appendix I.

4.2 DESKTOP-BASED DEDAC SYSTEM

4.2.1 System Design

Since raw loop actuation signals are accessible from the Input File in the Model 170 controller cabinet [21], it would be feasible to collect 60 Hz or higher frequency detector event data without interrupting the controller's normal operation. In the desktop-based DEDAC system, instead of obtaining data from the controller, a digital Input/Output (I/O) data acquisition card was connected to the wiring terminals of the controller's Input File. By polling the data address of the data acquisition card with a 60 Hz (or higher) sampling rate, high-frequency loop event data could be obtained.

Figure 4-1 illustrates an overview of the desktop-based DEDAC system design. As can be seen, the Input File is located right under the controller unit in the loop station cabinet. Loop actuation signals flow from loop detectors installed in the freeway pavement to the Input File, from where the signals flow to the Model 170 controller in the cabinet and the digital data acquisition card installed in the computer, simultaneously. Meanwhile, the event data collection software installed in the computer polls the data address of the data

acquisition card with a 60 Hz (or higher) sampling rate and saves the event data on a local disk. With this architecture, the desktop-based DEDAC system collects the exact real-time detector event data seen by the controller without interfering with the controller's normal operation (or requiring controller CPU time).

4.2.2 System Implementation

Before data collection and testing could occur, it was necessary to develop the detector event data collection program. The program was developed to run on a 32-bit Windows platform. The Application Program Interface (API) functions used for the implementation of the program are contained in the Microsoft® Platform Software Development Kit. The programming language used in implementing the program was Microsoft® Visual C.

4.2.2.1 High Resolution Timer

Since the desktop-based DEDAC system had to poll the data addresses of the digital data acquisition card at least 60 times per second, it was necessary to use a high-resolution timer for polling interval control and resolution control to make sure that the sampling rate was equal or higher than 60 Hz.

A multimedia timer was used for accurate polling interval control. A multimedia timer runs on its own thread (a path of execution through a program). Multimedia timer services allow applications to schedule periodic timer events (request and receive timer messages) with the greatest resolution possible for the hardware platform. For example, the utilization of a multimedia timer in the Musical Instrument Digital Interface (MIDI) sequencer maintains the pace of MIDI events within a resolution of 1 millisecond [40].

4.2.2.2 Multithreading

A multithreading programming technique was employed to complete parallel tasks control for the system. A thread is basically a path of execution through a program. It is also the smallest unit of execution that Win32 schedules. A thread consists of a stack, the state of the CPU registers, and an entry in the execution list of the system scheduler. Each thread shares all of the process's resources. In this program, aside from the threads generated by the operating system, some user-defined threads (a WRITE thread and multiple detector-status threads) also run in parallel.

Since disk operations are slow and the system polls data at a very high frequency, writing and reading data must be conducted in parallel. The system uses two buffers for temporary data storage. The event data read from digital data acquisition card data registers are saved in one of the buffers temporarily. Once the buffer is full, the other buffer takes over immediately. The WRITE thread then writes data in the buffer full of data from memory to a computer hard disk. The two buffers are used alternately to guarantee the reception of detector event data at high frequency.

The number of detector-status threads is equal to the number of dual-loop detectors or single-loop detectors from which the system collects event data. Each of the threads checks the status of its associated dual-loop detector (or single-loop detector) to see whether the status (on or off) has changed based on the latest input data. If the status does change, the associated indicator within the software will change correspondingly.

4.2.2.3 Equipment Needs

The desktop-based DEDAC system consists of three parts:

- Desktop computer and its accessories, including monitor, keyboard, and mouse.

The system testing was performed using a desktop computer configured with a Pentium III processor, running at an 850 MHz processing speed, and 256 MB of random access memory (RAM).

- Digital data acquisition card

A digital data acquisition card was required to provide input interface for a PCI-Bus computer. Since most freeway segments have five or fewer lanes in each direction, the digital data acquisition card should have at least 10 input channels in order to be able to collect data from five lanes simultaneously. Another consideration when choosing a digital data acquisition card is that the upper limit of input voltage must be higher than 24 volts, which is the upper limit of output voltage from the Input File.

PCI-IDIO-16, a digital data acquisition card recommended by WSDOT, was used in the system development. The PCI-IDIO-16 is a half-size card that provides an isolated digital input and output interface for PCI-Bus computers [41]. The card has sixteen optically isolated digital inputs for AC or DC control signals and sixteen solid-state switch outputs. For the purpose of this study, only ten isolated inputs were actually used for the data collection and system testing. Digital signals are connected to the card via a 78-pin D-type connector that extends through the back of the computer case. This card operates on Operating Systems Windows 98 or Windows 95.

- Connectors

A "Y" cable that divides the 78-pin D-type I/O connector down to two 37-pin DF-type connectors and two 37-pin DM-type connectors were used to make the connections between the digital I/O card and Cabinet Input File.

4.2.2.4 User Interface

The main dialog box and the setting menu comprise the user interface for the desktop-based DEDAC system.

4.2.2.4.1 Main Dialog Box

Figure 4-2 is the main dialog box of the program. It consists of four functional components:

1. Parameter Setting

Users are allowed to set up the following parameters:

- The time the data collection starts and the time it ends.

- Preferred timer resolution. The resolution ranges from 0 to 5 milliseconds according to the needs of different applications.

- Polling interval. This determines the polling rate of the program. For example, if the polling interval were set as 10, the polling rate would be 100 Hz.

2. Control Panel

The control panel contains all the control buttons used to start or stop the program. A digital clock is implemented to indicate the current system time.

3. Display Field

The display field presents real-time vehicle presence information. For each lane, when the dual-loop detector detects a vehicle passing by, the associated indicator will change its color to blue indicating the presence of the passing vehicle. The number of vehicles that have passed through the dual-loop detector is also recorded and shown below the indicator in the display field.

4. Status Report

The status report shows the progress of the data collection process. It records the times the data collection starts and ends. It also records the times when the two buffers switch. All the information is saved in a log file for future reference.

4.2.2.4.2 Setting Manual

As shown in Figure 4-3, two dialog boxes were designed and implemented under the setting menu. The dialog box named Loop Information provides an interface for users to input some background information such as loop station number, loop ID, data collection site, weather, etc. The dialog box named Personnel Information is used to input names of the data collection participants. This information will be saved at the beginning of the data file as a header for future reference.

4.2.3 System Testing

4.2.3.1 In-Laboratory Test

The reliability of the system was tested in-house at the WSDOT's ITS laboratory using a loop-detector simulator. The simulator takes traffic parameters such as flow rate and

occupancy value as inputs and outputs the corresponding loop actuation signals to simulate a loop's "on" or "off" state. By examining these "on" and "off" states the following individual vehicle data could be obtained: 1) time each vehicle arrives at the loop detector, 2) time each vehicle departs from the loop detector, and 3) presence time of each vehicle on the loop detector.

The reliability check consisted of two parts: a connection test and a system effectiveness test.

4.2.3.1.1 Connection Test

Connection refers to the physical input channel through which the signal flows from the Input File in the controller cabinet to the digital I/O card, which is then read by the system program. Sixteen signal indicators were implemented for the connection test; each of them was associated with an input channel. If the desktop-based DEDAC system detected a signal at one of the channels the indicator associated with that channel would turn blue; otherwise it would turn white. First, the simulator sent a signal to a randomly selected input channel; the indicator associated with that channel turned blue. This test was repeated until all sixteen channels had been tested with all associated indicators turning blue. The simulator then sent a signal to each of the sixteen input channels of the I/O card sequentially, and the result was that all sixteen indicators turned blue accordingly. From these results, it was determined that all sixteen input channels were detecting signals properly. It was also concluded that all sixteen input channels passed the connection test successfully.

4.2.3.1.2 Effectiveness Test

After passing the connection test, the effectiveness of the desktop-based DEDAC system was tested under different traffic conditions. The loop detector simulator was given flow rate and occupancy parameters that were used to create corresponding traffic event signals for the simulated loop detectors. The event data collection system being tested collected traffic event data from the simulated loops (i.e., vehicle arrival, departure, and presence times) and calculated the corresponding flow rates and occupancy values.

All 16 input channels were tested simultaneously. The input flow rate and occupancy values obtained for each channel are listed in Table 4-1. In this table, "Simulated" stands for the parameters that were input to the simulator to produce the simulated event signals, while "Calculated" refers to the data obtained from the data collection system calculations using the event data generated by the simulator. Since the simulator created the event data based on flow and occupancy data that were given inputs, the ability of the data collection system calculations to match these original input parameters was used as a test of the collection system's accuracy.

The input flow rates ranged from 3 to 18 vehicles per minute and the input occupancy values ranged from 6% to 36%. The simulated loop actuations signals were collected for 20 minutes. The collected data were then processed to obtain flow rate and occupancy values for each of the 16 channels. As shown in Table 4-1, the calculated flow rate and occupancy values perfectly matched those of the simulated parameter inputs for each channel.

The results from the two tests described above indicated that the desktop-based DEDAC system was able to accurately collect loop detector actuation signals with high sampling rates under a variety of traffic conditions.

4.2.3.2 Freeway Field Test

The desktop-based DEDAC system was also tested in the field to further verify its reliability and effectiveness. A description of the freeway field test is given in this section.

4.2.3.2.1 Data Collection Site

Two criteria had to be met when choosing the data collection site. First, the freeway segment where the loops were located (detector zone) had to be in the researchers' field of view so that it was possible for the researchers to do consistency checking, i.e., to examine whether or not the traffic information displayed in the program interface was reflecting what was really happening in the detector zone. Second, there should be a WSDOT traffic surveillance video camera available for traffic data recording. The videotaped traffic information would be processed to obtain ground-truth data for verification purposes.

Keeping these considerations in mind, loop station ES-163R located on Interstate 5 at NE 130th Street in Seattle, was chosen as the data collection site. Figure 4-4 shows a snapshot of the test site. This particular freeway section has four general-purpose (GP) lanes and one high-occupancy-vehicle (HOV) lane in the southbound direction. Each of the five lanes has a dual-loop detector installed in the pavement. Additionally, there is an on ramp in the same direction. The station cabinet is approximately 20 meters away from the freeway shoulder and the cabinet is approximately aligned with the five dual-loop detectors. For the

freeway field test, the five lanes were numbered 1 to 4 and HOV, with the rightmost lane (next to shoulder) identified as Lane 1 and the leftmost lane (next to median) as HOV.

4.2.3.2.2 In-Field Vehicle Presence Checking

The desktop-based DEDAC system collected loop event data from 2:00 p.m. to 3:00 p.m. on May 16, 2002. During this one-hour data collection period, when the system detected a vehicle occupying a dual-loop detector, the indicator corresponding to that lane on the screen's display field would turn blue signaling the vehicle's presence. The volume count for that lane would also increase by one. If the desktop-based DEDAC system were working properly, it would be able to detect every vehicle traversing the detector zone in real time.

Since it was extremely difficult to check every passing vehicle in real time, only the vehicles that traversed through the rightmost lane (Lane 1) were checked in the field during the first 20 minutes of data collection. During the first 20 minutes, 243 vehicles traversed the freeway segment through Lane 1 according to the manual count. All of them were successfully detected and signaled by the desktop-based DEDAC system. After the first 20 minutes, vehicles that traversed the detector zone through any of the five lanes were checked randomly. The system successfully detected and indicated the presence of these vehicles.

Loop event data were collected by the system during the one-hour field data collection. The traffic traversing all five lanes during that hour was also videotaped by the WSDOT video camera. For system synchronization purposes, the clock time of the loop detection system and that of the event data collection system were recorded with a digital video camera during the test.

4.2.3.2.3   Event Data Accuracy Checking

The accuracy of the loop detector event data were further evaluated using video ground-truth data. After the field data collection, the videotape provided by the WSDOT that had recorded the one-hour traffic was manually processed, frame-by-frame, to get individual vehicle information such as the time each vehicle appeared at a dual-loop detector and what the classification of that vehicle was (for estimation of length). The detector event data collected during the one-hour field test were also processed by applying the current WSDOT dual-loop algorithm's working mechanism to get individual vehicle arrival and departure times on both the upstream and downstream loops of each of the dual-loop detectors. Speed and length were also calculated for each vehicle. The individual vehicle data calculated using event data were called event-data-based traffic data hereafter in this research. The individual vehicle information obtained from these two data sources was compared for the first 20 minutes for each of the five lanes.

When a vehicle traversing the detector zone was observed on the videotape, the time stamp and its estimated length were recorded. The information was then compared to the vehicle information calculated by the system using the collected event data. If the calculated information showed that a vehicle passed over the detector at the same time, through the same lane with its calculated length close to what was observed from the videotape, that vehicle was marked as "detected."

As can be seen from Table 4-2, all vehicles that passed over the detector zone through Lane 1, Lane 3, Lane 4 and the HOV Lane during the first 20-minute period were successfully detected. In the remaining 40 minutes, individual vehicles in these four lanes

were randomly chosen from the videotape. All of them were found in the event-data-based individual vehicle data. It was concluded that the desktop-based DEDAC system was indeed able to collect accurate loop detector event data from these four dual-loop detectors in the field.

According to the video data, there were 435 vehicles traversing the detector zone through Lane 2 in the first 20-minute period. All of them were found in the event-data-based individual vehicle data. However, the event-data-based individual vehicle length was consistently shorter than that observed from the videotape. In other words, the event-data-based individual vehicle data only detected the presence of the passing vehicles. The cause of this error was further analyzed in Chapter 5.

4.2.4 Summary

Based on the results of the simulation tests and the freeway field tests, it was concluded that the proposed event data collection system is able to provide reliable high frequency loop detector event data. This system makes individual vehicle data collection possible. It also provides an approach for readily identifying loop malfunctions in the field. A prevailing advantage of the proposed system over the current system is that it makes the collection of loop detector event data independent of the controller's computing resource. This feature makes the system easy-to-employ at any loop station cabinets from which the detector event data need to be collected. Therefore, it is a reliable and practical system for transportation practitioners and researchers to collect accurate event data from loop detectors and such high frequency loop event data enable various kinds of transportation research and applications that could not otherwise be possible.

4.3 LAPTOP-BASED DEDAC SYSTEM

Although the desktop-based DEDAC system is a reliable and practical system for loop detector event data collection, integrating a bulky desktop computer in the system seriously limits its usability. Because of the large size of the desktop computer and monitor, the desktop-based DEDAC system cannot be placed inside the traffic cabinet, so data collection personnel must be present during the entire data collection. With such a cumbersome system, it would be extremely difficult for long-duration data collection, especially in inclement weather. Therefore, in the second phase, efforts were made to upgrade the desktop-based DEDAC to a laptop-based DEDAC in order to improve the system's usability.

4.3.1 System Design

Figure 4-5 illustrates an overview of the laptop-based DEDAC system design. As can be seen in Figure 4-5, there are two significant differences between the desktop-based DEDAC and the laptop-based DEDAC. The first, of course, is that the bulky desktop computer is replaced by a portable laptop. The other difference is that the data acquisition card is replaced by a USB digital I/O adapter.

4.3.2 System Implementation

4.3.2.1 Equipment Needs

The laptop-based DEDAC system consists of three parts:

- Laptop computer

  The system testing was performed using a laptop computer configured with a Pentium III processor, running at an 850 MHz processing speed, and 128 MB of random access memory (RAM). The operating system of the laptop is Windows ME.

- USB digital I/O adapter

  The USB digital I/O adapter was selected after an intensive product search and a consultation with technical support representatives of various manufacturers. The USB digital I/O adapter provides two parallel input ports, and in total 16 optically isolated input sensors. Each sensor can be used to interface a voltage input and then sense whether the voltage is on or off. Each of the 16 input sensors is isolated from every other sensor. Each sensor is also isolated with respect to the host PC ground. This means that signals such as low-level Alternate Current (AC) line voltage, motor servo voltage, and control relay signals can be "sensed" or read by the computer, without the risk of damage due to ground loops or ground faults [42].

  In addition, most modern operating systems do not allow direct hardware access. But the driver and the API functions provided by the manufacturer of the USB digital I/O adapter enable control over the hardware in Windows. So the laptop-based DEDAC system can operate on Windows 9X, Windows 2000, and Windows XP. This feature dramatically enhances the transferability and usability of the DEDAC system.

- Connectors and wires

  Multiple connectors and wires are needed to connect the two input ports to the traffic cabinet Input File.

4.3.2.2 Laptop-Based DEDAC Program

The program developed in the first phase was rewritten in the second phase using Microsoft® Visual C++ to improve software architecture and class encapsulation for easy software update and maintenance. The Microsoft® Foundation Classes (MFC) [40] was used for the implementation of the program. The same high-resolution timer and multithreading programming techniques were employed for high sampling rate control and parallel tasks control.

The laptop-based DEDAC program main interface is slightly different from that of the desktop-based DEDAC. In the first phase, the program main interface was designed to facilitate system testing. For example, the indicators were implemented to visually present the passage of vehicles. In the second phase, the program main interface was designed to facilitate long-duration data collection. Therefore, two more input fields were implemented under Parameter Settings to allow users to input the date the data collection starts and the date the data collection ends. Indicators implemented in the second phase were removed.

4.3.3 System Testing

The same set of tests that was employed for the desktop-based DEDAC system was also conducted on the laptop-based DEDAC system. The 16 input channels were tested randomly and then sequentially and all passed the connection test successfully. The effectiveness of the system was then tested under the same and various other simulated

traffic conditions. First, same flow rate and occupancy values were simulated for all the channels. Shown in Table 4-3, the system collected exactly what were simulated. Then, various flow rates and occupancy values were simulated for different channels. The laptop-based DEDAC system collected the simulated loop actuation signals for 24 hours. The flow rates and occupancy values calculated based on the 24-hour simulated data are summarized in Table 4-4. As can be seen in Table 4-4, for each channel, the collected flow rate and occupancy values exactly equal the flow rate and occupancy values simulated for that channel.

The results from the two tests described above indicated that the laptop-based DEDAC system was able to accurately collect loop detector actuation signals with high sampling rates under a variety of traffic conditions for long periods of data collection.

4.4   LAPTOP-BASED DEDAC VS DESKTOP-BASED DEDAC

The laptop-based DEDAC system greatly improves the DEDAC system's portability and usability. The physical dimensions of the USB adapter used to build the interface between the Input File and a laptop computer are 17.8 cm (7.0 in) in length, 13.3 cm (5.3 in) in width, and 3.8 cm (1.5 in) in height. The volume of the adapter is 0.9×10^{-3} m^3 (56 in^3). The physical dimensions of a regular laptop computer are 38.0 cm (15.0 in) in length, 30.0 cm (11.8 in) in width, and 6.5 cm (2.6 in) in height. The volume of a regular laptop computer is about 0.7×10^{-2} m^3 (450 in^3). So, the space the laptop-based DEDAC system occupies is only 0.8×10^{-2} m^3 (510 in^3). Because the size is so small, the laptop-based DEDAC system is portable and can be easily placed in a traffic cabinet for event data collection.

The improved portability in turn improves the usability of the DEDAC system. The system can now be placed in any cabinet for long-duration event data collection regardless of weather conditions. Data collection personnel are no longer required to be present aside after they set up the equipment. The laptop-based DEDAC can be used to collect event data for days and weeks as long as the hard disk is not exceeded. The availability of the long-duration event data greatly improves the usability of the DEDAC system.

As mentioned previously, most modern operating systems do not allow direct hardware access. Due to the limitation of the PCI-IDIO-16 digital data acquisition card, the desktop-based DEDAC system can only operate on operating systems Windows 9X. The laptop-based DEDAC, encouragingly, can operate on most of the common operating systems, including Windows 9X, Windows 2000, and Windows XP. The driver and the API functions provided by the manufacturer of the USB digital I/O adapter enable control over the hardware in Windows. This feature dramatically enhances the portability and usability of the DEDAC system in that the USB adapter can be easily plugged into any laptop with one of the Windows operating systems to form a laptop DEDAC system.

Speed Traps

Type 170 Cabinet

170 Controller

Input File

Real-Time Data Recorder

Digital I/O Card Installed

Y Cable

37 D-Type Connectors
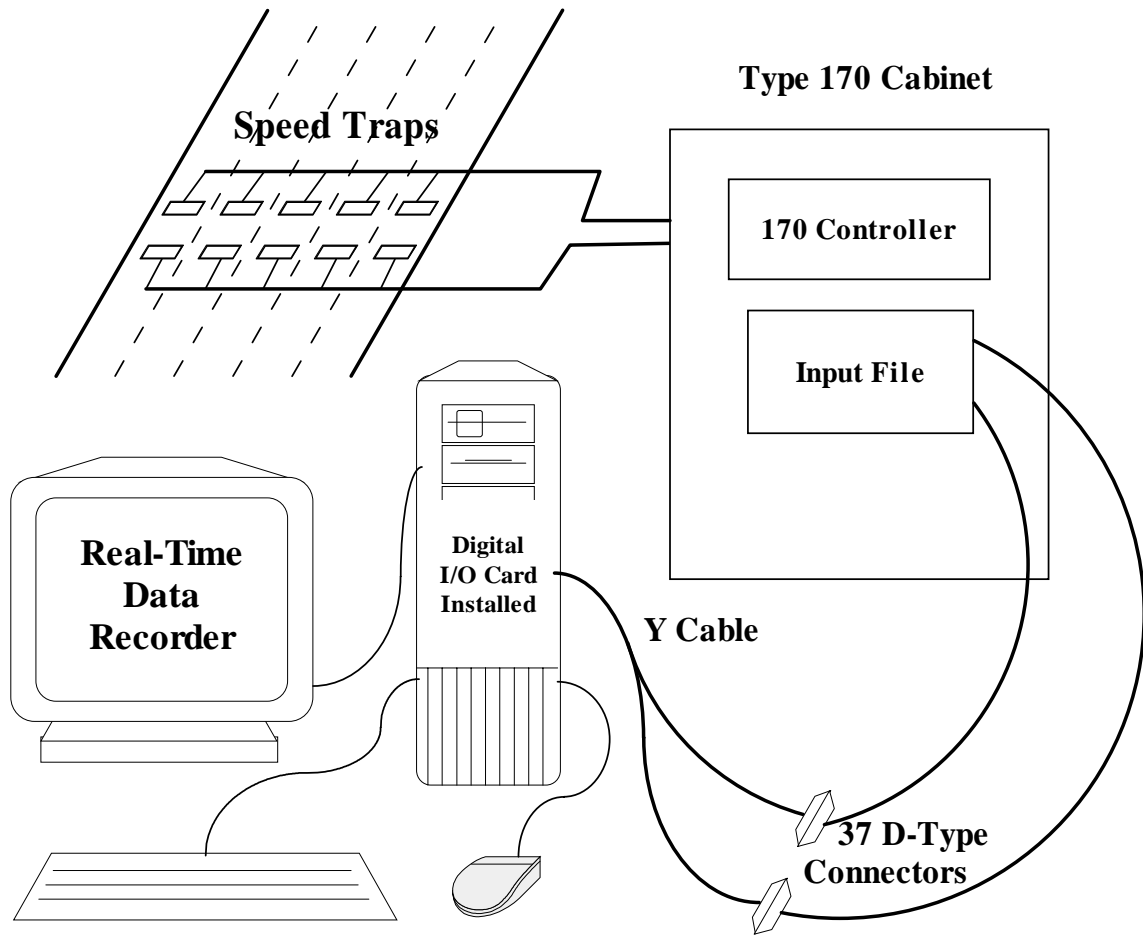
Figure 4-1. Overview of The Desktop-Based DEDAC System Design
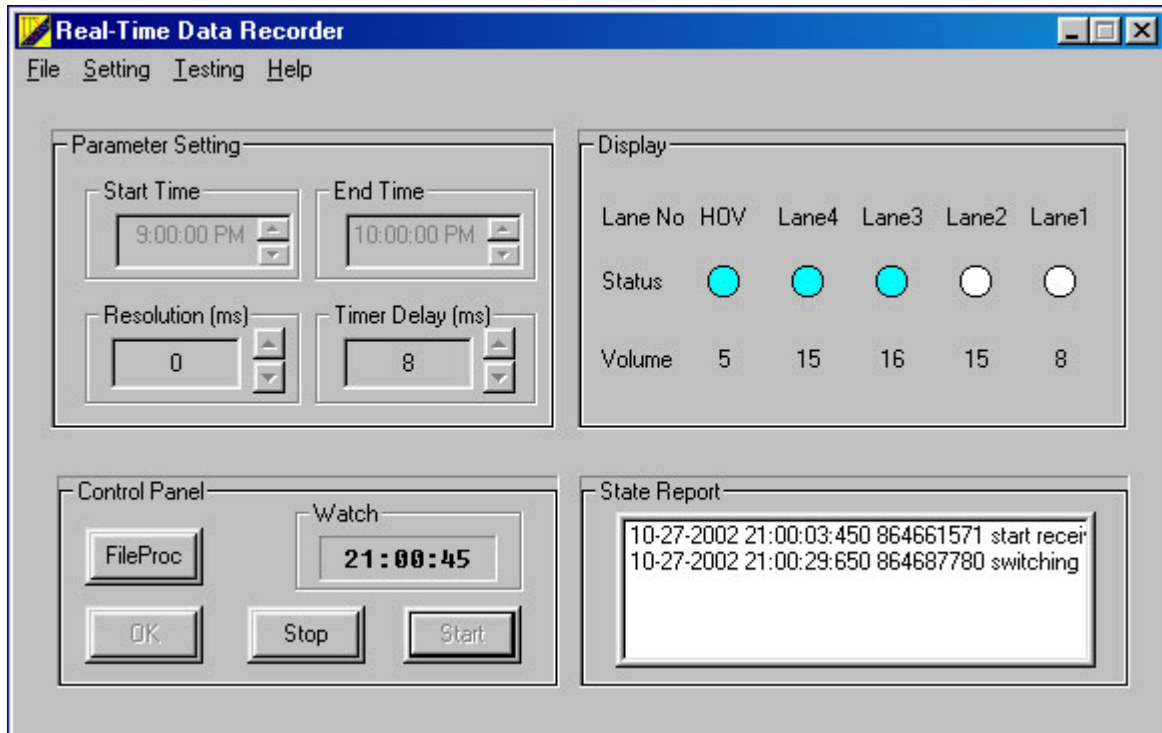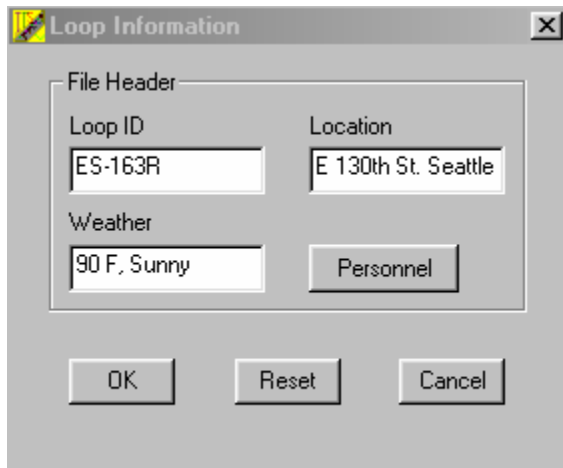
Figure 4-2. Desktop-Based DEDAC Program Main Interface
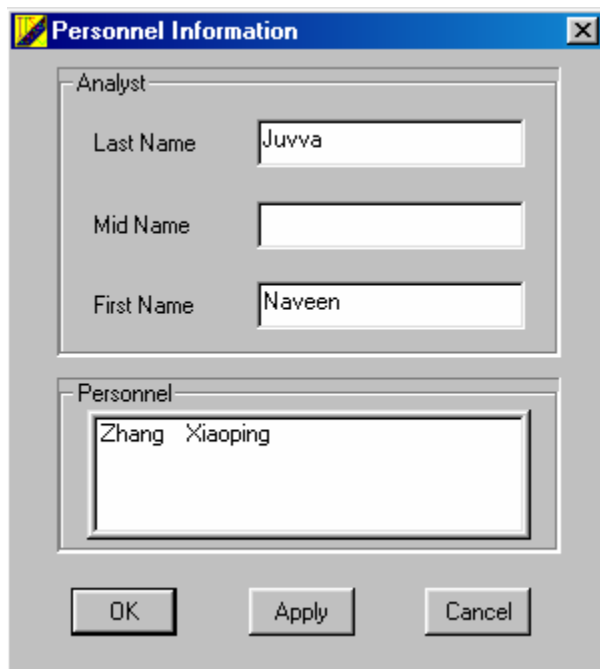
(a) Loop information, input dialog box

(b) Personnel information, input dialog box

Figure 4-3. Background Information: Input Dialog Boxes
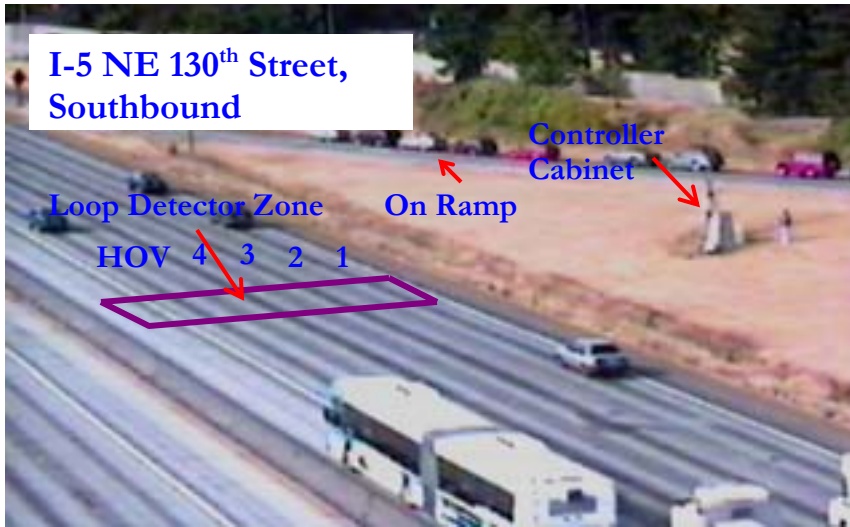
Figure 4-4. DEDAC Test Site (Station ES-163R at SB I-5 & NE 130th Street)

Type 170 Cabinet

USB Digital
I/O Adapter

170 Controller

Input File

Wires and
Connectors

USB Cable

Laptop with TDAC
Software Installed
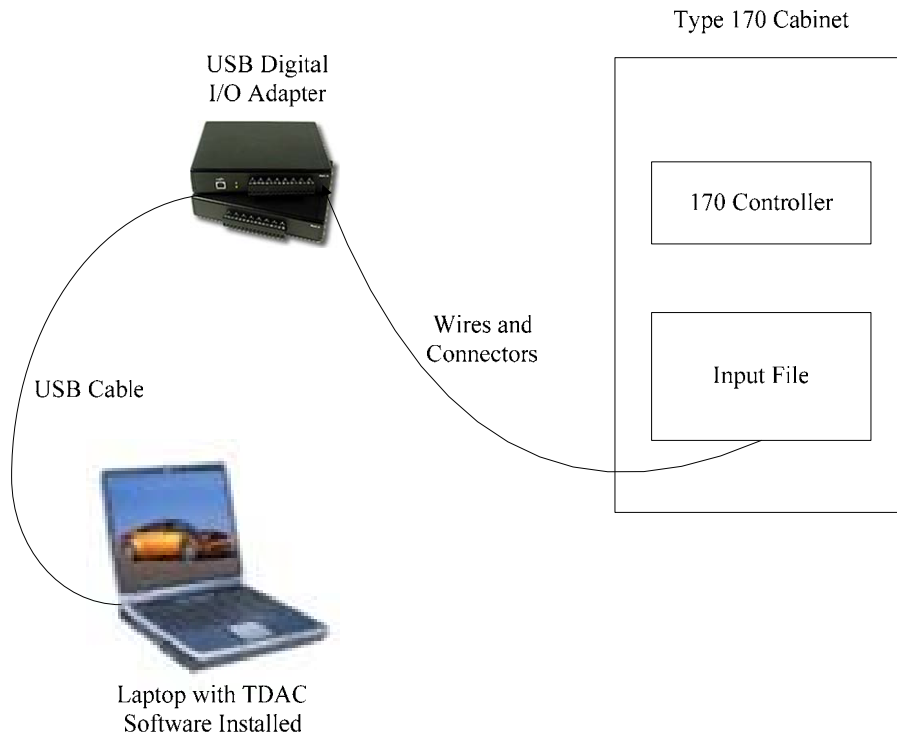
Figure 4-5. Overview of The Laptop-Based DEDAC System Design
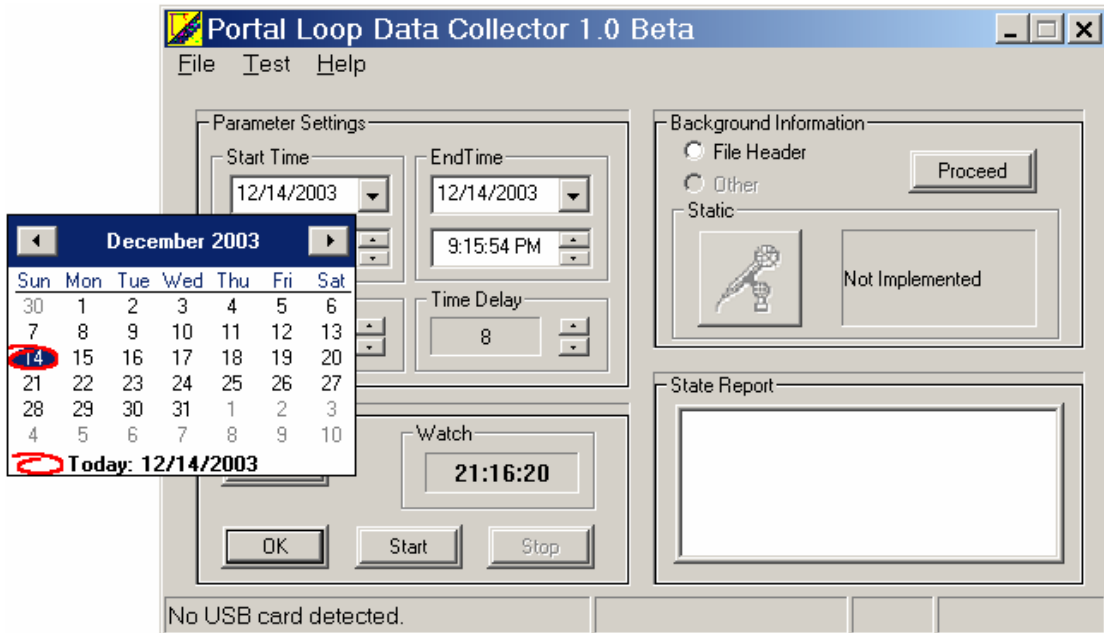
Figure 4-6. Laptop-Based DEDAC Program Main Interface

Table 4-1. Flow Rate and Occupancy Test Results (100% Accuracy)

Channel No.	Occupancy		Flow Rate	
	Simulated (%)	Calculated (%)	Simulated (vehs/min)	Calculated (vehs/min)
1	24	24	12	12
2	6	6	3	3
3	30	30	15	15
4	30	30	15	15
5	12	12	6	6
6	30	30	15	15
7	30	30	15	15
8	30	30	15	15
9	12	12	6	6
10	12	12	6	6
11	24	24	12	12
12	18	18	9	9
13	30	30	15	15
14	36	36	18	18
15	24	24	12	12
16	18	18	9	9

Table 4-2. Freeway Test Results

Lane No.		Lane 1	Lane 2	Lane 3	Lane 4	HOV
Volume Count (20-min Interval)	Calculated Based On Detector Event Data	243	435	506	546	99
	Observed By Processing Videotape	243	435	506	546	99

Table 4-3. Same Flow Rate and Occupancy Values Test Results (100% Accuracy)

Channel No.	Occupancy		Flow Rate	
	Simulated (%)	Calculated (%)	Simulated (vehs/min)	Calculated (vehs/min)
1	10	10	6	6
2	10	10	6	6
3	10	10	6	6
4	10	10	6	6
5	10	10	6	6
6	10	10	6	6
7	10	10	6	6
8	10	10	6	6
9	10	10	6	6
10	10	10	6	6
11	10	10	6	6
12	10	10	6	6
13	10	10	6	6
14	10	10	6	6
15	10	10	6	6
16	10	10	6	6

Table 4-4. Various Flow Rate and Occupancy Values Test Results (100% Accuracy)

Channel No.	Occupancy		Flow Rate	
	Simulated (%)	Calculated (%)	Simulated (vehs/min)	Calculated (vehs/min)
1	88	88	6	6
2	66	66	6	6
3	55	55	9	9
4	24	24	18	18
5	10	10	12	12
6	44	44	22	22
7	6	6	3	3
8	14	14	7	7
9	10	10	2	2
10	24	24	18	18
11	30	30	15	15
12	44	44	22	22
13	10	10	10	10
14	55	55	9	9
15	24	24	18	18
16	10	10	6	6

CHAPTER 5   DETERMINATION OF LOOP ERROR CAUSES

The inductive loop detection system is subject to errors, which might be caused by the system hardware malfunction, problematic system software, or both. On the hardware side, errors might be caused by an insufficiency of controller computing power or hardware malfunction. On the software side, the errors might be caused by coding bugs in the software or defects in the underlying algorithm.

In order to identify the error causes and how much they contribute to loop data inaccuracy, this research thoroughly examined the dual-loop detector detecting process. The research approach is covered in Chapter 3, and the data collection, data analysis, and major findings are covered in this chapter.

5.1   DATA COLLECTION

The one-hour event data and video data collected from five dual-loop detectors on May 16, 2002, at loop station ES-163R for testing the reliability and effectiveness of the DEDAC system were also used for determining dual-loop error causes. The aggregated 20-second dual-loop bin-volume data for the same one-hour period were downloaded from Traffic Data Acquisition and Distribution (TDAD) website at http://www.its.washington.edu/tdad/. The information obtained was then analyzed to investigate possible causes of dual-loop miscount and misclassification.

5.2   DATA ANALYSIS

As stated in Chapter 3, the causes of loop errors can be identified by thoroughly examining the dual-loop detector detecting process.   In this section, the collected information was analyzed by following the procedure described in the research approach.

5.2.1   TDAD-Based Volume vs. Video Ground-Truth Volume

TDAD-based and video ground-truth volume data were compared for each of the five lanes for the one-hour period, and the results are summarized in Table 5-1. As can be seen in this table, the five dual-loop detectors can be sorted in the order of Lane 3 > Lane 4 > HOV > Lane 1 > Lane 2 based on their vehicle detecting rates, with the dual-loop detector on Lane 3 (96.95% of the passing vehicles were detected) being the best and the one on Lane 2 (only 0.15% of the passing vehicles were detected) the worst. The results showed that despite one dual-loop detector counted vehicles favorably, the other four did not. It can be concluded that most dual-loop detectors at Station ES-136R did not work well at counting vehicles. Since the difference between the WSDOT 20-second volume data and video ground-truth data was notable, the quality of the collected event data needed to be evaluated. Therefore, event-data-based vehicle presence times were compared to those obtained from processing the videotape.

5.2.2   Event-Data-Based Volume vs. Video Ground-Truth Volume

The collected loop detector event data were processed to get individual vehicle information, such as vehicle arrival and departure times, speed, and length, for the same one-hour period by applying the current WSDOT dual-loop algorithm's working mechanism. Because it was

suspected that the 10% on-time percentage difference threshold value employed in the current WSDOT dual-loop algorithm filtered out a considerable amount of vehicles, no on-time difference threshold value was set when processing the event data in order to keep those vehicles that were filtered out by the current WSDOT dual-loop algorithm. The individual vehicle information was then compared with that obtained from processing videotape.

The event-data-based individual vehicle data were compared to the video ground-truth data for a 20-minute period, from 2:00 p.m. to 2:20 p.m., for each of the five lanes. The purpose of the comparison was to evaluate the quality of the collected event data. As can be seen from Table 5-2, all vehicles that passed over the detector zone during this period were successfully detected. Since there was no vehicle missing from the event-data-based individual vehicle data during this 20-minute period, it was concluded that the current WSDOT dual-loop algorithm worked favorably well on counting vehicles when the on-time difference validity check was not implemented to filter out vehicles. The result also indicated that the collected event data were good in terms of signaling the presence of passing vehicles.

Based on the findings from the two tests performed above, it was suspected that the 10% on-time percentage difference threshold value employed in the current WSDOT dual-loop algorithm contributed considerably to dual-loop detector miscount problem.

5.2.3 TDAD-Based Volume vs. Event-Data-Based Volume

The time a vehicle occupies a loop detector, the vehicle presence-time, also known as detector on-time, can be calculated by simply subtracting the time the vehicle arrives at the

detector from the time the vehicle leaves the detector. When a vehicle traverses a dual-loop detector, it sequentially occupies the paired single loops that form the dual-loop detector. Let OT_1 denote the total on-time at M loop, and OT_2 the on-time at S loop. The percentage difference (ΔT) between these two on-times with respect to OT_1 can be calculated using equation (5-1).

$$\Delta T = \frac{OT_2 - OT_1}{OT_1} \times 100 \qquad (5\text{-}1)$$

As stated in Section 1.1.2, the on-time difference check is one of the checks that the WSDOT dual-loop algorithm applies to verify the validity of the detector data. For an individual vehicle that passes over a speed trap, if the absolute of the on-time difference between M and S loops is larger than 10%, the WSDOT dual-loop algorithm will not calculate speed and length for this vehicle and drop it from total count with an error flagged. The WSDOT dual-loop detectors are only able to classify vehicles that pass over the detector zone without such an error flag.

In order to investigate how the on-time difference threshold affects dual-loop detectors' performance, volumes downloaded from TDAD were compared with those calculated using the collected event data without applying $\pm 10\%$ on-time threshold, and with those calculated with $\pm 10\%$ on-time threshold applied.

As can be seen from Table 5-3, the sum of 4-bin volumes calculated without $\pm 10\%$ on-time difference threshold was much higher than those of TDAD for each of the five lanes. But after the $\pm 10\%$ on-time threshold was applied, the calculated volumes dropped remarkably. These results indicated that the $\pm 10\%$ on-time difference threshold contributed

considerably to dual-loop detectors' undercount problem. The results in Table 5-3 also implied that the occupancy inconsistencies between the paired M and S loops were serious and needed to be analyzed.

5.2.4 On-Time Difference between Paired M and S Loops

The effectiveness of the WSDOT's dual-loop detectors in collecting vehicle count and classification data can be evaluated based on the on-time difference information. Possible causes of large on-time differences, indicating potential dual-loop detector malfunctions, can also be investigated. On-time mean percentage differences between paired M and S loops for the five dual-loop detectors are summarized in Table 5-4.

In Table 5-4, a negative number in the Mean field means the sensitivity of M loop is higher than that of S loop, while a positive number means the opposite. For Lanes 2, 3, and HOV, M loops are more sensitive than S loops. Whereas for Lanes 1 and 4, M loops are less sensitive than S loops. The absolute mean percentage difference ranged from 7.01 to 57.51 in the order of Lane 3 < Lane 4 < Lane HOV < Lane 1 < Lane 2, with Lane 3 having the smallest absolute percentage difference value and Lane 2 the highest value. This sequence is in the reverse order of Lane 3 > Lane 4 > Lane HOV > Lane 1 > Lane 2, which is the order of the dual-loop detector's detecting rates. This result showed that the higher the absolute on-time mean percentage difference, the lower the vehicle detecting rate. It was concluded that the large on-time difference considerably affected the dual-loop detector's capability of counting vehicles and possibly estimating individual vehicle lengths.

The on-time percentage difference distributions for Lanes 3 (the best lane) and 2 (the worst lane) were plotted in Figure 5-1 and Figure 5-2, respectively. As illustrated in Figure 5-

1, for Lane 3, the majority of the absolute on-time differences were smaller than 10%. This meant that the WSDOT dual-loop detection system should have been able to detect most of the vehicles that passed the detector zone in Lane 3 during the one-hour period. This conjecture was confirmed by the statistic in Table 5-3 that this dual-loop detector only undercounted 3.05% of the passing vehicles. This result indicated that the WSDOT dual-loop detector collects data from an overwhelming majority of the passing vehicles when the on-time difference between the two single-loop detectors is within the allowable (±10%) range.

This result was contrasted with the distribution curve in Figure 5-2. In Figure 5-2, the normal curve spans from –80 to 0 indicating that almost every on-time at the S loop of the dual-loop detector in Lane 2 was consistently shorter than its matching on-time at the M loop. It was obvious from the curve that most of the on-time differences were larger than 10%, the threshold for discarding event data. Thus, almost all of the vehicles that passed over the freeway segment in Lane 2 were not counted by the dual-loop detector. This conclusion was further verified by the one-hour volume data in Table 5-1. As shown in this table, 1315 vehicles passed over the detector zone through Lane 2 during the one-hour testing period, of which only two (0.15%) were detected by the dual-loop detection system.

Based on these results, it was strongly suspected that the S loop might be operating in an incorrect mode. Loop detectors can operate in two modes including "presence mode" and "pulse mode". Under normal operations, a loop detector operates in "presence mode", where the loop turns on and stays on as long as a vehicle is occupying it. While in "pulse mode", the loop detector produces a short output pulse when a vehicle enters the loop

detection zone. An experienced traffic operator at WSDOT confirmed that, during the data collection, the S loop was operating in "pulse mode." The mistake was corrected several days after the field test. It was concluded from the analysis performed above that a wrong mode setting which caused large on-time differences between a paired M and S loops significantly affected dual-loop detector performance.

5.3 SUMMARY OF DATA ANALYSIS

The main findings from data comparison are summarized as follows:

1. Under non-forced-flow traffic conditions, when both M and S loops appear to work properly, the main cause of dual-loop errors is the fact that the on-time difference between the two single loops in a dual-loop detector exceeds the WSDOT ±10% threshold value included in the current WSDOT algorithm. Sensitivity discrepancy between the two single loops is a direct cause of the large on-time difference.

2. No malfunctions were found that might indicate the insufficiency of computing power in the Model 170 controllers in the research. Further research may be needed to investigate the sufficiency of computing power of the current WSDOT 170 controllers.
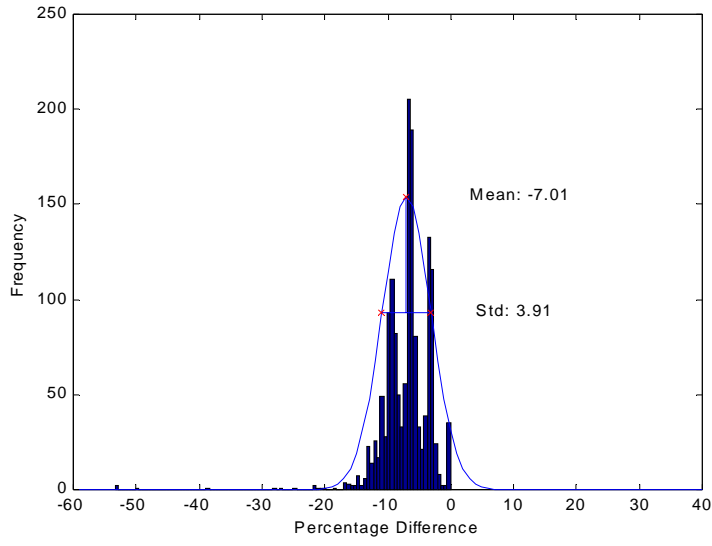
Figure 5-1. The Distribution of The Measured On-Time Percentage Difference at Lane 3
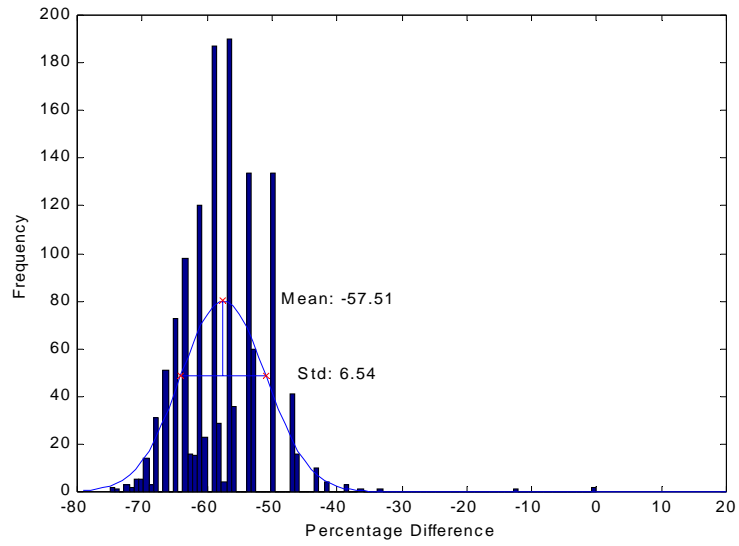
Figure 5-2. The Distribution of The Measured On-Time Percentage Difference at Lane 2

Table 5-1. Comparison between TDAD and Video Ground-Truth Volumes

Lane No.		Lane 1	Lane 2	Lane 3	Lane 4	HOV
Volume (One-Hour Interval)	V_T	123	2	1463	1291	153
	V_V	817	1315	1509	1652	357
	$\dfrac{V_T}{V_V} \times 100$	15.06	0.15	96.95	78.15	42.86

V_T = TDAD-based dual-loop volume

V_V = Video-ground-truth volume

Table 5-2. Comparison between Event-Data-Based and Video Ground-Truth Volumes

Lane No.		Lane 1	Lane 2	Lane 3	Lane 4	HOV
Volume Count	V_{ET}	243	435	506	546	99
(20-Min Interval)	V_V	243	435	506	546	99

V_{ET} = Event-data-based dual-loop volume

V_V = Video-ground-truth volume

Table 5-3. Comparison between TDAD and Event-Data-Based Volumes

Lane No.		Lane 1	Lane 2	Lane 3	Lane 4	HOV
Volume (One-Hour Interval)	V_{ET1}	817	1315	1509	1652	357
	V_{ET2}	114	2	1135	881	117
	V_T	123	2	1463	1291	153
	$\dfrac{V_T - V_{ET1}}{V_{ET1}} \times 100$	-84.95	-99.85	-3.05	-21.85	-57.14
	$\dfrac{V_T - V_{ET2}}{V_{ET2}} \times 100$	7.89	0	28.90	46.54	30.77

V_T = TDAD-based dual-loop volume

V_{ET1} = Event-data-based dual-loop volume, without 10% on-time threshold

V_{ET2} = Event-data-based dual-loop volume, with 10% on-time threshold

Table 5-4. On-Time Mean Percentage Differences between Paired M and S Loops

On-Time Percentage Difference (One-Hour Interval)		Lane 1	Lane 2	Lane 3	Lane 4	HOV
$\dfrac{OT_2 - OT_1}{OT_1} \times 100$	Mean	17.11	-57.51	-7.01	11.52	-12.71
	Standard Deviation	10.40	6.54	3.91	10.71	7.50

CHAPTER 6   DEVELOPMENT OF A NEW DUAL-LOOP ALGORITHM

With advances in technologies, the computing power of controllers has been dramatically increased. A new dual-loop algorithm that can filter out noise and correct erroneous loop actuation signals is needed to improve the performance of the current dual-loop detection system. In response to this need, a new version of the dual-loop algorithm written in a more advanced programming language (C# [40]) was developed in this research.

The new dual-loop algorithm begins with a noise filter and a postprocessor that screen out noise and correct erroneous actuation signals. The algorithm then matches downstream on-times to their upstream on-times. The matched on-time pairs are then used to calculate individual vehicle speed and length with error flags. When calculating speed and vehicle length, various checks are applied to test the validity of the data. If any of the checks fails, an appropriate error will be flagged. The new algorithm is also able to output individual vehicle arrival, departure, and presence times. All in all, the new dual-loop algorithm is much more flexible than the current WSDOT dual-loop algorithm in that it is capable of tolerating erroneous raw loop actuation signals and outputting acceptable speed and vehicle length information.

This chapter covers the design and implementation of the new dual-loop algorithm in the order of new dual-loop algorithm design, threshold setting, noise filter and postprocessor, paired on-time matching, and speed and length calculation.

6.1   NEW DUAL-LOOP ALGORITHM DESIGN

Figure 6-1 illustrates the responses of the two single loops when a vehicle passes a dual-loop detector. The time a vehicle occupies a loop detector, the vehicle presence-time, also known as detector on-time, can be calculated by simply subtracting the time the vehicle arrives at the detector from the time the vehicle leaves the detector.

As can be seen in Figure 6-1, when a vehicle traverses a dual-loop detector, it sequentially occupies the paired single loops that comprise the dual-loop detector. Paired single-loop detectors' on-times (T_{uon}, T_{don}) and the time for the vehicle to traverse from the M loop to the S loop, also called elapsed time (T_e), can be calculated using the following equations:

$$T_{uon} = t_{uoff} - t_{uon} \qquad (6\text{-}1)$$

$$T_{don} = t_{doff} - t_{don} \qquad (6\text{-}2)$$

$$T_{e1} = t_{don} - t_{uon} \qquad (6\text{-}3)$$

$$T_{e2} = t_{doff} - t_{uoff} \qquad (6\text{-}4)$$

Once detector elapsed time is available, speed can be calculated straightforwardly using equation 6-5 or 6-6 by dividing the distance between the two single loops with the elapsed time. The distance between the two single loops is measured from the leading edge of the M loop to that of the S loop or the rear edge of the M loop to that of the S loop. For increased reliability, speed can be calculated using equation 6-7 as the average of the two speeds calculated using equations 6-5 and 6-6.

$$S_1 = \frac{l_u + l_{ud}}{T_{e1}} \tag{6-5}$$

$$S_2 = \frac{l_d + l_{ud}}{T_{e2}} \tag{6-6}$$

$$S = \frac{S_1 + S_2}{2} \tag{6-7}$$

Where

S_1 = speed calculated using the distance from the leading edge of the M loop to that of the S loop and the elapsed time between the two points

S_2 = speed calculated using the distance from the rear edge of the M loop to that of the S loop and the elapsed time between the two points

S = average of S_1 and S_2

Vehicle speed and the single-loop on-times are then used to calculate vehicle length using either of the following equations:

$$l_{vu} = T_{uon} \times S - l_u \tag{6-8}$$
$$l_{vd} = T_{don} \times S - l_d \tag{6-9}$$

Where

l_{vu} = vehicle length calculated using M loop's on-time and length

l_{vd} = vehicle length calculated using S loop's on-time and length

When both of the two loops work properly (i.e., either of the two calculated lengths can be used to represent vehicle length), the average of the two calculated lengths (equation 6-10) can be used as the length of the target vehicle for increased reliability.

$$l_v = \frac{l_{vu} + l_{vd}}{2} \qquad\qquad (6\text{-}10)$$

Where

l_v = average of l_{vu} and l_{vd}

As discussed above, the dual-loop algorithm itself is very straightforward when the dual-loop detectors are working properly. However, as previously stated, many factors affect the performance of the loop detection systems, so various data validity checks are conducted in the new dual-loop algorithm. The factors being checked are the ones that dramatically affect dual-loop data quality and systems performance. These factors include match of M and S on-time pairs, length of elapsed times, upstream and downstream on-times, and difference between the upstream and downstream on-times. The validity checking process in the new dual-loop algorithm is shown in Figure 6-2. If any of the factors fails the validity check, an error flag will be generated along with the calculated speed and vehicle length.

The factors mentioned above are compared to predefined threshold values. They are checked in the order of elapsed times, upstream and downstream on-times, and on-time difference. The derivation of threshold values is described in the following section.

6.2 THRESHOLD SETTINGS

Threshold values for basic parameters can be determined according to the empirical range for speed (S_{min}, S_{max}) and the empirical range for vehicle length (l_{vmin}, l_{vmax}).

$$S_{min} < S < S_{max}$$
$$l_{vmin} < l_v < l_{vmax}$$

Since under congested traffic conditions when traffic is stop-and-go the speed is very unsteady, threshold values for some basic parameters such as detector on-time (T_{onmin}, T_{onmax}) and the elapsed time (T_{emin}, T_{emax}) cannot be determined. Therefore, threshold values for the basic parameters are only derived for traffic under non-forced-flow conditions in this research.

Once the threshold values for the basic parameters are determined, the range of other derived parameters such as detector on-time (T_{onmin}, T_{onmax}) and the elapsed time (T_{emin}, T_{emax}) can then be derived based on these empirical threshold values.

Since the length of the detector is fixed, the minimum and maximum on-time values can be easily calculated using the following equations:

$$T_{onmin} = \frac{l_u + l_{vmin}}{S_{max}} \qquad (6\text{-}11)$$

$$T_{onmax} = \frac{l_u + l_{vmax}}{S_{min}} \qquad (6\text{-}12)$$

and $T_{onmin} < T_{on} < T_{onmax}$

The minimum and maximum elapsed times can be calculated similarly using the following equations:

$$T_{emin} = \frac{l_u + l_{ud}}{S_{max}} \qquad (6\text{-}13)$$

$$T_{emax} = \frac{l_u + l_{ud}}{S_{min}} \qquad (6\text{-}14)$$

and $T_{emin} < T_e < T_{emax}$

The empirical threshold values of the basic parameters such as speed, vehicle length, loop dimensions, and loop spacing, are listed in Table 6-1. The derived parameters, such as minimum on-time, maximum on-time, minimum off-time, minimum elapsed time, maximum elapsed time, and their calculated threshold values are listed in Table 6-2.

6.3   ERROR CODING SCHEME

The current WSDOT error coding scheme is employed in the new dual-loop algorithm. The error types are coded in binary numbers. In the new dual-loop algorithm, 19 types of errors are flagged. Each type is represented by a single digit in a 19-digit binary number. These 19 errors are numbered from Type 1 to Type 19. A Type 1 error is represented by a value of "1" in the first digit (counting from right to left); a Type 2 error is represented by a value of "1" in the second digit; and so on and so forth. In other words, each of the digits in the binary number represents the type of error numbered using the position of the digit in the binary number.

For example: binary number 000 00000000 00000001 represents Type 1 error since the first digit of the binary number is "1", binary number 000 00000000 00010000 represents Type 5 error since the fifth digit of the binary number is "1", and so on and so forth.

The beauty of this error coding scheme is that the types of errors can be easily recognized when multiple errors occur when collecting data for a single vehicle. For example: if Type 1 and Type 5 errors both occur in a single-vehicle data, the error code that encodes these two types of errors in binary format is 000 00000000 00010001, which is the addition of the two error codes that represent Type 1 and Type 5 errors. The addition operation is illustrated in Figure 6-3. The first and the fifth digits equal to "1", so Type 1 and Type 5 errors are coded in this binary number.

In the dual-loop algorithm output, however, the error codes are converted from binary numbers to decimal numbers. For example, in the dual-loop algorithm output, a Type 5 error is represented by a decimal number 16 and a Type 8 error is represented by a decimal number 128. These decimal numbers need to be converted to binary numbers for quick identification of the types of errors.

6.4 SINGLE-LOOP ACTUATION SIGNAL NOISE FILTER AND POSTPROCESSOR

Almost all electronic signals are subject to noise. As stated previously in Chapters 2 and 5, the loop actuation signals are digital signals, which have two states – "on" or "off." These two states indicate whether or not the loop is being occupied; where "on" means occupied and "off" means not occupied. The duration of an "on" state is called a loop's on time. The "on" and "off" states can be combined to form an infinite number of "on" and "off"

sequences, but only some of them are valid signal sequences. Therefore, before using the loop actuation signals to calculate speed and vehicle length information, it is necessary to apply a noise filter to filter out random positive or negative false alarm noise or pulse breaks. A postprocessor should also be applied to catch any positive or negative false alarm signals induced or undetected by the noise filter with error flagged.

6.4.1 Introduction to the Noise Filter and Postprocessor

As can be seen in Table 6-2, the minimum on-time threshold value is 75 milliseconds. Because the sampling interval is 16 milliseconds, 75 milliseconds lead to a signal sequence of five 16-millisecond in length. Therefore, five 16-millisecond is a proper window size for the noise filter. For convenience, "0" is used to represent the "on" state, and "1" is used to represent the "off" state. The noise filter can then be represented by a 5-digit digital signal sequence. The noise filter developed in this research is pictorially represented as a Karnaugh map [46] in Table 6-3.

In the Karnaugh map, AB represents the first two digits of the 5-digit input signal sequence, DE represents the last two digits of the 5-digit input signal sequence, and C represents the digit (underlined) in the middle that needs to be determined by the noise filter. In total, there are 32 different 5-digit input signal sequences, which exhaust all the possible 5-digit combinations of "0"s and "1"s.

Because the new dual-loop algorithm aims at detecting as many passing vehicles as possible, the objective of this noise filter is to filter out noise, while still keeping as many on-time pulses as possible for each of the two single loops. Although some positive false alarm signals may be introduced in this process, they will be filtered out during the matching

process in the dual-loop algorithm. In this research, a positive false alarm is defined as the loop detector detects the presence of a vehicle when there is no vehicle occupying the loop; a negative false alarm is defined as the loop detector does not detect the presence of a vehicle when there is a vehicle occupying the loop.

The noise filter screens out the positive or negative false alarm noise by flipping the noise from its current state to its opposite state. In the noise filter a "0" in the middle of the input signal sequence will not be flipped to "1" unless the digit is preceded by two "1"s and succeeded by two "1"s; a "1" in the middle of the input sequence will not be flipped to "0" if the digit is preceded by two "1"s, or succeeded by two "1"s, or preceded by a "1" and succeeded by a "1". This will maintain as many on-time pulses as possible during the noise-filtering process. In the Karnaugh map, the digits that have been flipped are circled.

After being processed by the noise filter, the loop actuation signals will be sent to a postprocessor to filter out any positive or negative false alarm signal shorter than the on-time or off-time threshold value. The output loop actuation signals will then be used to calculate speed and vehicle-length information.

6.4.2 Illustration of the Noise Filter and Postprocessor

All the possible combinations of "0"s and "1"s can be classified into six groups, each of which can be reduced to and represented by a general signal sequence. The noise filter and the postprocessor are applied to each of these six representative signals to test their effectiveness. These processes are covered in Appendix II and illustrated in Figures II-1 to II-6.

6.4.3 Summary

In this section, a noise filter and a postprocessor were developed and their effectiveness was illustrated in Appendix II by processing six representative signal sequences. In each of the six cases, a negative false alarm noise or signal, a positive false alarm noise or signal, or both are flagged whenever it applies. Type 1 or Type 2 error in Table 6-4 is flagged to indicate a negative false alarm noise or positive false alarm noise respectively.

The noise filter and the postprocessor are designed to effectively screen out noise occurring in the raw loop actuation signals. The processed signals are used for matching M and S on-time pairs, which are then used to calculate individual vehicle speed and length.

6.5   PAIRED ON-TIME MATCHING

6.5.1   Introduction to the M and S Loop On-Time Pulses Matching Rules

After the noise filtering and post processing process, M loop and S loop signal sequences are processed simultaneously to match the M loop and S loop on-time pairs. As illustrated in Figure 6-1, when a vehicle traverses a dual-loop detector it first activates the M loop to generate an on-time pulse, then the S loop to generate another on-time pulse. So if a dual-loop detector is working properly and the car does not switch to another lane in between M and S loops, the on-time pulse generated by the M loop should have a matching pulse generated by the S loop. Therefore, for each on-time pulse in the M loop signal sequence, the paired on-time matching algorithm searches for the best matching on-time pulse in the S loop signal sequence. The following rules are applied during this matching process.

Rule 1: When a car traverses a dual-loop detector, it first occupies the M loop and then the S loop, so the S loop on-time match pulse should occur after the M loop on-time pulse.

Rule 2: The elapsed time from the M loop on-time pulse to its matching S loop on-time pulse should be longer than the minimum elapsed time threshold and shorter than the maximum elapsed time threshold.

Rule 3: If the identified on-time pulse in the S loop signal sequence does not meet the criterion stated in Rule 2, an error indicating that the elapsed time is shorter than the minimum threshold or greater than the maximum threshold is flagged. Type 3, Type 4, Type 5, and Type 6 error flags in Table 6-4 are used to indicate elapsed times that do not fall inside a valid range.

Rule 4: The M loop on-time pulse that does not have any matching pulse in the S loop signal sequence is filtered out as a positive false alarm signal. Type 2 error in Table 6-4 is flagged to indicate a positive false alarm signal.

Rule 5: The S loop on-time pulse that does not have a matching pulse in the M loop signal sequence is filtered out as a positive false alarm signal. Type 2 error in Table 6-4 is flagged to indicate a positive false alarm signal.

Rule 6: If one S loop on-time pulse satisfies the criterion in Rule 2 for two or more M loop on-time pulses, the one that immediately precedes the S loop on-time pulse

in the M loop on-time sequence is chosen to form a matching pair with the S loop on-time pulse.

Rule 7: If two or more S-loop on-time pulses satisfy the criterion in Rule 2 for an M loop on-time pulse, the S loop on-time pulse that immediately succeeds the M loop on-time pulse is chosen to form a matching pair with the M loop on-time pulse.

6.5.2 Illustration of the M and S Loop On-Time Pulses Matching Rules

All the positive false alarm pulses that could occur when matching for the M loop and S loop on-time pulse pairs can be classified into five cases. The application of the seven rules introduced above is illustrated in Appendix III by processing these five cases.

6.6 INDIVIDUAL VEHICLE SPEED CALCULATION

After the M loop and S loop on-time pulses matching, the matched on-time pulse pairs are used for calculating speed. As stated in Section 6.1, speed can be calculated using equations 6-5, 6-6, and 6-7. Shown in Figure 6-1, for each pair of M and S loop on-times, there are two elapsed times, T_{e1} and T_{e2}. In the new dual-loop algorithm, for each pair of M and S loop on-times, the validity of the elapsed times is checked. If either or both of the elapsed times fall outside of the valid range or the difference between the two elapsed times is greater than the elapsed time difference threshold value, the speed of the preceding vehicle will be used in the calculation considering that the speeds of two consecutive vehicles running on the freeway should not differ considerably under non-forced-flow traffic conditions. The process employed to calculate speeds is illustrated in the flow chart in Figure 6-4. In Figure

6-4, the vehicle for which speed and length data are calculated is represented by index *i*, and the vehicle that precedes the current one is represented by index *i-1*.

In the current WSDOT dual-loop algorithm, 10% is the percentage difference threshold value; therefore, for consistency, 10% is also used in this research as the difference threshold value. Since there is no document to help track the development of the current WSDOT algorithm, plus the engineer who designed the current WSDOT dual-loop algorithm is not available to answer questions, the origination of this 10% threshold value is not investigated in this research.

6.6.1   Illustration of Speed Calculation

For each pair of M and S loop on-times, elapsed times T_{e1} and T_{e2} are compared to the elapsed time threshold values, T_{emin} and T_{emax}, and the difference between T_{e1} and T_{e2} is compared to the elapsed time difference threshold value, $\Delta T_{e\_threshold}$, which is 10% in this research. There are four possible cases.

6.6.1.1   Case 1

In this case, both elapsed times fall in the valid range, i.e., $T_{emin} < T_{e1} < T_{emax}$ and $T_{emin} < T_{e2} < T_{emax}$ If the difference between T_{e1} and T_{e2} is smaller than the threshold value, both are used to calculate speeds by applying equations 6-5, 6-6, and 6-7.

If the difference between T_{e1} and T_{e2} is larger than the threshold value, the speed of the vehicle (if there is any) which precedes the current one is used to derive an elapsed time (T_e'). Then, of the two elapsed times, T_{e1} and T_{e2}, the one that is closer in value to T_e' will be used for speed calculation. In this case, Type 7 error is flagged.

If the difference between T_{e1} and T_{e2} is larger than the threshold value and the current vehicle is the first one for which speed is to be calculated, both T_{e1} and T_{e2} are used to calculate speeds. In this case, Type 7 error is flagged.

6.6.1.2 Case 2

In this case, the first elapsed time falls in the valid range, the second elapsed time falls outside of valid range, i.e., $T_{emin} < T_{e1} < T_{emax}$ and $T_{e2} < T_{emin}$ or $T_{e2} > T_{emax}$. In Case 2, Type 5 or Type 6 error is flagged.

If there is no vehicle preceding the current one, only T_{e1} is used for speed calculation because T_{e2} is not a valid value. If there is a vehicle preceding the current one, the speed of that vehicle is used to derive the elapsed time T_{e}'. If the difference between T_{e}' and T_{e1} is greater than the threshold value, only T_{e1} is used for speed calculation. Otherwise, the speed of the preceding vehicle is also used in speed calculation for the current vehicle for improved reliability. The reasoning behind this is that the speeds of the successive vehicles running on the freeway under non-forced-flow traffic conditions do not differ considerably.

6.6.1.3 Case 3

In this case, the first elapsed time falls outside of the valid range, the second elapsed time falls inside the valid range, i.e., $T_{e1} < T_{emin}$ or $T_{e1} > T_{emax}$ and $T_{emin} < T_{e2} < T_{emax}$. In Case 3, Type 3 error or Type 4 error is flagged.

Case 3 is similar to Case 2, so the speed calculation method in Case 2 is also applied in Case 3 except that T_{e2} rather than T_{e1} is used in speed calculation.

6.6.1.4 <u>Case 4</u>

In this case, neither of the two elapsed times falls inside the valid range, i.e., $T_{emin} > T_{e1}$ or T_{e1} $> T_{emax}$, and $T_{emin} > T_{e2}$ or $T_{e2} > T_{emax}$. In Case 4, two different errors are flagged. One is Type 3 or Type 4 error, and the other is Type 5 or Type 6 error.

In this case, the speed of the current vehicle is equal to the speed of the preceding vehicle because the speeds of successive vehicles running on the freeway should not differ considerably. If the current vehicle is the first one detected in the data collection, the speed is set to zero.

6.6.2 Summary

In this section, individual vehicle speed calculation was introduced and then illustrated. By checking the validity of the two elapsed times, possible errors will be flagged. These errors are summarized in Table 6-4. If any of the two elapsed times falls outside of the valid range, the reliability of the calculated speed for the current target vehicle can be improved by incorporating the speed of the preceding vehicle in the speed calculation.

After this process, the calculated speed for an individual vehicle is compared to the minimum and maximum threshold speed values, S_{min} and S_{max}. If the calculated speeds fall outside of the valid range, Type 13 or Type 14 error in Table 6-4 is flagged.

6.7 VEHICLE LENGTH CALCULATION

The calculated speed is then used to calculate individual vehicle length. As stated in Section 6.1, vehicle length can be calculated using equations 6-8, 6-9, and 6-10. In the new dual-loop algorithm, the validity of the two on-times is checked. If either or both of the on-times fall

outside of the valid range or the difference between the two on-times is greater than the on-time difference threshold value, errors will be flagged. The process employed to calculate vehicle lengths is illustrated in the flow chart in Figure 6-5.

6.7.1 Illustration of Length Calculation

When calculating a vehicle's length, the M and S loop on-times (T_{uon}, T_{don})are compared to the on-time threshold values, T_{onmin} and T_{onmax}, and the difference between T_{uon} and T_{don} is compared to the on-time percentage difference threshold value, $\Delta T_{on\_threshold}$, which is 10% in this research. There are four possible cases:

6.7.1.1 <u>Case 1</u>

In Case 1, both on-times fall in the valid range, i.e., $T_{onmin} < T_{uon} < T_{onmax}$ and $T_{onmin} < T_{don} < T_{onmax}$, so both are used for vehicle length calculation. If the difference between the two on-time values is greater than the on-time difference threshold, Type 12 error is flagged.

6.7.1.2 <u>Case 2</u>

In Case 2, the upstream loop on-time falls in the valid range but the downstream loop on-time falls outside of the valid range, i.e., $T_{onmin} < T_{uon} < T_{onmax}$ and $T_{don} < T_{onmin}$ or $T_{don} > T_{onmax}$. In this case, only upstream on-time value is used for vehicle length calculation and Type 10 or type 11 error is flagged.

6.7.1.3 <u>Case 3</u>

In Case 3, the downstream loop on-time falls in the valid range but the upstream loop on-time falls outside of the valid range, i.e., $T_{uon} < T_{onmin}$ or $T_{uon} > T_{onmax}$, and $T_{onmin} < T_{don} <$

T_{onmax}. In this case, only downstream on-time value is used for vehicle length calculation and Type 8 or Type 9 error is flagged.

6.7.1.4 <u>Case 4</u>

In Case 4, neither of the two on-times falls inside the valid range, i.e., $T_{uon} < T_{onmin}$ or $T_{uon} > T_{onmax}$, and $T_{don} < T_{onmin}$ or $T_{don} > T_{onmax}$. In this case, both on-times are used for length calculation and the Type 8 or Type 9 error and Type 10 or Type 11 error are flagged.

6.7.2 Summary

In this section, the individual vehicle length calculation method was introduced and then illustrated by processing four possible cases. In each of the four cases, possible errors were caught and flagged by checking the validity of the two on-times.

After this process, the calculated length of any individual vehicle is compared to the minimum and maximum threshold length values, l_{min} and l_{max}. If the calculated length falls outside of the valid range, Type 15 or Type 16 error is flagged. These two errors and their error codes are summarized in the 15th and 16th rows in Table 6-4.

6.8 SUMMARY

This chapter began with a brief discussion of the necessity for developing a new dual-loop algorithm. It then covered in detail the design and implementation of the algorithm with an emphasis on the new features that improve the tolerability of the WSDOT dual-loop detectors and therefore the performance of the dual-loop detection system. The advantages

of the new dual-loop algorithm over the current WSDOT dual-loop algorithm are summarized as follows:

1. The new dual-loop algorithm employs a thorough noise filtering and post processing process to filter out noise occurring in the raw loop actuation signals and to recover the on-time pulses broken by random noise. Since the current WSDOT dual-loop algorithm only has a crude noise filtering process, a tremendous amount of noise is overlooked resulting in the single-loop over-count problem. With the implementation of the noise filter and the postprocessor in the new dual-loop algorithm, the single-loop over-count problem is expected to be significantly alleviated.

2. The new dual-loop algorithm conducts various checks to test the validity of the individual vehicle data. If any of the checks fails an appropriate error will be flagged. The current WSDOT dual-loop algorithm also conducts some validity checks, but the data with error flags are simply discarded. The new dual-loop algorithm, however, keeps the individual vehicle data with error flags in the total count to reduce the dual-loop undercount problem.

3. The new dual-loop algorithm takes into account the fact that under non-forced-flow traffic conditions speeds of consecutive vehicles should not differ significantly. So if the calculated speed of the current vehicle is problematic, the speed of the preceding vehicle is used to adjust the calculated speed. The current WSDOT dual-loop

algorithm does not have this feature. If the calculated speed for an individual vehicle is erroneous, the current dual-loop algorithm simply flags an error.

These features and their functions were also tested in this research and the results are summarized in Chapter 7.
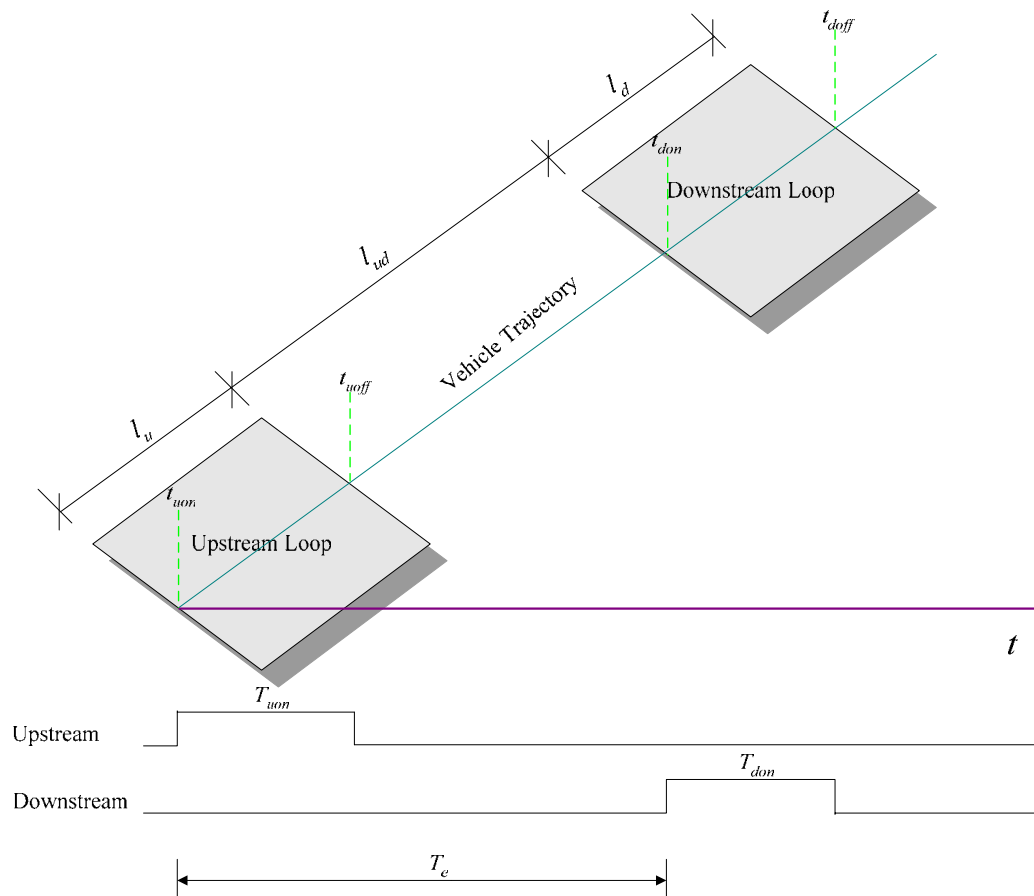
Where

t_{uon} = time when a vehicle hits the upstream loop's leading edge

t_{uoff} = time when a vehicle leaves the upstream loop's rear edge

t_{don} = time when a vehicle hits the downstream loop's leading edge

t_{doff} = time when a vehicle leaves the downstream loop's rear edge

l_u = length of the upstream loop

l_d = length of the downstream loop

l_{ud} = distance between the upstream and downstream single loops measured from the rear edge of the upstream loop to the leading edge of the downstream loop

T_{uon} = on-time at the upstream loop

T_{don} = on-time at the downstream loop

T_{e1} = elapsed time (leading edge to leading edge)

T_{e2} = elapsed time (rear edge to rear edge)

Figure 6-1. Illustration of A Vehicle Traversing A Dual-Loop Detector

Input:
 M and S On-Time
Sequences

Match M and S On-Time Pairs

Check the Validity of
Elapsed Times

Check the Validity of the
Calculated Speed

Check the Validity of M and S
On-Time Values

Check the Validity of the
Calculated Vehicle Length

Output:
 Vehicle Speed
 Vehicle Length
 Error Flags
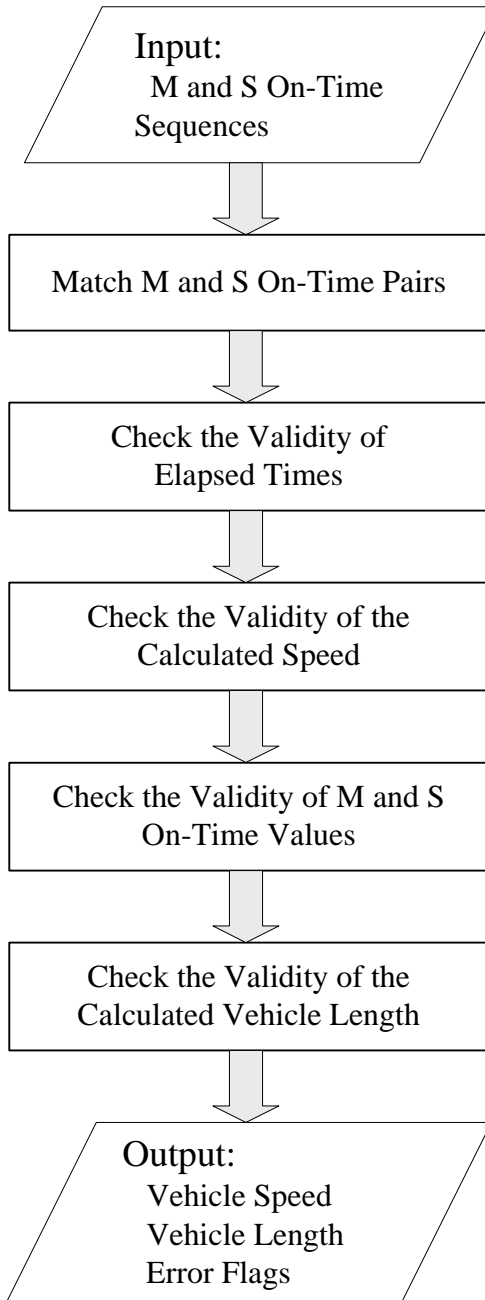
Figure 6-2. Validity Checks in The New Dual-Loop Algorithm

Type 1 Error

000 00000000 00000001

Type 5 Error

+   000 00000000 00010000

000 00000000 00010001

Type 5 Error   Type 1 Error
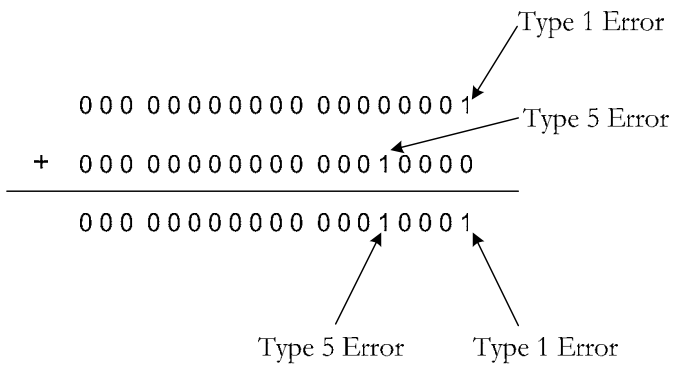
Figure 6-3. Error Coding Scheme (Addition of Two Error Codes)
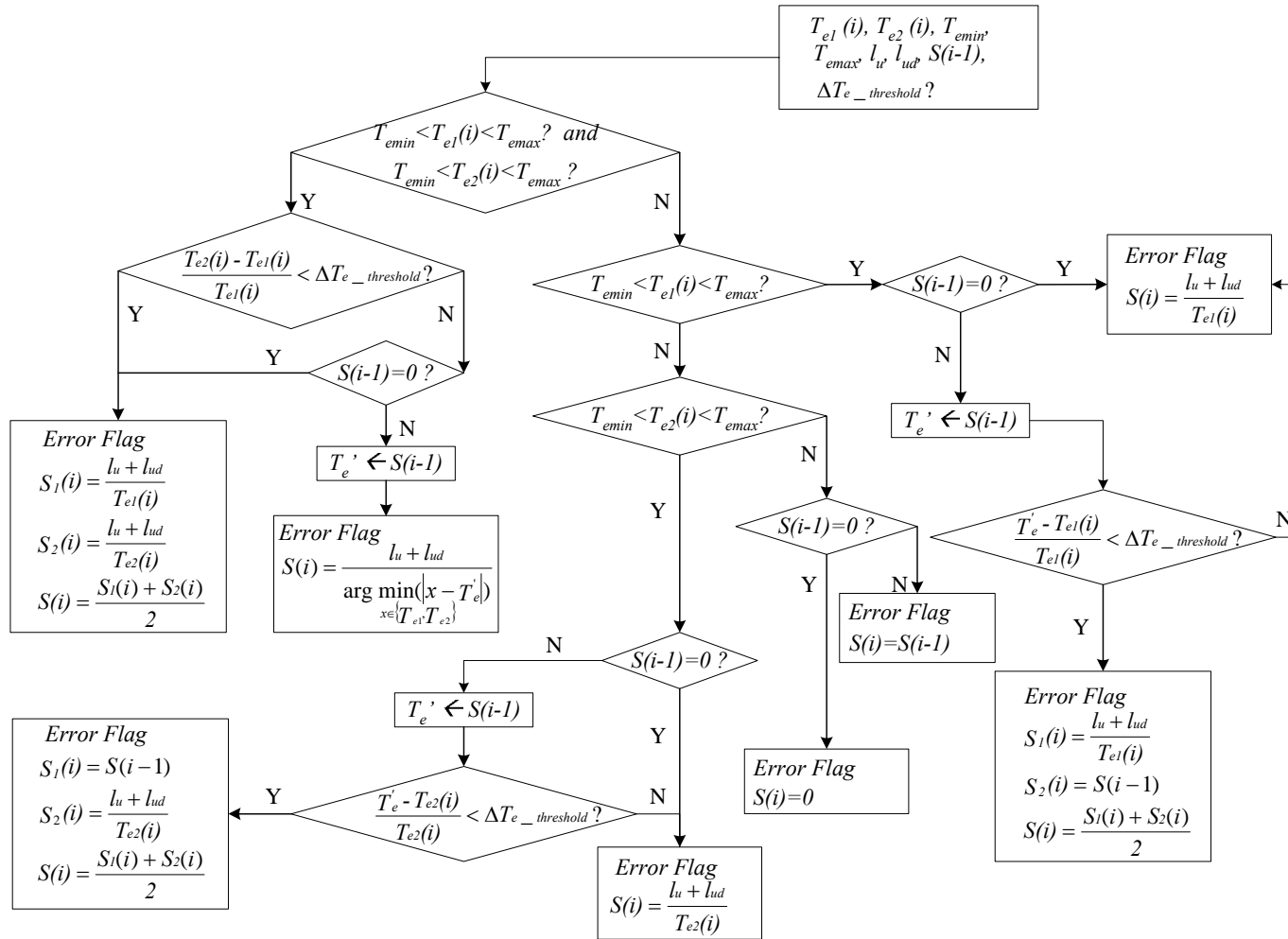
Figure 6-4. Speed Calculation Flow Chart

T_{uon}, T_{don}, T_{onmin}, T_{onmax}, l_u, l_d, l_{uv}, $\Delta T_{on\_threshold}$

$T_{onmin} < T_{uon} < T_{onmax}$? and $T_{onmin} < T_{don} < T_{onmax}$?

Y

N

$\dfrac{T_{don} - T_{uon}}{T_{uon}} > \Delta T_{on\_threshold}$?

N

Y

$T_{onmin} < T_{uon} < T_{onmax}$?

Y

N

$l_{vu} = T_{uon} \times S - l_u$

$l_{vd} = T_{don} \times S - l_d$

$l_v = \dfrac{l_{vu} + l_{vd}}{2}$

Error Flag

$l_{vu} = T_{uon} \times S - l_u$

$l_{vd} = T_{don} \times S - l_d$

$l_v = \dfrac{l_{vu} + l_{vd}}{2}$

Error Flag

$l_v = T_{uon} \times S - l_u$

$T_{onmin} < T_{don} < T_{onmax}$?

Y

N

Error Flag

$l_v = T_{don} \times S - l_d$

Error Flag

$l_{vu} = T_{uon} \times S - l_u$

$l_{vd} = T_{don} \times S - l_d$

$l_v = \dfrac{l_{vu} + l_{vd}}{2}$
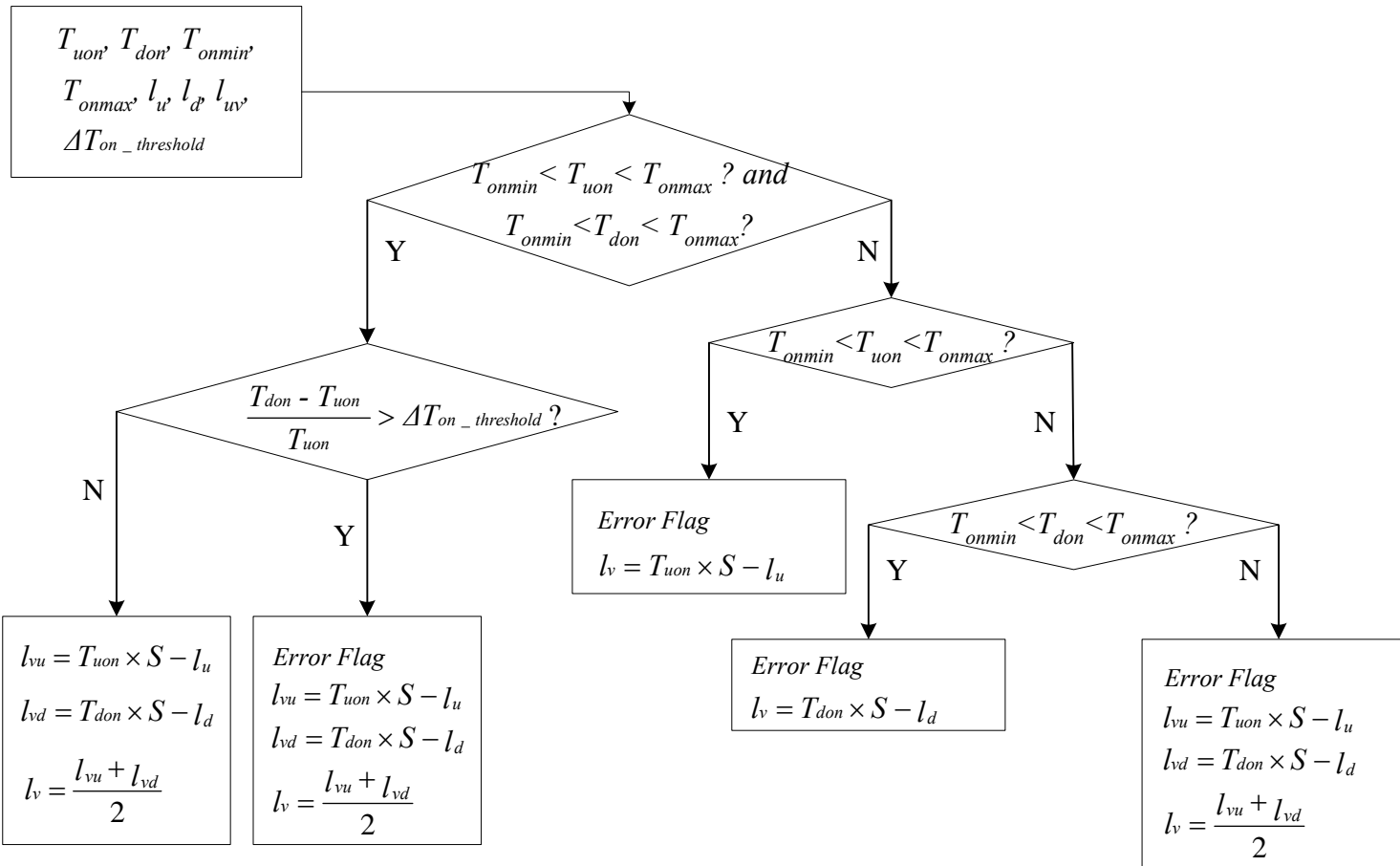
Figure 6-5. Vehicle Length Calculation Flow Chart

Table 6-1. Basic Parameters and Their Empirical Threshold Values

Parameter	Value	Explanation
Maximum Speed S_{max} (mph)	100	Speed limit on the Greater Seattle freeway network is 60 mph for most of the freeway segments. Speeding vehicles may travel at a speed higher than 80 mph. Only in some rare cases, such as emergency vehicles or car racing, vehicles may travel up to 100 mph. This value is also the maximum speed threshold value used in the current WSDOT dual-loop algorithm. Therefore, in the new dual-loop algorithm, the maximum speed threshold value is still 100 mph.
Minimum Speed S_{min} (mph)	5	When the traffic condition is congested or stop-and-go, the average speed can be as low as 5 mph. This is the minimum velocity that keeps a vehicle moving. This value is also the minimum speed threshold value used in the current WSDOT dual-loop algorithm. Therefore, in the new dual-loop algorithm, the minimum speed threshold value is still 5 mph.
Maximum Vehicle Length $l_{v\,max}$ (ft)	110	According to Washington State regulations, including 1) Guide for Uniform Laws and Regulations Governing Truck Size and Weight Among the WASHTO States [43] and 2) Washington State Commercial Vehicle Guide 2002-2003 [44], the permitted maximum vehicle length on the freeway network is 110 feet.
Minimum Vehicle Length $l_{v\,min}$ (ft)	5	The minimum vehicle length was decided based on the length of motorcycles. The length of a regular motorcycle is greater than 4.7 feet, which can be rounded up to 5 feet. In addition, this value is used in the current WSDOT dual-loop algorithm. Therefore, in the new dual-loop algorithm, the minimum vehicle length is still 5 feet.
Loop Spacing l_{ud} (ft)	16/17	According to WSDOT loop installation records, the spacing of a paired single-loop detectors is 16 feet or 17 feet. The spacing of two single-loop detectors, by definition, is the distance between the two single-loop detectors from the leading edge of the upstream detector to the leading edge of the downstream detector.
Loop Length l_u (ft)	6	The majority of the loops installed on the freeway network are 6′×6′ square loops. The dimension of the few round loops installed to replace broken square loops can also be considered 6′×6′ because studies show data collected by round loops do not differ significantly from those collected by square loops [45].

Table 6-2. Derived Parameters and Their Calculated Threshold Values

Derived Parameter	Value	Derivation
Minimum On-Time	75 ms OR 5 sample intervals	According to Equation (6-11), $T_{on\,min} = \dfrac{l_u + l_{v\,min}}{S_{max}}$, $T_{on\,min} = 75$ ms, when $S_{max} = 100$ mph, $l_u = 6$ ft, and $l_{v\,min} = 5$ ft.
Maximum On-Time	15818 ms OR 95 sample intervals	According to Equation (6-12), $T_{on\,max} = \dfrac{l_u + l_{v\,max}}{S_{min}}$, $T_{on\,max} = 15818$ ms, when $S_{min} = 5$ mph, $l_u = 6$ ft, and $l_{v\,max} = 100$ ft.
Minimum Off-Time	170 ms OR 10 sample intervals	According to Highway Capacity Manual, the minimum spacing between two consecutive vehicles is 25 feet, so $T_{off\,min} = 170$ ms, when $S_{max} = 100$ mph.
Minimum Elapsed Time $T_{e\,min}$	109 ms/116 ms OR 7 sample intervals	According to Equation (6-13), $T_{e\,min} = \dfrac{l_u + l_{ud}}{S_{max}}$, $T_{e\,min} = 109$ ms, when $S_{max} = 100$ mph, $l_u = 6$ ft, and $l_{ud} = 10$ ft. $T_{e\,min} = 116$ ms, when $S_{max} = 100$ mph, $l_u = 6$ ft, and $l_{ud} = 11$ ft.
Maximum Elapsed Time $T_{e\,max}$	2182 ms/2318ms OR 137/145 sample intervals	According to Equation (6-14), $T_{e\,max} = \dfrac{l_u + l_{ud}}{S_{min}}$, $T_{e\,max} = 2182$ ms, when $S_{min} = 5$ mph, $l_u = 6$ ft, and $l_{ud} = 10$ ft. $T_{e\,max} = 2318$ ms, when $S_{min} = 5$ mph, $l_u = 6$ ft, and $l_{ud} = 11$ ft.

Table 6-3. The Noise Filter in The Format of Karnaugh Map

CDE AB	000	001	010	011	100	101	110	111
00	0	0	0	0	⓪	⓪	⓪	1
01	0	0	0	0	⓪	⓪	1	1
10	0	0	0	0	⓪	⓪	⓪	1
11	0	0	0	①	1	1	1	1

Table 6-4. Types of Errors and Their Flags

Error Flag Type Index	Error Flag Code (Decimal)	Error Flag Code (Binary)	Error Flag Type
1	1	000 00000000 00000001	Negative false alarm noise/signal
2	2	000 00000000 00000010	Positive false alarm noise/signal
3	4	000 00000000 00000100	$T_{e\_1} < T_{e\,\min}$
4	8	000 00000000 00001000	$T_{e\_1} > T_{e\,\max}$
5	16	000 00000000 00010000	$T_{e\_2} < T_{e\,\min}$
6	32	000 00000000 00100000	$T_{e\_2} > T_{e\,\max}$
7	64	000 00000000 01000000	$\dfrac{T_{e\_2} - T_{e\_1}}{T_{e\_1}} > \Delta T_{e\_threshold}$
8	128	000 00000000 10000000	$T_{uon} < T_{on\,\min}$
9	256	000 00000001 00000000	$T_{uon} > T_{on\,\max}$
10	512	000 00000010 00000000	$T_{don} < T_{on\,\min}$
11	1024	000 00000100 00000000	$T_{don} > T_{on\,\max}$
12	2048	000 00000100 00000000	$\dfrac{T_{don} - T_{uon}}{T_{uon}} > \Delta T_{on\_threshold}$
13	4096	000 00010000 00000000	$S < S_{\min}$
14	8192	000 00100000 00000000	$S > S_{\max}$
15	16384	000 01000000 00000000	$l_v < l_{v\,\min}$
16	32768	000 10000000 00000000	$l_v > l_{v\,\max}$
17	65536	001 00000000 00000000	S loop false alarm
18	131072	010 00000000 00000000	M loop false alarm
19	262144	100 00000000 00000000	$T_{e\_1} = 0 \ or \ T_{e\_2} = 0$

CHAPTER 7   DATA ANALYSIS AND RESULTS

The effectiveness of the new dual-loop algorithm was evaluated by comparing the data calculated by applying the new dual-loop algorithm to those calculated by applying the current WSDOT dual-loop algorithm and video ground-truth data.

After developing a new dual-loop algorithm, a data collection site was selected to collect long duration detector event data. The new dual-loop algorithm was then applied to the collected event data to calculate individual vehicle data, such as vehicle arrival and departure times, vehicle speed and length, for each of the detected vehicles. Volume data obtained by applying the new dual-loop algorithm were compared to those calculated by the current WSDOT dual-loop algorithm for various time intervals. One-hour individual vehicle data calculated by the new dual-loop algorithm were compared to one-hour video ground-truth data to test the accuracy of the data collected. The results verified the effectiveness of the noise filter, the postprocessor, and the new dual-loop algorithm.

7.1   DATA COLLECTION

7.1.1   Loop Data Collection Site

According to a study [47] conducted by a researcher at Washington State University, the two most heavily used truck routes in King County are I-5 and State Route 167 (SR-167). SR-167, also known as the Valley Freeway, parallels I-5 through the Kent Valley between Puyallup and Interstate 405 (I-405). It receives an average of 907 trucks per day in summer and 702 per day in winter. Therefore, it was selected as a good candidate route for data collection for this research.

As requested by the Washington State Transportation Center (TRAC), the data collection site was located on the south end of SR-167. After comparing the performance among several dual-loop stations located along the south end of SR-167 as well as taking into account the availability of WSDOT video cameras, loop station ES-312D on SR-167, located at 34th Street NW in Auburn, was chosen as the data collection site. Figure 7-1 shows the location and a photograph of the data collection site. This particular freeway section has two GP lanes and one HOV lane in both the northbound and southbound directions. Each of the three lanes in both directions has a dual-loop detector installed in the pavement. There is a WSDOT traffic surveillance video camera located at 37th Street NW available for recording traffic.

7.1.2 Loop Data Collection

Loop detector event data were collected for more than three days from 3:00 p.m., November 20, 2003, to 10:00 a.m., November 24, 2003, from six dual-loop detectors: three in the northbound direction and three in the southbound direction. Traffic was recorded for four hours in the morning of November 21, 2003, using the WSDOT surveillance video camera. The weather was rainy on the day of data collection.

7.1.3 Ground-Truth Vehicle Length Data Collection

An ideal way of evaluating the accuracy of vehicle-length data calculated by applying the new dual-loop algorithm was to compare the calculated length of each detected vehicle to its true length. However, because of the shooting angle of the WSDOT surveillance camera, it was

unfeasible to measure the lengths of the vehicles in the camera's field-of-view. A different approach was needed to collect ground-truth vehicle length data.

Although vehicle lengths can't be measured when playing the videotape, types of vehicles, such as motorcycles, jeeps, passenger cars, pickup trucks, buses, trucks, etc., can be easily identified. For example, Volkswagen Beetles can be easily recognized on the videotape due to their unique shape. The true length of this type of vehicle can be easily obtained from their manufacturers or collected from parking lots. If there were some Volkswagen Beetles passing by the study site during the data collection period, the true length of this type of vehicle can be used to evaluate the accuracy of the length calculated by the new dual-loop algorithm. Therefore, vehicles that have a distinct shape and fixed length, or the variation of the length is less than 5% can be used to estimate the accuracy of the event-data-based length data.

Eleven types of vehicles with distinct shapes are identified in this research to be used to evaluate the accuracy of the calculated vehicle length data. These eleven types of vehicles include the following: motorcycle, Volkswagen Beetle, small jeep, passenger car, mini-van/Sport Utility Vehicle (SUV), small pickup, tractor, school bus, transit bus, dump truck/pup trailer combination, and car hauler. Appendix V has a photo of a representative vehicle for each of the eleven types. Of these eleven types of vehicles, Volkswagen Beetle, small jeep, tractor, school bus, transit bus, and car hauler are the ones with relatively fixed lengths. Passenger car, mini-van/SUV, small pickup, and dump truck/pup trailer combination are the ones with variable length, but the variation of the length is relatively

small. For convenience, the dump truck/pup trailer combination is referred to as dump-pup truck hereafter in this research.

7.2   DATA PROCESSING

Event data collected on November 21, 2003, were input to the new dual-loop algorithm to calculate 24-hour individual vehicle information, including individual vehicle arrival and departure times, speed, and vehicle length. The videotape provided by WSDOT with four hours of traffic recorded was digitized. Both the videotape and the digitized images were visually processed to obtain individual vehicle arrival times and vehicle class data in the northbound direction for one hour from 10:00 a.m. to 11:00 a.m. When classifying commercial vehicles, the Guide for Uniform Laws and Regulations Governing Truck Size and Weight among the WASHTO States [43] and Washington State Commercial Vehicle Guide [44] were used as two main references. These one-hour video data were used as video-ground-truth data in this research. Twenty-four hours of 20-second aggregated data collected on November 21, 2003, were also downloaded from the TDAD website.

7.3   EVALUATING THE EFFECTIVENESS OF THE NEW DUAL-LOOP ALGORITHM IN COUNTING VEHICLES

7.3.1   One-Hour Volume Comparison

In order to evaluate the effectiveness of the new dual-loop algorithm in counting vehicles, loop detector event data collected from 10:00 a.m. to 11:00 a.m. on November 21, 2003, were processed to get one-hour single-loop and dual-loop volumes. One-hour TDAD-based single-loop and dual-loop volumes were also downloaded for comparison purposes. These

two sets of one-hour volume data, together with the one-hour video-ground-truth volume data are summarized in Table 7-1. The event-data-based and TDAD-based single-loop volume data were each then compared to the video-ground-truth volume data to calculate over-count rates for each of the three lanes. The results are summarized in Table 7-2.

7.3.1.1 Single-Loop Volume Comparison

Table 7-1 shows that the event-data-based one-hour single-loop volume was almost equal to the video-ground-truth one-hour volume for each of the two GP lanes. During this one-hour period, the M and S loops on Lane 1 only over counted one and four vehicles respectively. The M loop on Lane 2 correctly counted all the passing vehicles, while the S loop only over-counted two vehicles. The M and S loops on the HOV lane correctly counted all the passing vehicles. As can be seen in Table 7-2, the highest event-data-based over-count rate was only 0.32% during this one-hour period.

In contrast to the event-data-based single-loop volumes, shown in Table 7-1, the TDAD-based one-hour single-loop volumes were consistently higher than the video-ground-truth volumes. The M and S loops on Lane 1 over-counted 46 and 53 vehicles, respectively. The M and S loops on Lane 2 over-counted 61 and 71 vehicles, respectively. The M and S loops on the HOV lane over-counted 16 and 13 vehicles, respectively. As can be seen in Table 7-2, the over-count rate ranged from 3.65% to 4.79%, which was much higher than the event-data-based over-count rate.

The difference between event-data-based single-loop over-count rates and TDAD-based over-count rates were calculated and the results were also summarized in Table 7-2. The over-count rate reductions indicated that the noise filter and the postprocessor

effectively filtered out noise and corrected raw loop actuation signals when processing this one-hour period of event data.

The TDAD-based single loop's over-count problem is, to a great extent, caused by positive false alarms. As previously defined in Chapter 5, a single loop's positive false alarm means the single loop detects the presence of a vehicle when in fact there is no vehicle present.

7.3.1.2 Dual-Loop Volume Comparison

One-hour event-data-based dual-loop volume and one-hour TDAD-based dual-loop volume were each compared to the one-hour video-ground-truth volume to calculate the undercount rate for each of the three lanes. The results are summarized in Table 7-3.

As shown in Table 7-3, during this one-hour period, the number of passing vehicles and each individual vehicle's arrival time, calculated by applying the new dual-loop algorithm using event data, exactly matched that of video-ground-truth data except for one occasion when a dump-pup truck (the combination of a dump truck and a pup trailer), shown in Figure 7-2, was counted as two vehicles by the new dual-loop algorithm due to too little metal in the long drawbar that connected the dump truck and the pup trailer so that the loop shuts off, indicating the end of the dump truck, prior to the pup trailer's arriving.

The TDAD-based dual-loop volumes, in contrast, consistently undercounted vehicles that passed the detector zone during the one-hour period. The dual-loop detectors on Lanes 1, 2, and HOV undercounted 93, 146, and 14 vehicles, respectively. The undercount rate was as high as 9.22%. These results proved that the new dual-loop

algorithm was able to improve the detection rate of the dual-loop detectors for this one-hour period.

Based on the results described above, the one-hour TDAD-based volumes (both single-loop and dual-loop volumes) and event-data-based volumes (both single-loop and dual-loop volumes) were sorted by magnitude in descending order as follows:

$$V_M \text{ (or } V_S) \geq V_{EM} \text{ (or } V_{ES}) \geq V_{ET} \geq V_T$$

Where,

V_M = TDAD-based M loop volume

V_S = TDAD-based S loop volume

V_T = TDAD-based dual-loop volume

V_{EM} = Event-data-based M loop volume

V_{ES} = Event-data-based S loop volume

V_{ET} = Event-data-based dual-loop volume

In summary, the noise filter, the postprocessor, and the improved dual-loop algorithm considerably reduced the single-loop positive false alarm rate and noticeably improved the dual-loop detector detection rate for this one-hour period. These enhancements significantly improved the performance of both single-loop and dual-loop detectors for counting vehicles.

7.3.2 Twenty-Four-Hour Volume Comparison

In order to catch most of the differences between event-data-based volume and TDAD-based volume, these two sets of data were compared for an entire day. Twenty-four hours of volumes calculated using event data collected on November 21, 2003, were compared to those downloaded from the TDAD website. The comparison results are summarized in Table 7-4.

As shown in Table 7-4, for each of the three lanes, TDAD-based M and S loops were consistently detecting more vehicles than the T loop. This result was not surprising since normally the single loops tend to over-count vehicles, whereas the dual loops tend to undercount vehicles. For each of the three lanes, the 24-hour volume collected by the M loop was very close to that collected by the S loop (difference less than 1%). From these results, it seemed that the M and S loops were in good working order during the 24-hour data collection period.

However, when compared to the 24-hour volume calculated from event data, one found that the single-loop (M or S) volume calculated using event data was considerably higher than that collected by the TDAD single loop (M or S) for each of the three lanes. The percentage differences between these two sets of volumes were calculated and the results are summarized in Table 7-5. As can be seen in Table 7-5, the differences in percentage ranged from 10.56% to 13.94%. These results conflicted with the ones shown in Section 7.3.1 that TDAD-based single-loop volumes were higher than those calculated using event data. As mentioned previously, the TDAD-based M and S loops seemed to be in good working order; so the question became what might have caused this discrepancy.

By examining the collected raw loop detector event data and the 20-second aggregated data downloaded from TDAD website, it was discovered that the TDAD-based single loops and dual loops did not detect any of the passing vehicles from midnight to 6:29:13 a.m. As shown in Table 7-6, during this period, all data entries were zeros in the TDAD-based volume field while the event data showed the presence of vehicles in each of the three lanes. In other words, the TDAD-based volumes were missing volume data for more than six hours. This explained why the 24-hour volumes detected by TDAD-based single-loop detectors (M and S) were lower than those calculated using event data.

Since the laptop-based DEDAC system actually detected the presence of vehicles in the 6.5-hour period, the three dual-loop detectors were not stuck in the "off" state. The cause of the loop detection system's malfunction at this particular location needed further investigation.

In order to make the event-data-based volume and TDAD-based volume comparable, event-data-based volume was calculated for the 17.5-hour period from 6:29:13 a.m. to 11:59:59 p.m. for each of the three lanes. Volumes and comparison results were summarized in Tables 7-7 and 7-8. As can be seen in Table 7-7, event-data-based single-loop volume was lower than the TDAD-based single-loop volume for each of the three lanes. The difference, shown in Table 7-8, ranged from 3.77% to 5.40%. The event-data-based dual-loop volume was higher than the TDAD-based dual-loop volume for each of the three lanes. The 24-hour volume comparison results further showed that the noise filter and the postprocessor reduced the single-loop over-count rates and the new dual-loop algorithm increased the dual-loop detection rate.

7.4 EVALUATING THE EFFECTIVENESS OF THE NEW DUAL-LOOP ALGORITHM IN MEASURING VEHICLE LENGTH

As mentioned previously, one-hour video data were processed to obtain individual vehicle arrival time and vehicle type. The observed individual vehicle information was then compared to the event-data-based individual vehicle information for the same one-hour period. The accuracy of the event-data-based vehicle length data was then evaluated using the vehicle length data collected for the identified eleven types of vehicles. The mean length and standard deviation of these eleven types of vehicles are summarized in Tables 7-9 and 7-10.

In Table 7-9, mean vehicle length and standard deviation were calculated using samples with no error flags. In Table 7-10, mean vehicle length and standard deviation were calculated using all the samples regardless of error flags. One can find from a rough comparison of these two sets of data that, for most of the vehicle classes, the mean calculated using all the samples belonging to a class regardless of error flags was slightly greater than that calculated only using samples without error flags. This might indicate that when a flag occurs the measured length of the subject vehicle tends to be greater than when there is no flag.

7.4.1.1 Motorcycle

Only one motorcycle passed over the data collection site during the one-hour period. It was detected without error flags. The calculated speed of the motorcycle was 72.44 miles per hour and the calculated length was 5.90 feet. It was observed from the videotape that the motorcycle was indeed traveling at a speed faster than that of other vehicles on the roadway

segment at that moment. It was extremely difficult to get the length of this motorcycle because it was impossible to get the information such as its model and manufacturer by observing the videotape. However, according to the information released by some motorcycle manufacturers, the wheel-based length of a regular motorcycle ranges from 4.76 feet to 5.74 feet, so the overall length of a regular motorcycle should not be longer than 8.20 feet. In addition, ground-truth motorcycle length data collected during the research showed that the length of a regular motorcycle was about 7.00 feet. So the calculated length of 5.90 feet fell in the valid range, but was slightly shorter than its true length.

7.4.1.2 Volkswagen Beetle

There were six Volkswagen Beetles traversing the detector zone during the one-hour period. All of them were detected without error flags. According to the information posted on the Volkswagen manufacturer's website, the length of a Beetle is 13.50 feet. Ground-truth length data collected during the research verified that the length of the Beetles was 13.50 feet. The calculated length of the three Beetles that passed over Lane 1 ranged from 11.00 to 11.02 feet. The mean was 11.01 feet and the standard deviation was 0.01 feet. The calculated length of the other three Beetles that passed over Lane 2 ranged from 12.51 to 12.55 feet. The mean was 12.52 feet and the standard deviation was 0.02 feet. The results showed that the dual-loop detectors underestimated the length of these Volkswagen Beetles by 1.00 to 2.50 feet.

7.4.1.3 Short Jeep

There were eleven small jeeps traversing the data collection site during the one-hour period. One of the small jeeps that passed over Lane 2 was detected with error flags. The calculated lengths of the two short jeeps that passed over Lane 1 were 9.85 and 9.58 feet, respectively. The mean was 9.71 feet and the standard deviation was 0.19 feet. The calculated length of the six short jeeps that passed over Lane 2 ranged from 9.45 to 12.40 feet. The mean was 10.42 feet and the standard deviation was 1.26 feet. The calculated length of the three short jeeps that passed over Lane HOV ranged from 9.45 to 13.80 feet. The mean was 11.44 feet and the standard deviation was 2.22 feet. Ground-truth length data collected in the research indicated that the length of the small jeeps ranged from 11.70 to 13.50 feet. The results showed that the dual-loop detectors on Lane 1 underestimated the length of small jeeps by about 1.50 feet. The dual-loop detectors on Lane 2 and Lane HOV seemed to measure the length of small jeeps with acceptable accuracy.

7.4.1.4 Passenger Car

There were 1280 passenger cars passing the detector zone during the one-hour period, of which 1202 were detected without error flags. If only considering passenger cars detected without error flags, the calculated mean passenger-car length was 13.75 feet (standard deviation 1.42 feet), 13.88 feet (standard deviation 1.35 feet), and 14.68 feet (standard deviation 1.58 feet), for Lane 1, Lane 2, and Lane HOV, respectively. By adding in the passenger cars detected with error flags, the mean length slightly increased by 0.09 to 0.33 feet. According to the ground-truth data collected in the research, the length of a passenger car ranged from 11.00 to 19.00 feet, and the majority of the cars were longer than 15.00 feet.

Therefore, the results indicated that the dual-loop detectors slightly underestimated the length of passenger cars in that one-hour period.

7.4.1.5 Mini-Van and SUV

There were 951 mini-vans and SUVs traversing the detector zone during the one-hour period, of which 807 were detected without error flags. Considering only vehicles detected without error flags, the calculated mean length of the two types of vehicles was 15.16 feet (standard deviation 2.95 feet), 14.78 feet (standard deviation 2.25 feet), and 15.87 feet (standard deviation 2.02 feet), for Lane 1, Lane 2, and Lane HOV, respectively. By adding in the vehicles detected with error flags, the mean length slightly increased by about 0.42 to 0.61 feet. According to vehicle length information released by auto manufacturers and ground-truth length data collected in the research, the majority of these two types of vehicles are longer than 16.00 feet. Therefore, the dual-loop detectors slightly underestimated the length of mini-vans and SUVs during the one-hour period.

7.4.1.6 Pickup Truck

There were 461 pickup trucks traversing the detector zone during the one-hour period, of which 405 were detected without error flags. Considering only pickup trucks detected without error flags, the calculated mean length was 15.86 feet (standard deviation 1.88 feet), 15.34 feet (standard deviation 2.00 feet), and 16.76 feet (standard deviation 2.30 feet) for Lane 1, Lane 2, and Lane HOV, respectively. By adding in the pickup trucks detected with error flags, the mean length slightly increased by 0.30 to 0.81 feet. According to ground-truth length data collected in the research, the length of a pickup truck ranges from 15.40 feet to

19.80 feet. So the dual-loop detectors slightly underestimated the length of pickup trucks during the one-hour period.

7.4.1.7 Tractor

There were 19 tractors (twelve on Lane 1 and seven on Lane 2) traversing the detector zone during the one-hour period; all of them were detected without error flags. The average length of the tractors was 21.14 feet (standard deviation 3.70 feet) and 22.19 feet (standard deviation 3.11 feet), for Lane 1 and Lane 2, respectively. According to ground-truth tractor length data collected at the Port of Seattle, the length of a tractor ranges from 19.40 to 27.40 feet. Most of the tractors were longer than 23.00 feet. Therefore, the length of the tractors that passed over the detector zone was slightly underestimated.

7.4.1.8 School Bus

There were only two school buses traversing the detector zone on Lane 1 during the one-hour period, both were detected with error flags. The two school buses differed in size. The smaller school bus was detected as 24.96 feet long and the larger one was detected as 41.96 feet long. According to school bus dimension information released by school bus manufacturers and the ground-truth school bus length data collected at a school bus parking lot, the length of the smaller school bus should be between 20.00 and 25.00 feet. The length of the large school bus should be between 35.00 and 40.00 feet. The dual-loop-measured lengths of these two school buses were approximately equal to their true lengths.

7.4.1.9 <u>Transit Bus</u>

There were three transit buses traversing the detector zone on Lane 1 during the one-hour period, two of which were detected without error flags. According to the information posted on the Metro website, the length of regular transit buses is 40.00 feet. The ground-truth length of a regular transit bus collected at a bus stop was 41.50 feet. The calculated length of the two buses detected with no error flags was 39.17 and 41.75 feet, respectively. The results indicated that the calculated length for each of the two buses was very close to its true length and the dual-loop detector on Lane 1 correctly measured the length of the buses.

The length of the transit bus detected with error flags was 45.65 feet, which was 5.65 feet longer than the length of a regular transit bus. The flag code was 2112, which was the sum of flag code 64 (error type 7) and flag code 2048 (error type 12). The two errors indicated that when the length of transit bus was calculated, the two elapsed times differed by more than 10% and so did the two on-times.

7.4.1.10 <u>Dump-Pup Trucks</u>

There were 33 dump-pup trucks traversing the detector zone during the one-hour period, of which 18 passed over Lane 1 and 15 passed over Lane 2. Of the 18 vehicles that passed over Lane 1, one was mistakenly read as two vehicles due to too little metal in the long drawbar. According to the ground-truth data collected at a construction site during the research, the length of the dump-pup trucks could be as long as 70.00 to 75.00 feet when the drawbar between the dump truck and the pup trailer is fully extended. The fully extended drawbar could be as much as 15.00 feet longer than its original contracted length. So the length of the entire dump-pup trucks could be as short as 55.00 to 60.00 feet.

Of the 32 dump-pup trucks, 27 (14 on Lane 1 and 13 on Lane 2) were detected with no error flags, five (three on Lane 1 and two on Lane 2) with error flags. On Lane 1, the length measured without error flags ranged from 62.00 feet to 74.72 feet and the average was 70.59 feet. On Lane 2, the length measured without error flags ranged from 62.00 feet to 79.19 feet and the average was 69.34 feet. The range of the measured length spanned from 62.00 feet to 79.19 feet. The results were not surprising because drawbars are extendible. In summary, the measured length of the dump-pup trucks fell in the reasonable range. For Lane 1, if adding in the vehicles detected with error flags, the average length increased slightly. For Lane 2, by adding in the vehicles detected with error flags, the average length decreased slightly.

7.4.1.11 Car Hauler

There were eight car haulers traversing the detector zone during the one-hour period, of which seven passed over Lane 1 and one passed over Lane 2. They were all detected without error flags. According to the ground-truth length data collected during the research, the length of a regular car hauler with a capacity of ten passenger cars was 75.00 feet. The car haulers that passed over Lane 1 all have a capacity of ten cars. The detected length of these car haulers ranged from 70.29 feet to 81.62 feet and the standard deviation is 3.90 feet. It was difficult to tell from the videotape whether or not the car hauler detected as 81.62 feet long was longer than the one detected as 70.29 feet, due to the shooting angle of the WSDOT surveillance camera; thus no further evaluation was conducted. Nonetheless, the results showed the measured length of the car haulers on Lane 1 fell in the reasonable range.

The car hauler that passed over Lane 2 had a capacity of five cars. The measured length of this car hauler was 61.43 feet. The accuracy of the measured length was not evaluated because the ground-truth length data were not collected for car haulers with a capacity of five cars. One can find from processing the videotape that the car hauler with a capacity of five cars was noticeably shorter than that with a capacity of ten cars.

7.5 EVALUATING THE EFFECTIVENESS OF THE NEW DUAL-LOOP ALGORITHM IN CLASSIFYING VEHICLES

In order to evaluate how accurately the new dual-loop algorithm classifies vehicles, one-hour video-based vehicle classification data were compared to the same one-hour event-data-based vehicle classification data. The length ranges used by the current WSDOT dual-loop algorithm to classify vehicles into one of four bins were also adopted to classify observed vehicles when processing the video data to classify vehicles detected by the new dual-loop algorithm. When observing the video, if the author was <u>certain</u> about the bin class of an observed vehicle, the vehicle was assigned to that bin; if the author was not certain about the bin class of a vehicle because the length of the vehicle was close to one of the bin threshold values, the vehicle was dropped from the ground-truth sample. In other words, only vehicles classified by the author with confidence (based on the ground-truth sample) were used to evaluate the accuracy of vehicle classification data calculated by the new dual-loop algorithm.

Event-data-based vehicle classification data were compared to the video-based vehicle classification data. The results are summarized in Table 7-11. As shown in this table, 1144 (91% of the total number of vehicles that passed Lane 1), 1519 (96% of the total number of vehicles that passed Lane 2), and 328 (98% of the total number of vehicles that

passed Lane HOV) vehicles that passed Lane 1, Lane 2, and Lane HOV respectively were classified into bins when manually processing the video ground-truth data. The selected samples accounted for an overwhelming majority of the vehicles that passed the dual-loop detection zone during that one-hour period and these samples were used to evaluate the accuracy of the new dual-loop algorithm and the current WSDOT algorithm. Of these vehicles, all but the dump-pup truck previously mentioned were classified into the same bins as the ground-truth sample by the new dual-loop algorithm for all three lanes.

In order to evaluate how much the new dual-loop algorithm improved the quality of the vehicle classification data, the one-hour TDAD-based aggregated data were also examined to identify the vehicles that were correctly classified by the current WSDOT dual-loop algorithm. The results are also summarized in Table 7-11. As shown in this table, the WSDOT dual-loop algorithm correctly classified the majority of the vehicles for each of the three lanes. For Bin1, more than 90% of the vehicles were correctly classified. For Bin2, 77% and 58% of the vehicles were correctly classified for Lane 1 and Lane 2, respectively. For Bin3, 80% and 70% of the vehicles were correctly classified for Lane 1 and Lane 2, respectively. For Bin4, 83% and 67% of the vehicles were correctly classified for Lane 1 and Lane 2, respectively.

By comparing the number of vehicles that were correctly classified by the new dual-loop algorithm to that by the current WSDOT dual-loop algorithm, one can find that the new dual-loop algorithm correctly classified significantly more vehicles than the current WSDOT dual-loop algorithm, especially Bin2, Bin3, and Bin4 vehicles where the new algorithm correctly classified up to 42% more vehicles than the current WSDOT algorithm.

It can be concluded from the above results that the new dual-loop algorithm correctly classified the overwhelming majority of the vehicles that were classified into bins when processing the video data for this one-hour period. The new dual-loop algorithm considerably increased the capability of dual-loop detectors to accurately classify vehicles.

7.6   ERROR TYPES AND THEIR FREQUENCIES

In this research, nineteen error types were defined to catch all possible errors that may occur during the dual-loop detection process. Errors occurred after preprocessing and their occurrence frequencies for one-hour, twenty-four hours, and three days are summarized in Tables IV-1, IV-2, and IV-3 in Appendix IV. As can be seen in these three tables, the overwhelming majority of the errors consisted of three error types including types 5, 7, and 12. Error Type 5 means that the second elapsed time is shorter than the minimum elapsed time. This type of error accounted for about 15% of total errors. Error Type 7 means that the percentage difference between the two elapsed times is greater than the threshold value, 10%. This type of error accounted about 42% of total errors. Error Type 12 means the percentage difference between the upstream loop and the downstream loop is greater than the threshold value, 10%. This type of error accounted for about 40% of total errors.

In addition, the one-hour data analysis showed that if the vehicles detected with error flags were taken away from the total count, a substantial amount of the passing vehicles would not be counted. In the northbound direction, 12.6% of the passing vehicles on Lane 1, 13.5% on Lane 2, and 8.4% on Lane HOV were detected with errors flagged. In the southbound direction, 12.2% of the passing vehicles on Lane 1, 10.5% on Lane 2, and 24.4% on Lane HOV were detected with errors flagged. Therefore, keeping the vehicles

detected with error flags in the total count considerably improved the capability of the dual-loop detector to count vehicles.

7.6.1 Error Types and Vehicle Classes

To find out what types of vehicles tend to induce error flags, errors were summarized with respect to vehicle types for the one-hour period for which video-ground-truth data were obtained and the results are included in Table 7-12 and visually presented in Figure 7-3.

On Lane 1, 47.4% of the errors occurred on trucks and 32.0% of the errors occurred on mini-vans or SUVs. The results indicated that trucks, mini-vans, and SUVs are the types of vehicles on which errors are more likely to occur.

On Lane 2, 37.2% of the errors occurred on Mini-Vans or SUVs, 26.1% of the errors occurred on passenger cars, 20.5% of the errors occurred on pickup trucks, and 15.8% of the errors occurred on trucks. The results may seem inconsistent with what was concluded according to the results from Lane 1 in that the proportion of total errors occurring for trucks on Lane 2 was half of that occurring for trucks on Lane 1. However, when taking into account the fact that the truck volume on Lane 2 was half of the truck volume on Lane 1 and the total traffic volume on Lane 2 was 1.5 times higher than that on Lane 1, trucks were still the type of vehicles most likely to induce error flags.

This conclusion became more convincing when summarizing the error occurrence frequencies with respect to vehicle classes classified based on vehicle length. All the vehicles detected during the one-hour period were classified into four bins according to their lengths, with vehicles in Bin1 shorter than or equal to 26 feet, vehicles in Bin2 longer than 26 feet but shorter than or equal to 39 feet, vehicles in Bin3 longer than 39 feet and shorter than or equal to 65 feet, and vehicles in Bin4 longer than 65 feet. Table 7-13 has the summary of the

results and Figure 7-4 visually shows the comparison of percentage of vehicles detected with errors among four bins for the two GP lanes.

As shown in Table 7-13 and Figure 7-4, for the two GP lanes, the overwhelming majority of the Bin4 vehicles were detected with error flags, the majority of the Bin3 vehicles were detected with error flags, and about half of the Bin2 vehicles were detected with error flags. It can be concluded that the longer the vehicle the more possible that the vehicle is detected with error flags. Since most of the trucks fall in Bin3 and Bin4 and Bin3 and Bin4 vehicles are more likely to induce error flags, it is justifiable to conclude that trucks are more likely to induce error flags when they are detected by dual-loop detectors.

7.7 DATA ANALYSIS SUMMARY

The data analysis results can be summarized as follows:

1. Single-loop detectors' positive false alarm rates were reduced considerably after applying a noise filter and a postprocessor. This indicated that the noise filter and the postprocessor can effectively filter out a tremendous amount of noise that would otherwise be counted as vehicles.

2. The new dual-loop algorithm kept vehicle information detected with error flags in the total count. This considerably improved the capability of dual-loop detectors to count vehicles and detect trucks.

3. For most of the vehicle classes, the average vehicle length calculated using all the samples belonging to a class regardless of error flags was slightly longer than that calculated using only samples without error flags.

4. The three dual-loop detectors in the study tended to slightly underestimate the length of short vehicles such as Volkswagen Beetles, short jeeps, passenger cars, SUVs, mini-vans, pickup trucks, and tractors.

5. The three dual-loop detectors in the study estimated the lengths of transit buses with satisfactory accuracy.

6. The three dual-loop detectors in the study estimated the lengths of dump-pup trucks with satisfactory accuracy except for one occasion when a dump-pup truck was counted separately as a single-unit truck and a trailer.

7. The new dual-loop algorithm worked very well when classifying vehicles into four bins if the lengths of the vehicles were not close to the bin threshold values. The new dual-loop algorithm correctly classified significantly more vehicles than the current WSDOT dual-loop algorithm, especially Bin2, Bin3, and Bin4 vehicles

8. The overwhelming majority of the errors consisted of three error types including Type 5, Type 7, and Type 12. Error Type 5 means that the second elapsed time is

shorter than the minimum elapsed time. Error Type 7 means that the percentage difference between the two elapsed times is greater than the threshold value. Error Type 12 means that the percentage difference between the on-time of the upstream loop and that of the downstream loop is greater than the threshold value. These three types of errors are primarily caused by the large sensitivity discrepancy between the paired single-loop detectors.

9. Bin3 and Bin4 vehicles are more likely to induce error flags and most of the trucks fall in these two bins; it is justifiable to conclude that trucks are more likely to induce error flags when they are detected by dual-loop detectors.

Schematic of the Data Collection Site
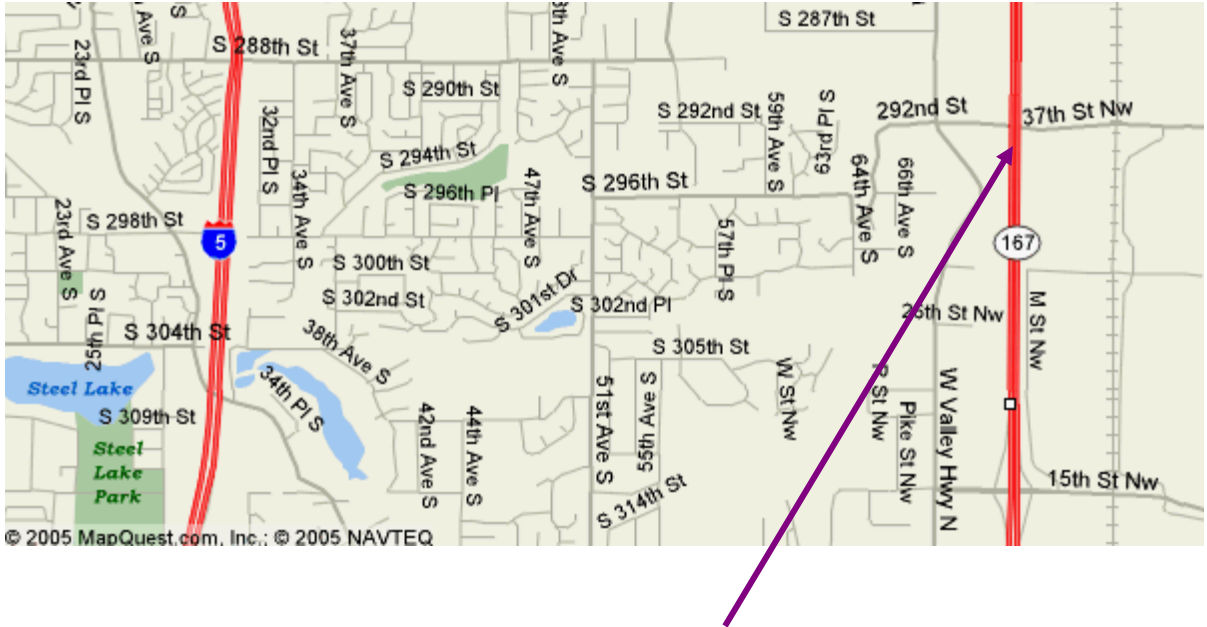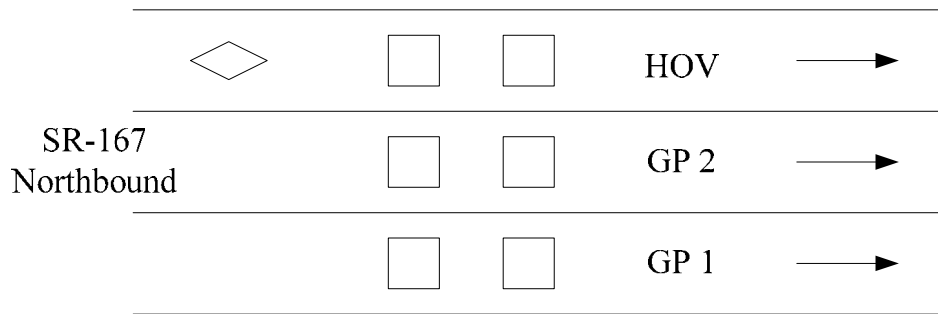

Figure 7-1. Data Collection Site (ES-312D on SR-167 at 34th Street NW)

Figure 7-2. The Misclassified Dump-Pup Truck

Lane 1: Vehicle Class vs. Error Type

Lane 2: Vehicle Class vs. Error Type

HOV Lane: Vehicle Class vs. Error Type
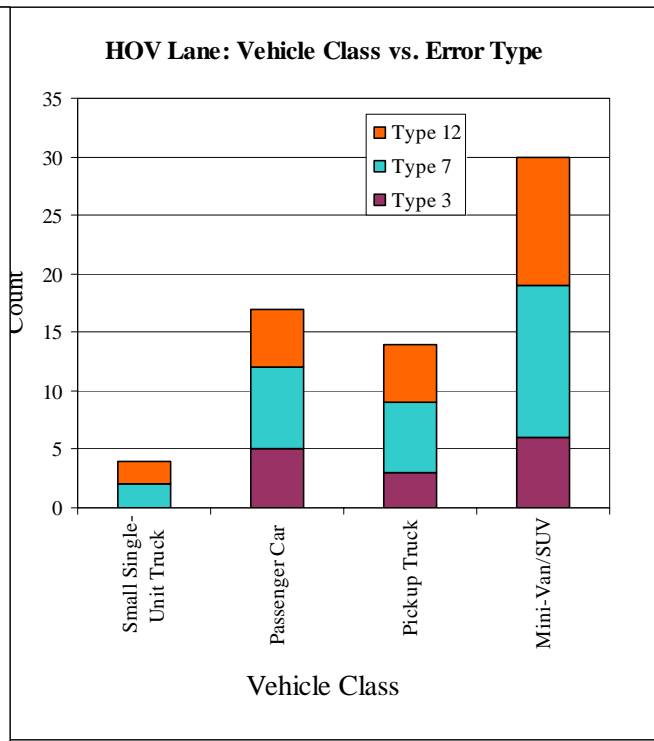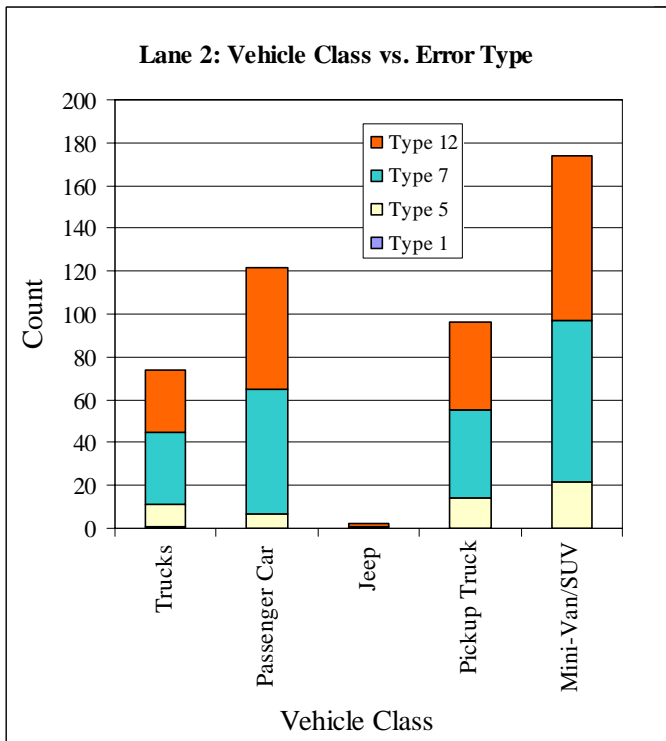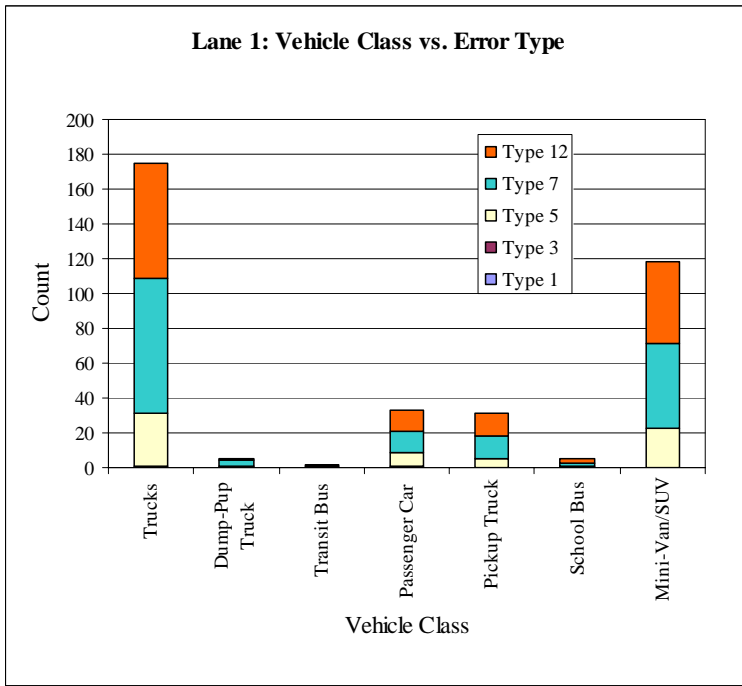
Figure 7-3. Vehicle Classes vs. Error Type
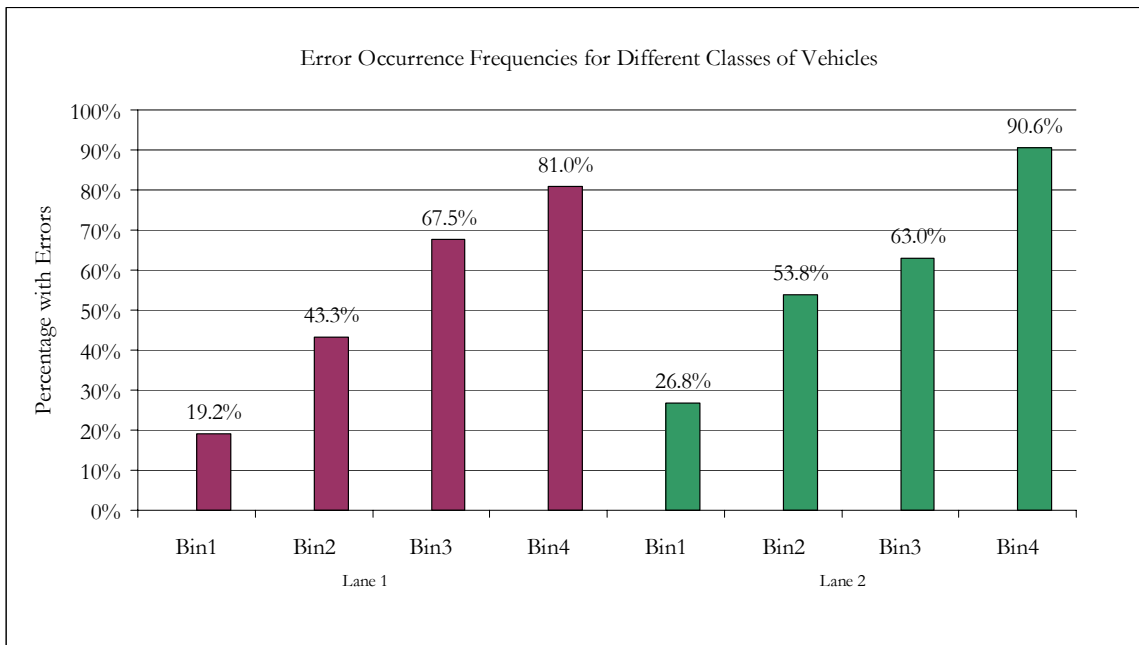
Figure 7-4. Error Occurrence Frequencies for Different Classes of Vehicles

Table 7-1. Single-Loop and Video-Ground-Truth Volumes (One Hour)

Lane No	TDAD-Based		Event-Data-Based		Video-Ground-Truth
	V_M	V_S	V_{EM}	V_{ES}	V_v
Lane 1	1308	1315	1263	1266	1262
Lane 2	1644	1654	1583	1585	1583
HOV	350	347	334	334	334

V_M = TDAD-based M loop volume

V_S = TDAD-based S loop volume

V_{EM} = Event-data-based M loop volume

V_{ES} = Event-data-based S loop volume

V_V = Video-ground-truth volume

Table 7-2. Single-Loop Over-Count Rates (One Hour)

Lane No	TDAD-Based		Event-Data-Based		Over-Count Rate Reduction	
	M loop $\dfrac{V_M - V_V}{V_V}$	S loop $\dfrac{V_S - V_V}{V_V}$	M loop $\dfrac{V_{EM} - V_V}{V_V}$	S loop $\dfrac{V_{ES} - V_V}{V_V}$	M loop $\dfrac{V_M - V_{EM}}{V_V}$	S loop $\dfrac{V_S - V_{ES}}{V_V}$
Lane 1	3.65%	4.19%	0.08%	0.32%	3.57%	3.87%
Lane 2	3.85%	4.49%	0.00%	0.13%	3.85%	4.36%
Lane HOV	4.79%	3.89%	0.00%	0.00%	4.79%	3.89%

V_M = TDAD-based M loop volume

V_S = TDAD-based S loop volume

V_{EM} = Event-data-based M loop volume

V_{ES} = Event-data-based S loop volume

V_V = Video-ground-truth volume

Table 7-3. Dual-Loop Undercount Rates (One Hour)

Lane No	V_T	V_{ET}	V_V	$\dfrac{V_T - V_V}{V_V}$	$\dfrac{V_{ET} - V_V}{V_V}$
Lane 1	1169	1263	1262	-7.37%	0.08%
Lane 2	1437	1583	1583	-9.22%	0.00%
Lane HOV	320	334	334	-4.19%	0.00%

V_T = TDAD-based dual-loop volume

V_{ET} = Event-data-based dual-loop volume

V_V = Video-ground-truth volume

Table 7-4. Summary of 24-Hour TDAD-Based and Event-Data-Based Volumes

Lane No	TDAD-Based			Event-Data-Based		
	V_M	V_S	V_T	V_{EM}	V_{ES}	V_{ET}
Lane 1	20357	20504	18014	23655	23655	23626
Lane 2	23813	23936	21096	27468	27461	27439
HOV	6867	6807	6245	7678	7676	7673

V_M = TDAD-based M loop volume

V_S = TDAD-based S loop volume

V_T = TDAD-based dual-loop volume

V_{EM} = Event-data-based M loop volume

V_{ES} = Event-data-based S loop volume

V_{ET} = Event-data-based dual-loop volume

V_V = Video-ground-truth volume

Table 7-5. TDAD-Based and Event-Data-Based 24-Hour Volumes Comparison

Lane No	$(V_M - V_{EM})/\ V_{EM}$	$(V_S - V_{ES})/\ V_{ES}$	$(V_T - V_{ET})/\ V_{ET}$
Lane 1	-13.94%	-13.32%	-23.75%
Lane 2	-13.31%	-12.84%	-23.12%
HOV	-10.56%	-11.32%	-18.61%

V_M = TDAD-based M loop volume

V_S = TDAD-based S loop volume

V_T = TDAD-based dual-loop volume

V_{EM} = Event-data-based M loop volume

V_{ES} = Event-data-based S loop volume

V_{ET} = Event-data-based dual-loop volume

V_V = Video-ground-truth volume

Table 7-6. TDAD-Based and Event-Data-Based Volumes (12:00 a.m. to 6:29 a.m.)

Lane No	TDAD-Based			Event-Data-Based		
	V_M	V_S	V_T	V_{EM}	V_{ES}	V_{ET}
Lane 1	0	0	0	4046	4049	4045
Lane 2	0	0	0	4521	4519	4516
HOV	0	0	0	1163	1163	1163

V_M = TDAD-based M loop volume

V_S = TDAD-based S loop volume

V_T = TDAD-based dual-loop volume

V_{EM} = Event-data-based M loop volume

V_{ES} = Event-data-based S loop volume

V_{ET} = Event-data-based dual-loop volume

Table 7-7. TDAD-Based and Event-Data-Based Volumes (6:29a.m. to 11:59 p.m.)

Lane No.	TDAD-Based			Event-Data-Based		
	V_M	V_S	V_T	V_{EM}	V_{ES}	V_{ET}
Lane 1	20357	20504	18014	19609	19606	19581
Lane 2	23813	23936	21096	22947	22942	22923
HOV	6867	6807	6245	6515	6513	6510

V_M = TDAD-based M loop volume

V_S = TDAD-based S loop volume

V_T = TDAD-based dual-loop volume

V_{EM} = Event-data-based M loop volume

V_{ES} = Event-data-based S loop volume

V_{ET} = Event-data-based dual-loop volume

Table 7-8. TDAD-Based and Event-Data-Based 18-Hour Volumes Comparison

Lane No.	$(V_M-V_{EM})/V_{EM}$	$(V_S-V_{ES})/V_{ES}$	$(V_T-V_{ET})/V_{ET}$
Lane 1	3.81%	4.58%	-8.00%
Lane 2	3.77%	4.33%	-7.97%
HOV	5.40%	4.51%	-4.07%

V_M = TDAD-based M loop volume

V_S = TDAD-based S loop volume

V_T = TDAD-based dual-loop volume

V_{EM} = Event-data-based M loop volume

V_{ES} = Event-data-based S loop volume

V_{ET} = Event-data-based dual-loop volume

Table 7-9. Calculated Mean Lengths for Eleven Types of Vehicles (No Error Flags)

Lane No		Motorcycle	Beetle	Short Jeep	Passenger Car	Van/SUV	Pickup	Tractor	School Bus	Transit Bus	Construction Vehicle	Car Hauler
Lane 1	Count	0	3	2	390	298	165	12	0	2	14	7
	Mean	----	11.01	9.71	13.75	15.16	15.86	21.14	---	39.96	70.59	75.17
	Std Dev	----	0.01	0.19	1.42	2.95	1.88	3.70	---	1.12	3.03	3.90
Lane 2	Count	0	3	5	670	396	201	7	0	0	13	1
	Mean	----	12.52	10.42	13.88	14.78	15.34	22.19	----	----	69.34	61.43
	Std Dev	----	0.02	1.26	1.35	2.25	2.00	3.11	----	----	5.72	----
HOV	Count	1	0	3	142	113	39	0	0	0	0	0
	Mean	5.90	----	11.44	14.68	15.87	16.76	----	----	----	----	----
	Std Dev	----	----	2.22	1.58	2.02	2.30	----	----	----	----	----

Table 7-10. Calculated Mean Lengths for Eleven Types of Vehicles (with Error Flags)

Lane No		Motorcycle	Beetle	Short Jeep	Passenger Car	Van /SUV	Pickup	Tractor	School Bus	Transit Bus	Construction Vehicle	Car Hauler
Lane 1	Count	0	3	2	402	346	178	12	2	3	17	7
	Mean	----	11.01	9.71	13.84	15.76	16.16	21.14	33.44	41.86	71.36	75.17
	Std Dev	----	0.01	0.19	1.67	3.28	2.20	3.70	11.99	3.38	3.73	3.90
Lane 2	Count	0	3	6	729	478	238	7	0	0	15	1
	Mean	----	12.52	10.05	14.21	15.39	16.15	22.19	----	----	69.90	61.43
	Std Dev	----	0.02	1.46	1.95	2.75	2.83	3.11	----	----	5.49	----
HOV	Count	1	0	3	149	127	45	0	0	0	0	0
	Mean	5.90	----	11.44	14.85	16.29	17.40	----	----	----	----	----
	Std Dev	----	----	2.22	1.81	2.52	2.74	----	----	----	----	----

Table 7-11. One-Hour Vehicle Classification Data

Bin No.	Lane 1					Lane 2					Lane HOV				
	V_V	V_E	V_T	$\frac{V_E}{V_V}$	$\frac{V_T}{V_V}$	V_V	V_E	V_T	$\frac{V_E}{V_V}$	$\frac{V_T}{V_V}$	V_V	V_E	V_T	$\frac{V_E}{V_V}$	$\frac{V_T}{V_V}$
Bin1	973	973	914	100%	94%	1463	1463	1326	100%	91%	328	328	306	100%	93%
Bin2	39	39	30	100%	77%	12	12	7	100%	58%	0	0	0	----	----
Bin3	44	44	35	100%	80%	20	20	14	100%	70%	0	0	0	----	----
Bin4	88	87	73	99%	83%	24	24	16	100%	67%	0	0	0	----	----
Subtotal	1144	1143	1052	99.9%	92.0%	1519	1519	1363	100.0%	89.7%	328	328	306	100%	93.3%

V_v = Number of vehicles that were classified into bins when processing the videotape
V_E = Number of vehicles that were classified into the same bins by the new dual-loop algorithm and by processing the videotape
V_T = Number of vehicles that were classified into the same bins by the current WSDOT dual-loop algorithm and by processing the videotape

Table 7-12. Error Occurrence Frequencies on Different Types of Vehicles

Lane 1						
Vehicle Class	Type 1	Type 3	Type 5	Type 7	Type 12	Sub Total	% of Total
Trucks	1	0	30	78	66	175	47.4%
Dump-Pup Truck	0	0	1	3	1	5	1.4%
Transit Bus	0	0	0	1	1	2	0.5%
Passenger Car	0	1	8	12	12	33	8.9%
Pickup Truck	0	0	5	13	13	31	8.4%
School Bus	0	0	1	2	2	5	1.4%
Mini-Van/SUV	0	0	23	48	47	118	32.0%
Grand Total	369						

Lane 2					
Vehicle Class	Type 1	Type 5	Type 7	Type 12	Sub Total	% of Total
Trucks	1	10	34	29	74	15.8%
Passenger Car	0	7	58	57	122	26.1%
Jeep	0	0	1	1	2	0.4%
Pickup Truck	0	14	41	41	96	20.5%
Mini-Van/SUV	0	22	75	77	174	37.2%
Grand Total	468					

HOV Lane				
Vehicle Class	Type 3	Type 7	Type 12	Sub Total	% of Total
Small Single-Unit Truck	0	2	2	4	6.2%
Passenger Car	5	7	5	17	26.2%
Pickup Truck	3	6	5	14	21.5%
Mini-Van/SUV	6	13	11	30	46.2%
Grand Total	65				

Table 7-13. Error Occurrence Frequencies on Different Classes of Vehicles

Lane 1

Vehicle Class	Type 1	Type 3	Type 5	Type 7	Type 12	Total with Flags	Total of One-hour	% with Flags
Bin1	0	1	37	78	77	193	1005	19.2%
Bin2	0	0	2	12	12	26	60	43.3%
Bin3	0	0	13	20	19	52	77	67.5%
Bin4	1	0	16	47	34	98	121	81.0%

Lane 2

Vehicle Class	Type 1	Type 5	Type 7	Type 12	Total with Flags	Total of One-hour	% with Flags
Bin1	0	43	176	177	396	1479	26.8%
Bin2	0	2	6	6	14	26	53.8%
Bin3	0	5	14	10	29	46	63.0%
Bin4	1	3	13	12	29	32	90.6%

HOV Lane

Vehicle Class	Type 3	Type 7	Type 12	Total with Flags	Total of One-hour	% with Flags
Bin1	14	28	23	65	331	19.6%
Bin2/Bin3/Bin4	0	0	0	0	0	0

CHAPTER 8   CONCLUSIONS AND RECOMMENDATIONS

8.1   CONCLUSIONS

In this research, the WSDOT dual-loop detection system was thoroughly examined and possible error causes were identified. There are a variety of loop error causes. When both single-loop detectors seem to work properly under non-forced-flow traffic conditions, the major cause for the dual-loop undercount problem is the large on-time difference caused by the sensitivity discrepancy between the two single loops because the current WSDOT dual-loop algorithm discards vehicles detected with on-time difference greater than the 10% threshold value.

Based on the identified error causes, a new dual-loop algorithm that can handle erroneous raw loop actuation signals was developed in this research. The new dual-loop algorithm can successfully filter out noise and alleviate the dual-loop miscount and misclassification problems caused by the large on-time difference between paired M and S loops. The dual-loop detection system could become a good truck data source after implementing the new dual-loop algorithm if the sensitivity discrepancy between paired single-loop detectors can be adjusted so that the on-time difference of the two single-loop detectors that form a dual-loop detector falls within a reasonable range.

A portable DEDAC system was also developed in this research for event data collection. A prevailing advantage of the DEDAC system is that it makes the collection of loop detector event data independent of the controller's computing resources. This

feature makes the system easy-to-employ at any loop station cabinets from which the detector event data need to be collected. Therefore, it is a reliable and practical system for transportation practitioners and researchers to collect accurate event data from loop detectors. Such high frequency loop event data enable various kinds of transportation research and applications that could not otherwise be possible.

8.2   RECOMMENDATIONS

8.2.1   Collection of Ground-Truth Vehicle Length Data

As stated in Chapter 7, the vehicle length data calculated by the new dual-loop algorithm were evaluated using eleven types of vehicles for which the range of the ground-truth length data were collected; the vehicle classification data calculated by the new dual-loop algorithm were evaluated using the samples for which the author was <u>certain</u> about their bin classes by observing the videotape. To make it possible to evaluate the accuracy of the calculated length for every single vehicle that passes the dual-loop detector zone, one can collect each vehicle's license plate or vehicle model data from which vehicle length can be obtained. The license plate or vehicle model data can be collected by using a video camera to record the traffic during the event data collection. The video camera should be placed at a location and zoom closely enough to the detector zone so that the license plate or model of any passing vehicle can be recognized when processing the videotape. For those loop detector zones where WSDOT surveillance cameras are available, the WSDOT surveillance cameras should be first considered for vehicle model data collection. If the shooting angle of the surveillance cameras is too acute to record

the vehicle's license plate or model information, a portable video camera should be brought to the field for the ground-truth vehicle length data collection.

8.2.2 Identification of Sensitivity Discrepancy

As identified in the data analysis, the relatively large sensitivity discrepancy between the two single-loop detectors that form a dual-loop detector is the main cause for dual-loop data errors. A quick remedy method that does not involve replacing any part of the system hardware or software would be to adjust the sensitivities of the two single-loop detectors so that the mean on-time difference is less than 10% for the passing vehicles under non-forced-flow traffic conditions. With sensitivity adjustment, these dual-loop detectors should be able to collect a majority of the passing vehicles.

An accurate way to identify the sensitivity discrepancy for a dual-loop detector would be to collect event data from its M and S loops and then calculate the on-time difference. However, there are about 1020 dual-loop detectors [45] on the Greater Seattle freeway network and it would be extremely labor-intensive and time-consuming to collect event data from each individual dual-loop detector on the dual-loop detection system. So, a more feasible method to identify the on-time difference should be sought.

For single-loop detectors, event data are aggregated into 20-second volume and scan-count, which can be divided by 12 to get lane-occupancy. Lane-occupancy multiplied by 20 seconds and then divided by 100 equals a loop's total on-time time during the 20-second interval. The total on-time time is then the sum of all the individual vehicles' on-times during that 20-second interval. Theoretically, when a vehicle traverses

a dual-loop detector, if the sensitivity discrepancy causes the on-time of the dual-loop detector's M loop to be greater than that of its S loop, the 20-second lane-occupancy would show the same pattern, i.e., lane-occupancy detected by M loop is greater than that detected by S loop.

In light of this, the mean lane-occupancy difference calculated using one-hour 20-second aggregated single-loop scan-count data were compared with the mean on-time difference calculated using the event data collected during the same one-hour period. The comparison results are summarized in Table 8-1. As can be seen in this table, for each of the four GP lanes, the scan-count percentage difference, ΔSC, was very close to the on-time percentage difference, ΔOT, calculated using event data. Therefore, comparing the difference between scan counts collected from paired single-loop detectors is a practical method to identify dual-loop detectors with large on-time difference and sensitivity discrepancy.

Although the aggregated-data-based lane-occupancy can represent the sensitivity discrepancy between the M and S loops for each of the dual-loop detectors embedded beneath the four GP lanes, the dual-loop detector for the HOV lane seemed to have larger difference, about 45%, between the aggregated-data-based lane-occupancy difference and the event-data-based on-time difference. In order to find out the causes, the one-hour volume data collected by the M and S loops were calculated for all five lanes. The results are summarized in Table 8-2. As can be seen in this table, for each of the four GP lanes, the volume collected by the M loop differed slightly from that collected by the S loop. For the HOV lane, however, the volume collected by the M loop

differed considerably from that collected by the S loop. By comparing the volume data collected on the HOV lane to the ground-truth volume data in Table 5-1 for the same lane, the M loop was found to greatly overestimate volume. It was concluded that the M loop on the HOV lane was malfunctioning. Thus the calculated lane-occupancy difference cannot represent the sensitivity discrepancy.

8.2.3 Elimination of Sensitivity Discrepancy

Based on the above analysis, a quick remedy method would be to develop a software package to process 20-second aggregated data to identify malfunctioning loops and calculate the lane-occupancy difference between M and S loops for each of the dual-loop detectors on the Seattle freeway network. The identified malfunctioning loops should be quickly inspected and repaired by WSDOT technicians. The calculated lane-occupancy differences can be used to help adjust loop detectors with sensitivity discrepancy.

This sensitivity setting adjustment becomes possible with the availability of the laptop-based DEDAC system. Adjustments that eliminate the sensitivity discrepancies based on a reasonable set of rules without further research into the absolute sensitivity levels should still improve the system so that the dual-loop detectors will be able to collect a majority of the passing vehicles without replacing any part of the current WSDOT dual-loop detection system.

Although adjusting the sensitivities to remove loop sensitivity <u>differences</u> will significantly improve the accuracy of the dual loop data, further research is needed to determine the correct <u>absolute</u> sensitivity levels as well. Therefore, a recommended

follow-up research project includes developing a program to be integrated into the current laptop-based DEDAC system. The program should calculate the sensitivity adjustment needed to calibrate every dual-loop detector that has a sensitivity discrepancy between the two single-loop detectors. A sensitivity adjustment that not only eliminates the sensitivity discrepancies but also identifies the correct <u>absolute</u> sensitivity levels for the loops would greatly improve dual-loop accuracy.

Table 8-1. Mean Scan-Count Difference vs. Mean On-Time Difference

Mean Scan-Count Difference between M and S Loops in Percentage						
Lane No.		Lane 1	Lane 2	Lane 3	Lane 4	HOV
M Loop	Mean	71.83	135.91	159.36	129.73	51.45
	Standard Deviation	38.29	47.65	49.98	47.36	33.26
S Loop	Mean	85.78	53.58	150.26	145.17	39.53
	Standard Deviation	46.35	16.34	43.83	51.16	25.98
$\Delta SC = \dfrac{SC_S - SC_M}{SC_M} \times 100$		19.41	-60.58	-5.71	11.90	-23.17

Mean On-Time Difference between M and S Loops in Percentage					
Lane No.	Lane 1	Lane 2	Lane 3	Lane 4	HOV
$\Delta OT = \dfrac{OT_S - OT_M}{OT_M} \times 100$	17.11	-57.51	-7.01	11.52	-12.71

Difference between ΔSC and ΔOT in Percentage					
Lane No.	Lane 1	Lane 2	Lane 3	Lane 4	HOV
$\dfrac{\Delta OT - \Delta SC}{\Delta SC} \times 100$	-11.86	-5.07	22.83	-3.18	-45.14

SC_S = Scan count measured by S loop

SC_M = Scan count measured by M loop

OT_M = Event-data-based M loop on-time data

OT_S = Event-data-based S loop on-time data

Table 8-2. M and S Volumes Comparison

Lane No.	Lane 1	Lane 2	Lane 3	Lane 4	HOV
V_M	812	1326	1522	1678	491
V_S	828	1323	1512	1686	376
$\frac{V_S - V_M}{V_M} \times 100$	1.97	-0.23	-0.66	0.48	-23.42

V_M = TDAD-based M loop volume

V_S = TDAD-based S loop volume

BIBLIOGRAPHY

1. The Freight Story: A National Perspective on Enhancing Freight Transportation. FHWA-OP-030004. Federal Highway Administration, 2002. U.S. Department of Transportation, Washington, D.C. Available at http://ops.fhwa.dot.gov/freight/publications/freight%20story/operat.htm. Accessed on December 6, 2003.

2. Transportation Statistics Beyond ISTEA: Critical Gaps and Strategic Responses. Bureau of Transportation Statistics, BTS98-A-01, 1998. U.S. Department of Transportation, Washington, D.C.

3. Quick Responses Freight Manual Final Report (1996). Prepared for Federal Highway Administration. U.S. Department of Transportation, the Travel Model Improvement Program. Report No. DTFH61-93-C-00075.

4. A Concept for a National Freight Data Program. Transportation Research Board Special Report 276. National Research Board, Washington, D.C., 2003. Available at http://trb.org/publications/sr/sr276.pdf. Accessed on December 6, 2003.

5. Hallenbeck, M. E, E. McCormack, J. Nee, and D. Wright. Freight Data from Intelligent Transportation System Devices. Research Report WA-RD 566.1.

Washington State Transportation Center (TRAC), Washington State Department of Transportation.

Available at http://depts.washington.edu/trac/bulkdisk/pdf/566.1.pdf.

6. Margiotta, R. 1998. ITS as a Data Resource: Preliminary Requirements for a User Service. Office of Highway Policy Information, Federal Highway Administration. Available at www.fhwa.dot.gov/ohim/its/itspage.htm. Accessed on December 6, 2003.

7. Pumrin, S. and D. J. Daily. Dynamic Camera Calibration in Support of Intelligent Transportation Systems (ITS). In *Transportation Research Record: Journal of Transportation Research Board, No.1804.* National Research Council, Washington, D.C., pp. 77-84.

8. Kilger, M. Video-Based Traffic Monitoring. International Conference on Image Processing and its Applications, 7-9 April 1992, Maastricht, Netherlands, pp. 89-92.

9. Fathy, M. and M.Y. Siyal. An Image Detection Technique Based on Morphological Edge Detection and Background Differencing for Real-Time Traffic Analysis. Pattern Recognition Letters, Vol. 16, No. 12, December 1995, pp. 1321-1330.

10. Ali, A.T. and E.L. Dagless. Computer Vision for Automatic Road Traffic Analysis. ICARCV 90, Proceedings of the International Conference on Automation, Robotics and Computer Vision, 19-21 September 1990, pp. 875-879.

11. Fathy, M. and M.Y.Siyal, Real-Time Image Processing Approach to Measure Traffic Queue Parameters. IEE Proceedings - Vision, Image and Signal Processing, Vol.142, No.5, October 1995, pp. 297-303. 1995 IEEE International Conference on Systems, Man and Cybernetics, Vol.1, 22-25 October 1995, Vancouver, British Columbia, Canada, pp. 679-683.

12. Dickinson, K.W. and R.C. Waterfall. Video Image Processing for Monitoring Road Traffic. IEE International Conference on Road Traffic Data Collection, December 1984, pp. 105-109.

13. Ashworth, R., D.G. Darkin, K.W. Dickinson, M.G. Hartley, C.L. Wan, and R.C. Waterfall. Applications of Video Image Processing for Traffic Control Systems. Second International Conference on Road Traffic Control, 14-18 April 1985, London, UK, pp. 119-122.

14. Mulcare, M. and D. Manor. Intelligent Microwave Radar: Multiple Zone Presence Detector. Proceedings of the International Conference on Application of new Technology to Transport Systems. Melbourne, Australia, May 1995. Vol. 2. pp 105-113.

15. Wang, J., C. E. Ryerson, and D. Manor. The Road Traffic Microware Sensor (RTMS). Vehicle Navigation and Information Systems Conference. Conference Record of Papers. 1992. pp 83-90.

16. Weber, N. A. Verification of Radar Vehicle Detection Equipment. South Dakota Department of Transportation. Report Number: SD98-15-F.

17. Chang, E. Real-World Traffic Detector Testbed System Design. IEEE International Conference on Intelligent Vehicles. Proceedings of the 1998 IEEE International Conference on Intelligent Vehicles. Vol. 2. 1998. pp646-649.

18. Bergan, A. T., R. L. Sabounghi, J. Fung, B. Zimmerman, and R. Bushma. Traffic Surveillance and Management Technologies: Video and Acoustic. Third World Congress on Intelligent Transport Systems. Orlando, Florida. 1996.

19. Loukakos, D. Other Road-Side Detectors: ITS Decision Report. ITD Decision Report. 2001. pp5.

20. WSDOT Intermodal Data Linkages Freight ITS Operational Test Evaluation Final Report. Part 2: Freight ITS Traffic Data Evaluation. Washington State Department of Transportation. Transportation Research Center (TRAC) 2003.

21. Traffic Detector Handbook (Second Edition). Institute of Transportation Engineers. Washington, DC, 1997.

22. Zhang, X., Y. Wang, and N. L. Nihan. Investigating Dual-Loop Errors Using Video Ground-Truth Data. Proc. ITS America 2003 Annual Meeting, Minneapolis, Minnesota, 2003.

23. Chen, L. and A. May. Traffic Detector Errors and Diagnostics. In *Transportation Research Record: Journal of Transportation Research Board, No. 1132*. National Research Council, Washington, D.C., pp 82-93.

24. Nihan, N. L. and M. Wong. Improved Error Detection Using Prediction Techniques and Video Imaging. Final Report, Washington State Department of Transportation and Transportation Northwest, TNW95-01.

25. Cleghorn, D., F. L. Hall, and D. Garbuio. Improved Data Screening Techniques for Freeway Traffic Management Systems. In *Transportation Research Record: Journal*

of Transportation Research Board, No. 1320. National Research Council, Washington, D.C., pp 17-23.

26. Payne, J. and S. Thompson. Malfunction Detection and Data Repair for Induction-Loop Sensors Using I-880 Database. In *Transportation Research Record: Journal of Transportation Research Board, No. 1570.* National Research Council, Washington, D.C., pp 191-201.

27. Skabardonis, A., Petty, K., Noeimi, H., Rydzewski, D. and Varaiya, P. I-880 Field Experiment: Data-Base Development and Incident Delay Estimation Procedures. In Transportation Research Record 1554, TRB, National Research Council, Washington D.C., 1996, pp. 204-212.

28. Nihan, N. L. Aid to Determining Freeway Metering Rates and Detecting Loop Errors. *Journal of Transportation Engineering, Vol 123, No 6.* ASCE, November/December 1997, pp454-458.

29. Jacobson, L., N. L. Nihan, and J. Bender. Detecting Erroneous Loop Detector Data in a Freeway Traffic Management System. In *Transportation Research Record: Journal of Transportation Research Board, No. 1287.* National Research Council, Washington, D.C., pp151-166.

30. Turochy, R. E. and B. L. Smith. A New Procedure for Detector Data Screening in Traffic Management Systems. Preprint CD-ROM. Transportation Research Board Annual Meeting. Washington, D.C., 2000. Paper no. 000842.

31. Park E. S., S. Turner, and C. H. Spiegelman. Empirical Approaches to Outlier Detection in ITS Data. In *Transportation Research Record: Journal of Transportation Research Board, No.1840.* National Research Council, Washington, D.C., pp. 21-30

32. Coifman, B. Using Dual Loop Speed Traps to Identify Detector Errors. In *Transportation Research Record: Journal of Transportation Research Board, No. 1683.* National Research Council, Washington, D.C., pp 47-58.

33. Coifman, B. Event Data Based Traffic Detector Validation Tests. *Preprint CD-ROM.* Transportation Research Board Annual Meeting, Washington. D.C., 2002.

34. Daily, D.J. and Z. Wall. An Algorithm for the Detection and Correction of Errors in Archived Traffic Data. *Preprint CD-ROM.* Transportation Research Board Annual Meeting, Washington, DC, 2003.

35. Chen, C., J. Rice, A. Skabardonis, and P. Varaiya. Detecting Errors and Imputing Missing Data for Single Loop Surveillance Systems. *Preprint CD-ROM.* Transportation Research Board Annual Meeting, Washington, DC, 2003.

36. Coifman, B., D. Lyddy, and A. Skabardonis. The Berkeley Highway Laboratory-Building on the I-880 Field Experiment. *Proc. IEEE ITS Council Annual Meeting.* IEEE, 2000, pp 5-10.

37. Coifman, B. Improved Velocity Estimation Using Single Loop Detectors. *Transportation Research: Part A*, Vol 35, No. 10, 2001, pp. 863-880.

38. Coifman, B. Estimating Travel Times and Vehicle Trajectories on Freeways Using Dual Loop Detectors. *Transportation Research: Part A*, 2002, Vol 36, No 4, 2002, pp. 351-364.

39. Coifman, B. Using Dual Loop Speed Traps to Identify Detector Errors. In *Transportation Research Record: Journal of Transportation Research Board, No. 1683.* National Research Council, Washington, D.C., pp 47-58.

40. Microsoft Developer Network Library (MSDN). http://www.msdn.microsoft.com/library/ Accessed July 6, 2003.

41. Model PCI-IDIO-16 User Manual. File #: MPCI-IDIO-16.B2. http://www.acces-usa.com/manuals/pci-idio-16.pdf. Accessed July 6, 2003.

42. SuperLogics USB 8207 adapter User Manual.
http://www.SuperLogics.com. Accessed June 6, 2003.

43. Guide for Uniform Laws and Regulations Governing Truck Size and Weight Among the WASHTO States. Adopted by the WASHTO Policy Committee, January 2000. Western Association of State Highway and Transportation Officials. http://www.wsdot.wa.gov/freight/mcs/WASHTOtruckGuide.pdf. Accessed December 20, 2004.

44. Washington State Commercial Vehicle Guide, 2002-2003. Washington State Department of Transportation.
http://www.wsdot.wa.gov/freight/mcs/CommercialVehicleGuide2002-03.pdf. Accessed December 20, 2004.

45. Discussion via emails with WSDOT senior engineer, Mr. Mark Morse. December 15, 2003.

46. Holdsworth, B., and R. C. Woods. Digital Logic Design. Oxford, Newnes, 2002. ISBN: 0750645822.

47. Painter, K. M., Washington State Freight Truck Origin and Destination Study: Pierce County. EWITS Research Report Number 21-Pierce, January 1998. http://ewits.wsu.edu/reports/research/err21pierce.pdf.

APPENDICES

APPENDIX I DETECTOR EVENT DATA COLLECTION (DEDAC) SYSTEM USER MANUAL

Notice

The information in this manual is provided for reference only. The author does not assume any liability arising out of the application of the DEDAC system.

Introduction

Detector Event Data Collection (DEDAC) System is a loop detector event data collection system developed in this research. The system is able to sample loop actuation signals at high sampling rates and then save the collected event data in real time without interfering with the detector controller's normal operation. The system consists of the following major components: an event data collection program called "DEDAC", a USB digital I/O adapter, a laptop computer, multiple connectors, and multiple wires.

System Architecture

Figure I-1 illustrates an overview of the DEDAC system design. As can be seen in this figure, the Input File is located right under the controller unit in the loop station cabinet. Loop actuation signals flow from loop detectors installed in the freeway pavement to the Input File, from where the signals flow to the Model 170 controller in the cabinet and the digital adapter, simultaneously. Meanwhile, the event data collection software, DEDAC program, installed in the laptop computer polls the data address of the USB digital I/O adapter with a high sampling rate in real time and saves the event data on a local disk.

The USB Digital I/O Adapter

The USB digital I/O adapter can be purchased from this website: www.superlogics.com. Here is the link to the description of this particular product (Part# 8207): http://www.superlogics.com/usb-digital-input-output/io/8207/9-766.htm. The USB

digital I/O adapter should be installed by following the instructions in the adapter User Manual, which can be downloaded from this link: http://www.superlogics.com/manuals/8207.pdf.

Installation Procedure

Building Connections

If loop event data are collected from fewer than four dual loops, either Port A or Port B of the I/O adapter and two 25-Pin connectors, one D-type Male (DM) and one D-type Female (DF), are needed for building the connections. If loop event data are collected from four to eight dual loops, both ports and four 25-Pin connectors, two DM and two DF, are needed.

Figure I-2 shows the connections built for collecting data from eight dual loops. The two DM connectors are wired to the onboard removable screw terminals on the two ports of the I/O adapter. The I/O adapter and the laptop computer are connected by the USB A to B cable. The two DM connectors are connected to the two DF connectors (not shown in this figure) that are wired to the Input File in the controller cabinet. Each of the self-built 25-pin DM and DF connectors should have eight data pins and the rest of the pins are grounded.

When wiring the DF connector, the assignment of data pins should be consistent with that of the DM connector. This way, data channels can be built up by connecting a DM connector with a DF connector. Loop actuation signals flow from the Input File to the I/O adapter via the connection built by the connectors and the wires then to the laptop computer via the USB A to B cable.

When wiring the wires to the wiring terminals of the Input File and the onboard removable screw terminals on the I/O adapter, one should note which loop in the Input File is connected to which Port Bit of the digital I/O adapter.

Installing the USB Digital I/O Adapter

The USB digital I/O adapter is shipped with a software CD and a USB A to B cable. When installing the I/O adapter, the software should be installed before the hardware. Choose **Install Software** at the beginning of the CD. Select the **Digital I/O** software drivers and install **SeaIO** prior to installing the hardware. After installing the software, connect the USB cable to the I/O adapter with the other end connecting to a laptop computer [42]. Please refer to the hardware manufacturer's user manual for detailed instructions.

Running the DEDAC Software

After the hardware has been successfully installed, the DEDAC software can be installed. Download the DEDAC software from TransNow website (www.transnow.org). Copy DEDAC.exe and DataDevice.dll to the laptop computer. Double-click on DEDAC.exe to start the program. Figure I-3 is the DEDAC program main interface.

The program main interface was designed to facilitate long-duration data collection. The Start Time and End Time are where users should input the date and time at which the data collection starts and the date and time at which the data collection ends. Figure I-4 shows the pop-up window from where users input date information.

Users need to select a timer resolution and a polling interval. The recommended value for the timer resolution is zero. The recommended value for the polling interval is one half of the sampling interval of the controller. For example, if the sampling rate of a controller is 100 Hz, the recommended polling interval is 5 milliseconds.

After setting up the four parameters, the DEDAC program is ready to be started. There are two ways to start the program:

1. Users can set up the start and end times and then start the program by clicking the OK button. Upon clicking on the OK button, the program will direct the users to create a file to where the collected data will be stored. The program will not start collecting data until the computer system clock time reaches the Start Time and will not stop until the computer system clock time reaches the End Time. Data collected from the Start Time to the End Time are saved. The program can also be terminated any time after it starts by clicking on the Stop button. In this case, data collected before terminating the program will be saved.

2. Users can start the program by clicking on the Start button to start collecting data immediately. Upon clicking on the Start button, the program will direct users to create a file to where the collected data will be stored. Users can terminate the program and therefore stop collecting data by clicking on the Stop button. Data are collected from the time the program starts to the time the program ends.
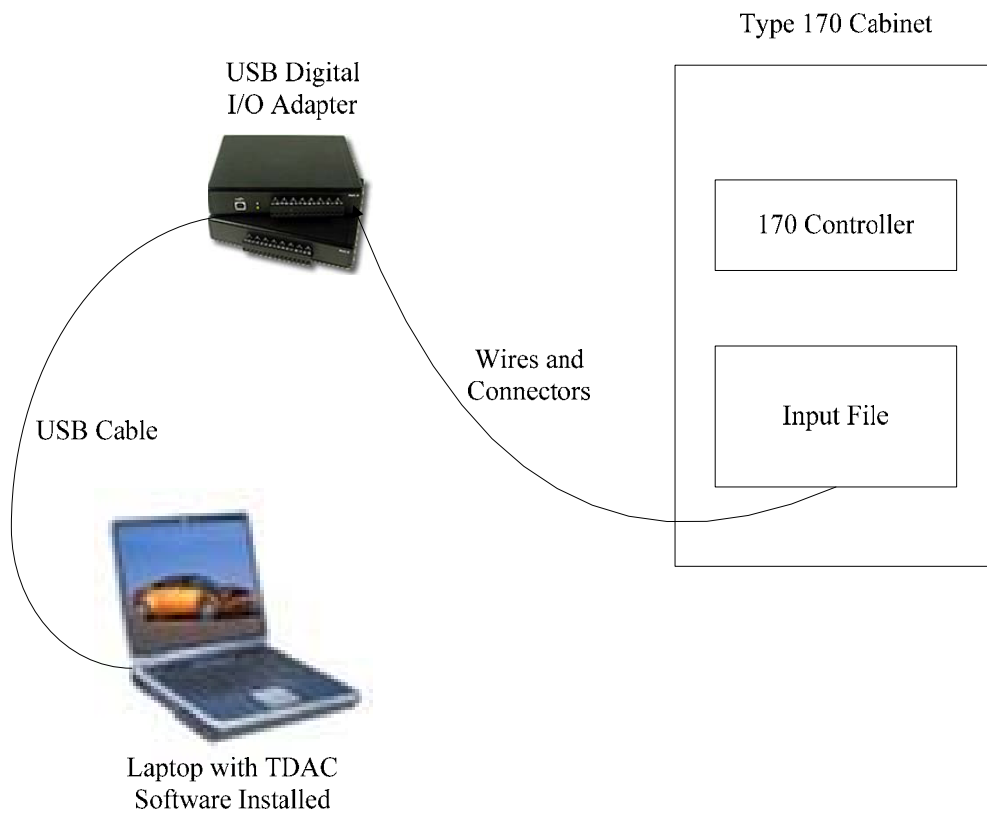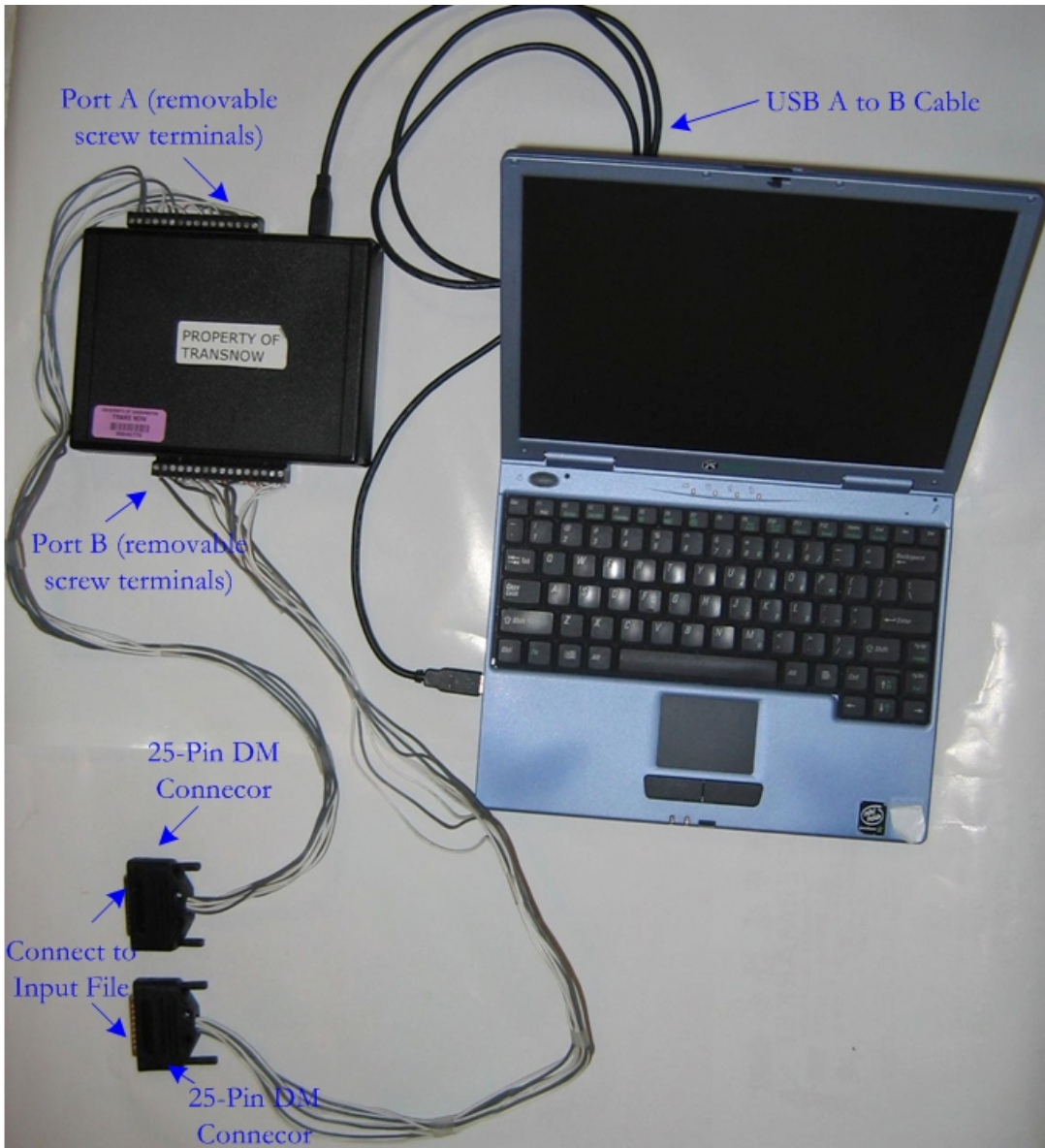
Figure I-1 DEDAC System Design

Figure I-2 Illustration of the Connections for Collecting Data from Eight Dual Loops
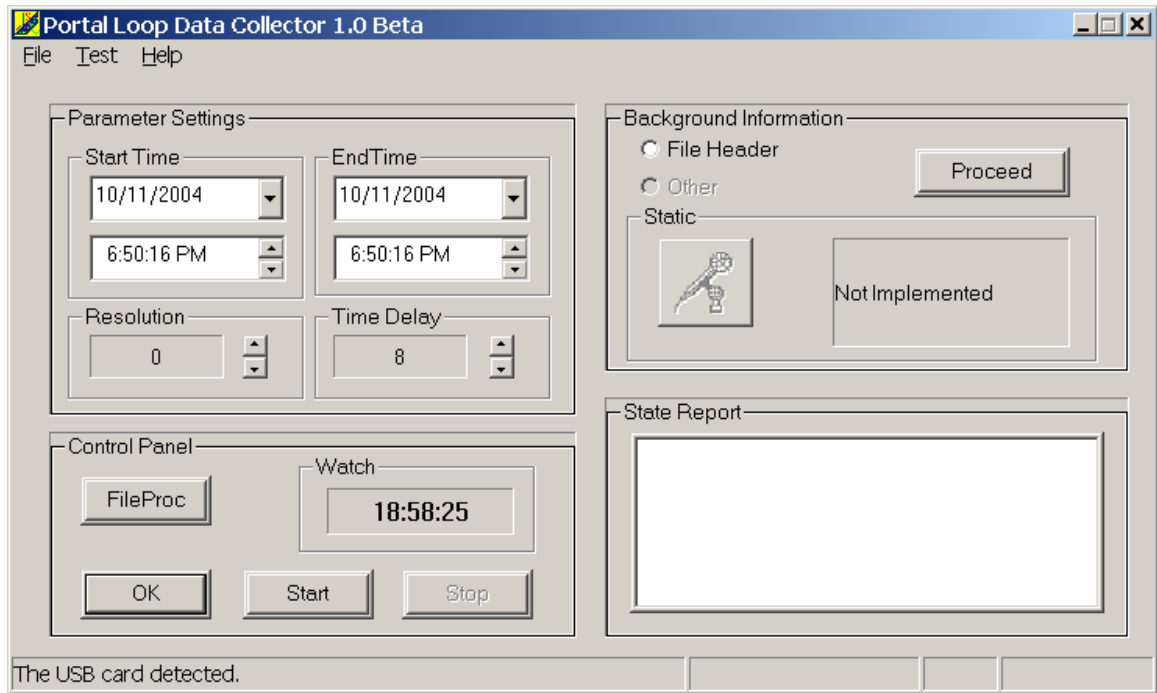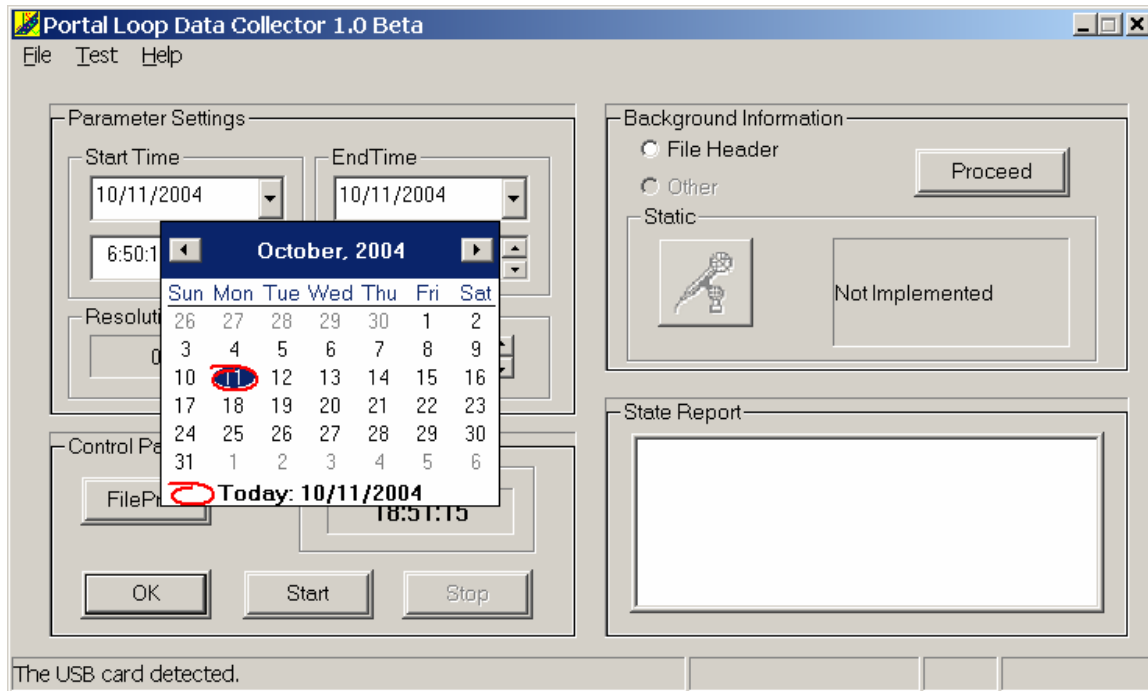
Figure I-3 DEDAC Program Main Interface

Figure I-4 DEDAC Program Main Interface (Enter Date Information)

APPENDIX II ILLUSTRATION OF THE NOISE FILTER AND POSTPROCESSOR

All the possible combinations of "0"s and "1"s can be classified into six groups, each of which can be reduced to and represented by a general signal sequence. The noise filter and postprocessor are applied to each of these six representative signals to test their effectiveness. These processes are illustrated in Figures II-1 to II-6.

Case 1

The original signal sequence in Case 1 represents those signal sequences with random single-digit noise occurring intermittently when a loop detector is in the "on" state and noise can be easily filtered out by the noise filter.

As can be seen in Figure II-1, the on-time signal sequence is broken into small pieces. After being processed by the noise filter, the noise is filtered out and the broken on-time pulse is reconstructed.

Case 2

The original signal sequence in Case 2 represents those signal sequences with random single-digit and two-digit noise occurring through a loop detector's on-time pulse and the noise occurring right before the loop detector changes state from "on" to "off." This occurrence of noise forces the noise filter to sacrifice the last digit of the on-time pulse.

Shown in Figure II-2, three negative false alarm noises occurred in the "on" state and a single-digit positive false alarm noise occurred in the "off" state in the original signal sequence. These four noises are labeled in the original signal sequence.

When this signal sequence is being filtered, the four noises are correctly identified and filtered by the noise filter. However, the noise filter mistakenly identifies the last digit of the on-time pulse as a single-digit positive false alarm noise because as stated in Section 6.4.1 and illustrated in Table 6-3, if a "0" digit is preceded and succeeded by two or more "1"s, this digit is treated as a positive false alarm noise and flipped from 0 to 1.

After being processed by the noise filter, the broken on-time pulse in the original signal sequence is reconstructed at the price of sacrificing its last on-time digit. This side effect of the noise filter cannot be caught and corrected by the postprocessor.

Case 3

The original signal sequence in Case 3 represents those signal sequences with random single-digit noise occurring when a loop detector is in the "off" state. The random noises occur in a way such that they can "fool" the noise filter to introduce a positive false alarm signal which is caught by the subsequent postprocessor.

Shown in Figure II-3, three positive false alarm noises occurred in the "off" state in the original signal sequence. These three positive false alarm noises are labeled in the original signal sequence. The first one is an isolated single-digit noise. The second one is a two-digit noise followed immediately by the third one, which is also a single-digit noise.

When this signal sequence is being filtered, the second and the third positive false alarm noises are ignored; instead, the digit between these two positive false alarm noises is mistakenly identified as a single-digit negative false alarm noise by the noise filter. After being processed by the noise filter, the first positive false alarm noise is

filtered out. The mistakenly identified negative false alarm noise is flipped from its "off" state to "on" state, which merges the second and the third positive false alarm noises together to form a short on-time pulse of four sample intervals. As calculated in Section 6.2, the length of a valid on-time pulse should be greater than or equal to five sample intervals. Since this short on-time pulse is shorter than the minimum on-time threshold, it is filtered out as a positive false alarm signal by the subsequent postprocessor.

In summary, in this case, the noises are successfully filtered out by the joint effort of the noise filter and the postprocessor. Despite a positive false alarm signal being introduced by the noise filter, it is later caught and removed by the subsequent postprocessor.

Case 4

The original signal sequence in Case 4 represents those signal sequences with random noise occurring right before and right after a loop detector changes its state from "on" to "off."

As shown in Figure II-4, in the original signal sequence, five negative false alarm noises occur breaking part of the on-time pulse into pieces right before the loop detector changes its state, and then three positive false alarm noises occur right after the loop detector changes state from "on" to "off." These eight noises are labeled the original signal sequence.

The noise filter correctly recognizes all eight noises. After being processed by the noise filter, the five negative false alarm noises and the three positive false alarm noises are filtered out.

One may argue, however, that the first positive false alarm noise could also be the last digit of the on-time signal because the last negative false alarm noise is filtered out and the "on" state could be extended to include the first positive false alarm. In this case, the broken on-time pulse in the original signal sequence is reconstructed at the price of sacrificing its last on-time digit. This side effect of the noise filter cannot be caught and corrected by the postprocessor.

Case 5

The original signal sequence in Case 5 represents those signal sequences with multiple-digit noise that is immune to the noise filter but sensitive to the postprocessor, i.e., the noise goes through the noise filter undetected, but is caught by the postprocessor.

Shown in Figure II-5, three three-digit negative false alarm noises occur in the original signal sequence. These three negative false alarm noises are labeled in the original signal sequence. As stated in Section 6.3.1 and illustrated in Table 6-3, if a "1" is preceded by another two "1"s, succeeded by another two "1"s, or preceded by a "1" and succeeded by another "1", it is not changed by the noise filter. So, after being processed by the noise filter, the original signal sequence does not change at all and the three negative false alarm noises still exist. But since the length of the three-digit negative false alarm noise is shorter than the minimum off-time threshold values, all three noises are filtered out by the postprocessor. In this case, it is the postprocessor that reconstructs the on-time pulse.

Case 6

The original signal sequence in Case 6 represents those signal sequences with random noise occurring when a loop detector is in the "on" state. The random noises occur in a way such that they can "fool" the noise filter to introduce a negative false alarm signal, which is later caught by the postprocessor.

Shown in Figure II-6, seven negative false alarm noises occur in the original signal sequence. These seven noises are labeled in the original signal sequence. The noise filter recognizes six of the seven false alarm noises except for the sixth one because it mistakenly identifies the single-digit between the fifth and the sixth false alarm noises as a single-digit positive false alarm noise, which is also labeled in the original signal sequence.

After being processed by the noise filter, part of the on-time pulse is recovered. However, the noise filter induces a negative false alarm signal by flipping the mistakenly identified single-digit positive false alarm noise from "on" to "off" because the flipped digit then merges with the sixth negative false alarm noise to form a negative false alarm signal. Since this negative false alarm signal only contains four sample intervals, it is later removed by the postprocessor.

In this case, the noises are successfully filtered out by the joint effort of the noise filter and the postprocessor. Despite a negative false alarm signal being introduced by the noise filter, it is later caught and removed by the subsequent postprocessor.

Summary

A noise filter and a postprocessor were developed and their effectiveness was illustrated by processing six representative signal sequences. Type 1 or Type 2 error in Table 6-4 is flagged whenever a negative false alarm noise/signal or positive false alarm noise/signal occurs.

The noise filter and the postprocessor are designed to effectively screen out noise occurring in the raw loop actuation signals. The processed signals are used for matching M and S on-time pulse pairs, which are then used to calculate individual vehicle speed and length.
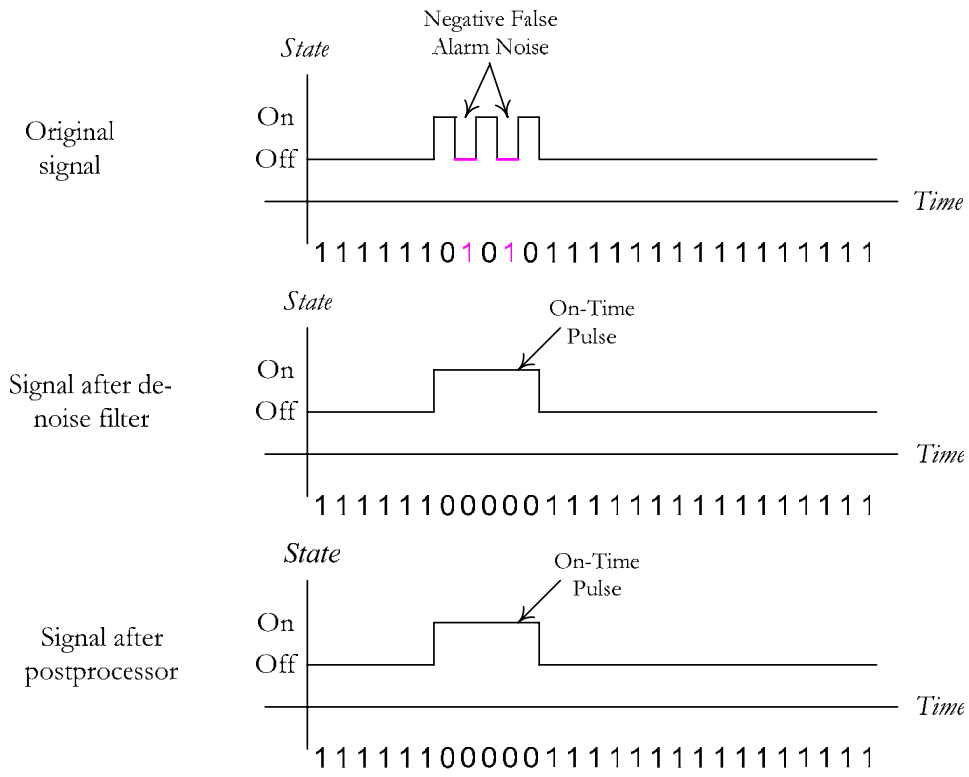
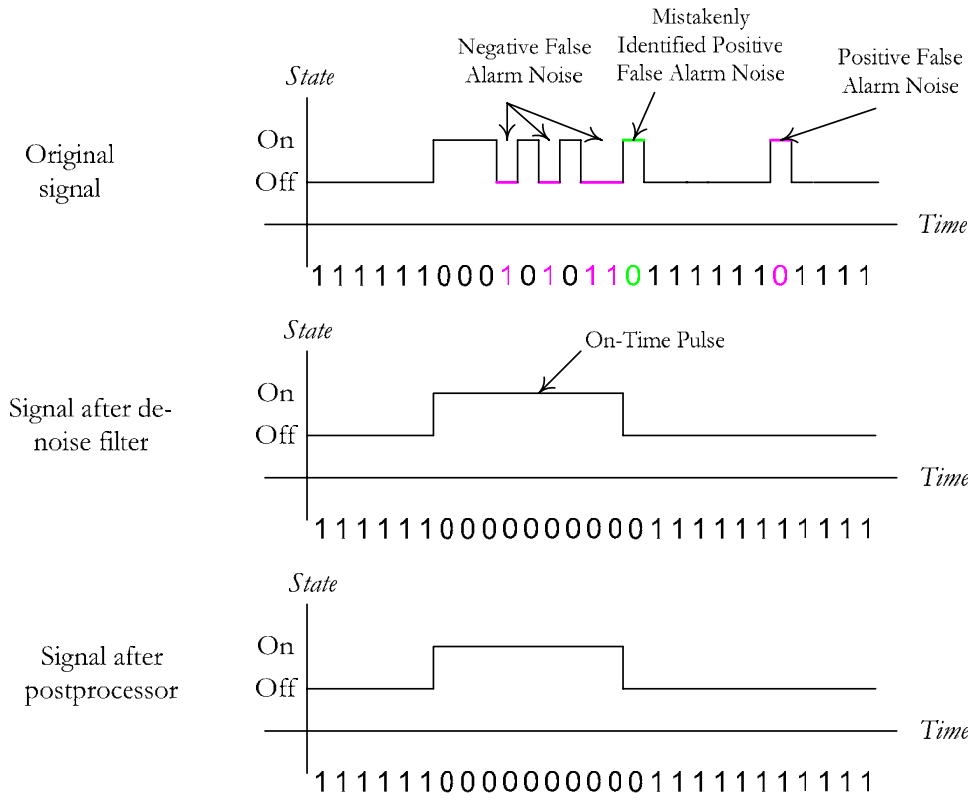Figure II-1. Illustration of Noise Filter and Postprocessor (Case 1)

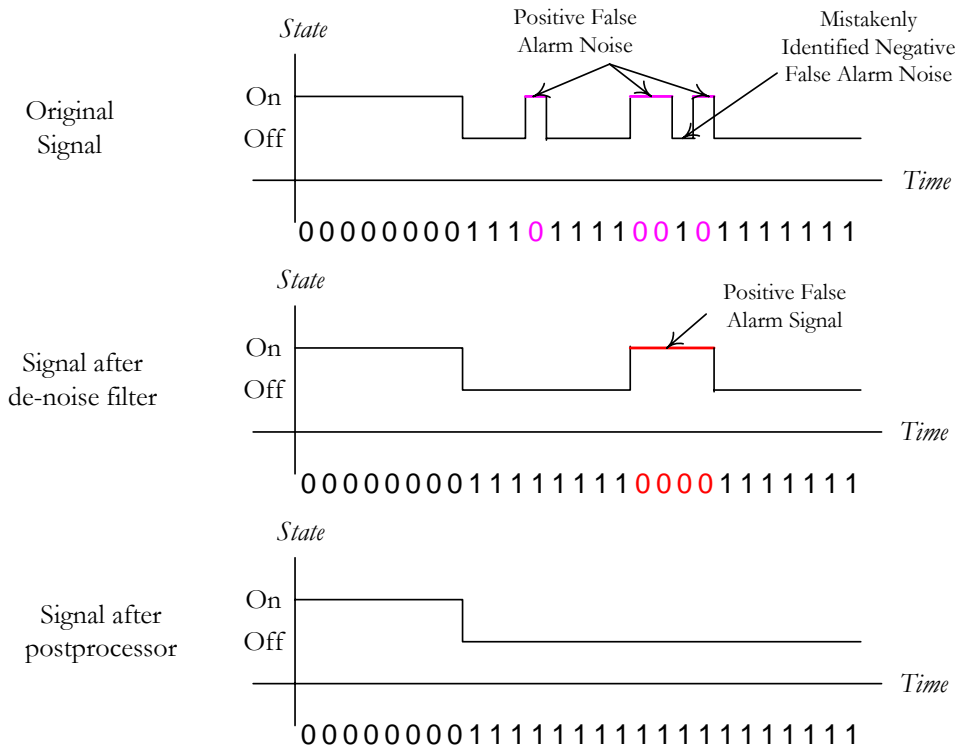Figure II-2. Illustration of Noise Filter and Postprocessor (Case 2)

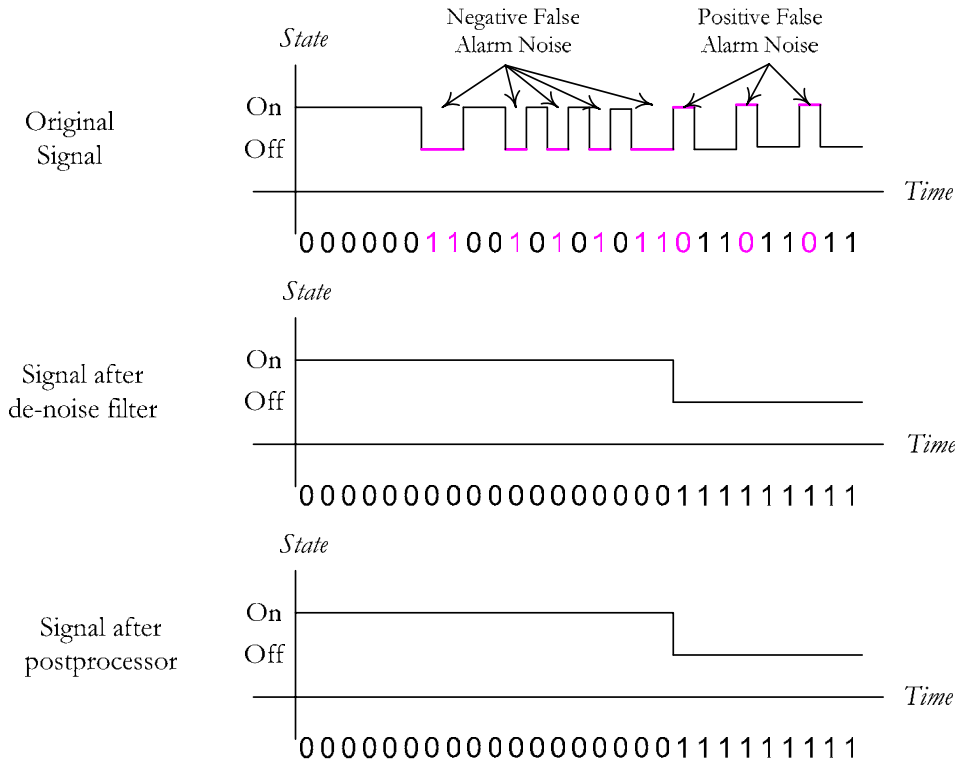Figure II-3. Illustration of Noise Filter and Postprocessor (Case 3)

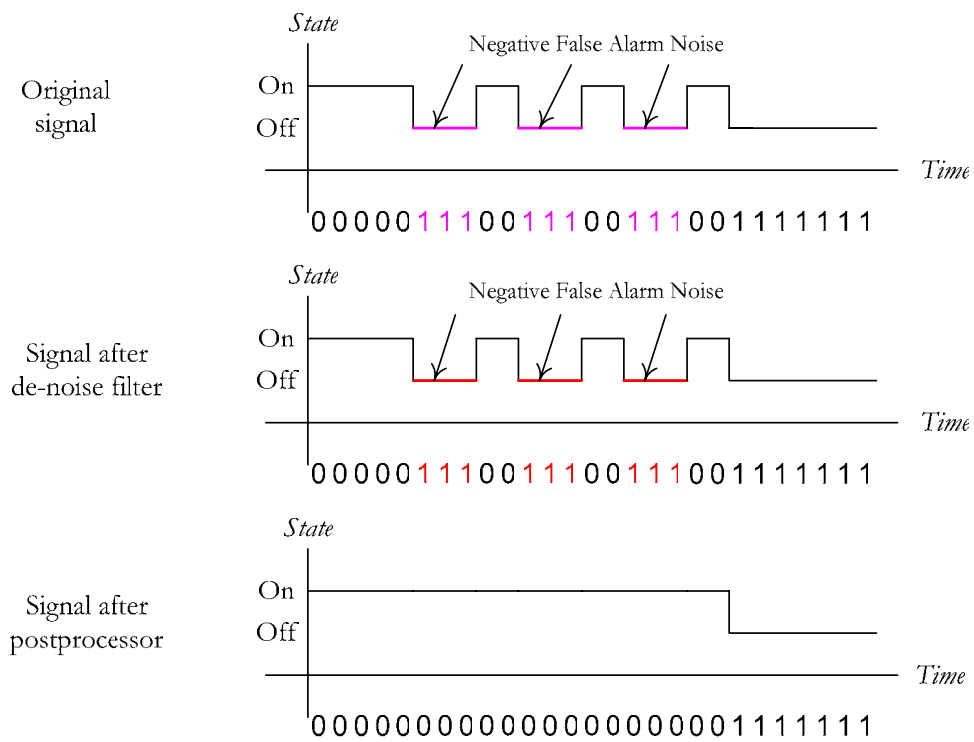Figure II-4. Illustration of Noise Filter and Postprocessor (Case 4)

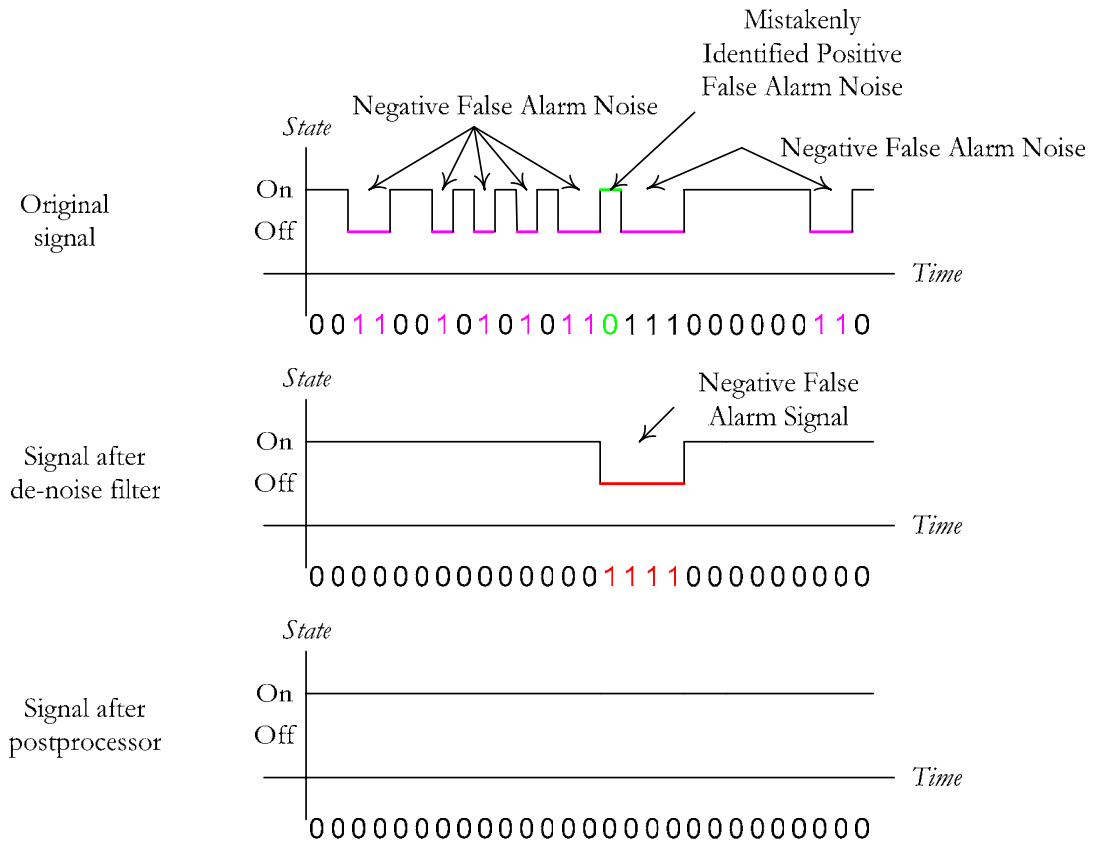Figure II-5. Illustration of Noise Filter and Postprocessor (Case 5)

Figure II-6. Illustration of Noise Filter and Postprocessor (Case 6)

APPENDIX III ILLUSTRATION OF THE M AND S LOOP ON-TIME PULSES MATCHING RULES

Case 1

In Case 1, a positive false alarm occurs in the S loop signal sequence and needs to be skipped or screened out during the matching process. The rules employed in this case include Rule 1, Rule 2, and Rule 5.

Case 1 is illustrated in Figure III-1. As can be seen in this figure, S loop on-time pulse S_j succeeds M loop on-time pulse M_i, and the elapsed time, $T_e(i, j)$, from M_i to S_j is greater than the minimum elapsed time threshold and smaller than the maximum elapsed time threshold. So, according to Rule 1 and Rule 2, S_j is matched to M_i.

On-time pulse S_{j-1}, however, cannot be matched to any M loop on-time pulse. The M loop on-time pulse, M_{i-1}, which immediately precedes S_{j-1}, forms an on-time pair with S_{j-2}. So, according to Rule 5, S_{j-1} is filtered out as a positive false alarm.

Case 2

In Case 2, a positive false alarm occurs in the M loop signal and needs to be skipped or screened out during the matching process. The rules employed in this case include Rule 1, Rule 2, and Rule 4.

Case 2 is illustrated in Figure III-2. As can be seen in this figure, S loop on-time pulse S_j succeeds M loop on-time pulse M_i, and the elapsed time, $T_e (i, j)$, from M_i to S_j is greater than the minimum elapsed time threshold and smaller than the maximum elapsed time threshold. So, according to Rule 1 and Rule 2, S_j is matched to M_i.

On-time pulse M_{i-1}, however, cannot be matched to any S loop on-time pulse. The S loop on-time pulse, S_j, which immediately succeeds M_{i-1}, forms an on-time pair with M_i. In addition, the elapsed time from M_{i-1} to S_j is greater than the maximum elapsed time threshold. So, according to Rule 4, M_{i-1} is filtered out as a positive false alarm.

Case 3

In Case 3, the elapsed time between the M loop on-time pulse and its matching S loop on-time pulse is greater than the maximum elapsed time threshold. The rules employed in this case include Rule 1 and Rule 3.

Case 3 is illustrated in Figure III-3. As can be seen in this figure, S_j immediately succeeds M_i and is the only S loop on-time pulse that can be matched to M_i. Although the elapsed time between M_i and S_j is greater than the maximum elapsed time threshold, according to Rule 1 and Rule 3, M_i and S_j form paired on-time pulses.

Case 4

In Case 4, an S loop on-time pulse can be matched to two M loop on-time pulses. This S loop on-time pulse forms an on-time pair with the M loop on-time pulse that immediately precedes it. The rules employed in this case include Rule 1, Rule 2, and Rule 6.

Case 4 is illustrated in Figure III-4. As can be seen in this figure, according to Rule 1 and Rule 2, S_j can be matched to two of M loop on-time pulses, M_{i-1} and M_i, because the elapsed time from either of these two on-time pulses to S_j is greater than the

minimum elapsed time threshold and smaller than the maximum on-time threshold. Then, according to Rule 6, S_j is matched to M_i because M_i immediately precedes S_j.

Case 5

In Case 5, an M loop on-time pulse can be matched to two S loop on-time pulses. This M loop on-time pulse forms an on-time pair with the S loop on-time pulse that immediately succeeds it. The rules employed in this case include Rule 1, Rule 2, and Rule 7.

Case 5 is illustrated in Figure III-5. As can be seen in this figure, according to Rule 1 and Rule 2, M_j can be matched to either of two S loop on-time pulses, S_j and S_{j+1}, because the elapsed time from M_j to either of the S loop on-time pulses falls in the valid range. Then, according to Rule 7, S_j is matched to M_i because S_j immediately succeeds M_i.
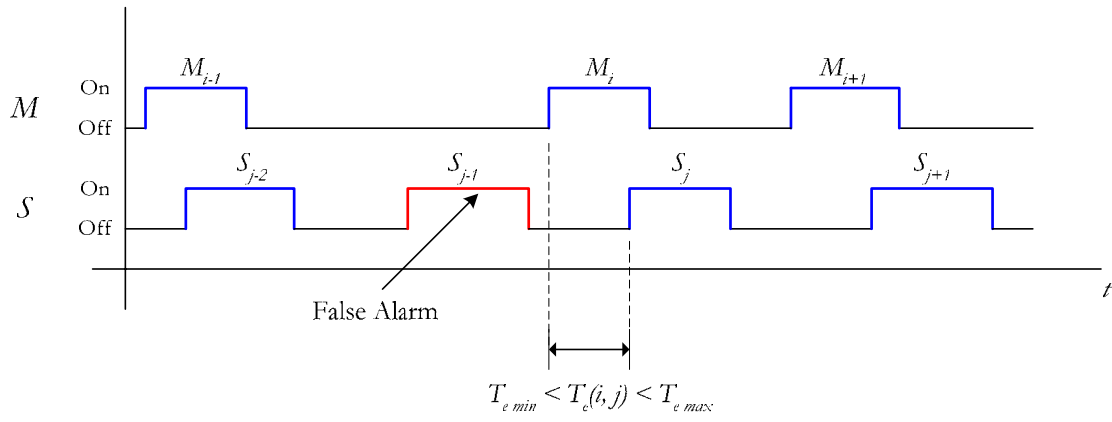
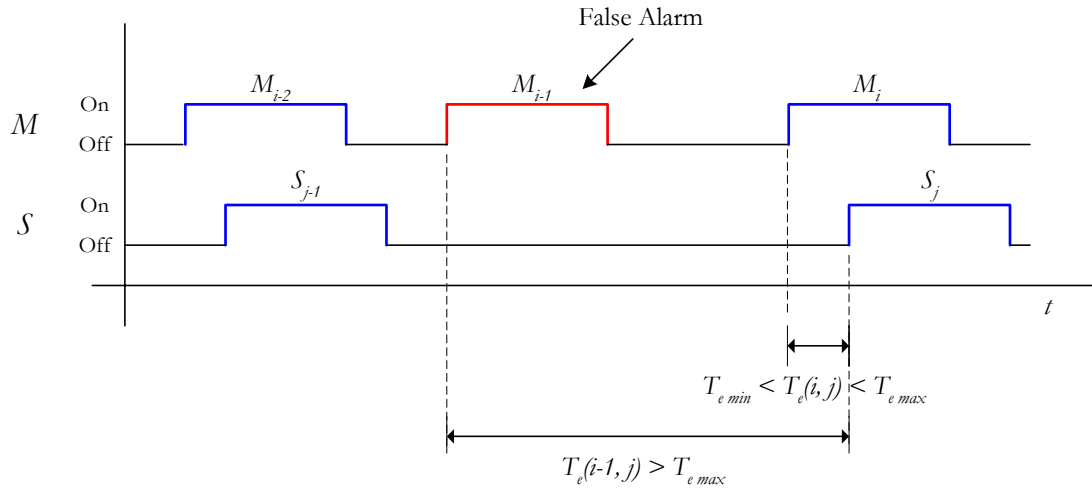Figure III-1. M Loop and S Loop On-Time Matching (Case 1)

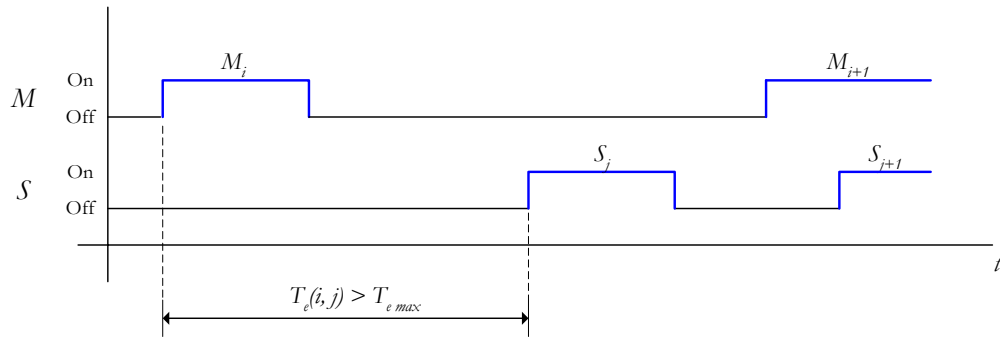Figure III-2. M Loop and S Loop On-Time Matching (Case 2)

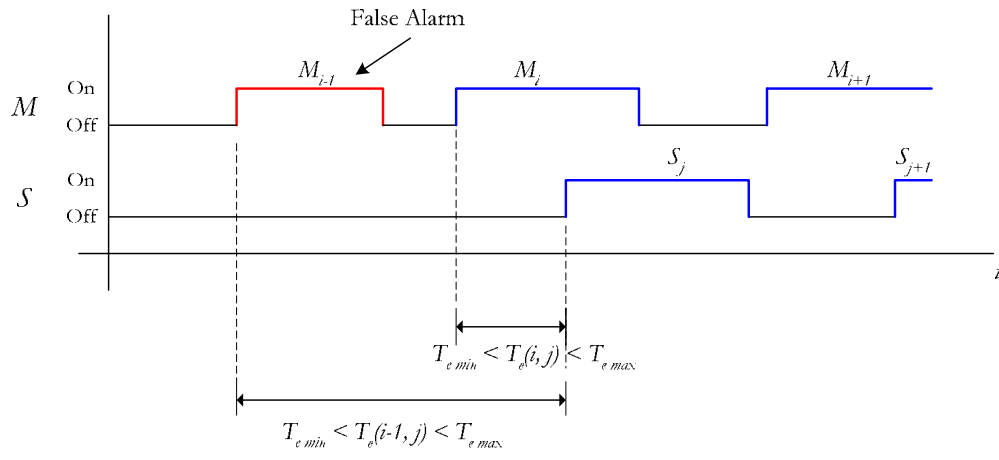Figure III-3. M Loop and S Loop On-Time Matching (Case 3)

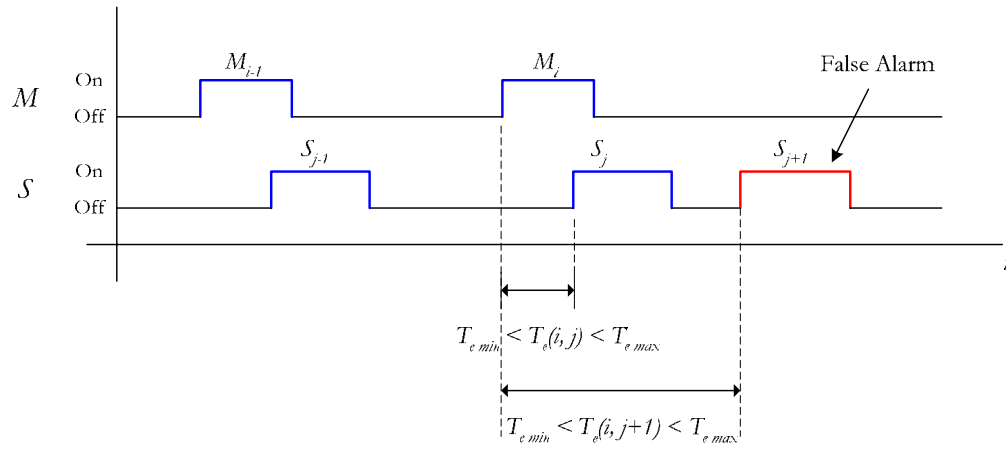Figure III-4. M Loop and S Loop On-Time Matching (Case 4)

Figure III-5. M Loop and S Loop On-Time Matching (Case 5)

APPENDIX IV DATA ERROR FREQUENCY DISTRIBUTION

Table IV-1. Data Error Frequency Distribution Based on One-hour Data

Flag Type	Flag Code	Northbound						Southbound					
		Lane 1		Lane 2		Lane HOV		Lane 1		Lane 2		Lane HOV	
		Count	Percentage	Count	Percentage	Count	Percentage	Count	Percentage	Count	Percentage	Count	Percentage
1	1	1	0.26%	1	0.21%	0	0.00%	1	0.34%	0	0.00%	0	0.00%
2	2	1	0.26%	2	0.42%	0	0.00%	2	0.69%	1	0.38%	1	0.34%
3	4	1	0.26%	0	0.00%	0	0.00%	0	0.00%	0	0.00%	0	0.00%
4	8	0	0.00%	0	0.00%	0	0.00%	0	0.00%	0	0.00%	0	0.00%
5	16	68	17.99%	53	11.18%	14	21.54%	48	16.49%	47	17.87%	90	31.03%
6	32	0	0.00%	0	0.00%	0	0.00%	0	0.00%	0	0.00%	0	0.00%
7	64	159	42.06%	210	44.30%	28	43.08%	117	40.21%	101	38.40%	97	33.45%
8	128	0	0.00%	0	0.00%	0	0.00%	0	0.00%	0	0.00%	0	0.00%
9	256	0	0.00%	0	0.00%	0	0.00%	0	0.00%	0	0.00%	0	0.00%
10	512	0	0.00%	0	0.00%	0	0.00%	0	0.00%	0	0.00%	0	0.00%
11	1024	0	0.00%	0	0.00%	0	0.00%	0	0.00%	0	0.00%	0	0.00%
12	2048	144	38.10%	206	43.46%	23	35.38%	112	38.49%	97	36.88%	96	33.10%
13	4096	0	0.00%	0	0.00%	0	0.00%	0	0.00%	0	0.00%	0	0.00%
14	8192	0	0.00%	0	0.00%	0	0.00%	0	0.00%	0	0.00%	0	0.00%
15	16384	0	0.00%	0	0.00%	0	0.00%	1	0.34%	3	1.14%	1	0.34%
16	32768	0	0.00%	0	0.00%	0	0.00%	0	0.00%	0	0.00%	0	0.00%
17	65536	4	1.06%	2	0.42%	0	0.00%	7	2.41%	7	2.66%	3	1.03%
18	131072	1	0.26%	0	0.00%	0	0.00%	3	1.03%	7	2.66%	2	0.69%
19	262144	0	0.00%	0	0.00%	0	0.00%	0	0.00%	0	0.00%	0	0.00%

Table IV-2. Data Error Frequency Distribution Based on 24-Hour Data

Flag Type	Flag Code	Northbound						Southbound					
		Lane 1		Lane 2		Lane HOV		Lane 1		Lane 2		Lane HOV	
		Count	Percentage	Count	Percentage	Count	Percentage	Count	Percentage	Count	Percentage	Count	Percentage
1	1	12	0.15%	10	0.12%	0	0.00%	4	0.06%	8	0.14%	4	0.05%
2	2	9	0.11%	16	0.20%	0	0.00%	15	0.23%	22	0.39%	7	0.08%
3	4	3	0.04%	13	0.16%	2	0.12%	3	0.05%	6	0.11%	6	0.07%
4	8	3	0.04%	11	0.14%	0	0.00%	75	1.14%	31	0.55%	22	0.25%
5	16	1251	15.25%	719	8.91%	224	13.42%	770	11.69%	643	11.39%	2104	24.01%
6	32	3	0.04%	13	0.16%	0	0.00%	74	1.12%	32	0.57%	17	0.19%
7	64	3607	43.98%	3734	46.25%	780	46.73%	2906	44.11%	2443	43.26%	3317	37.86%
8	128	0	0.00%	0	0.00%	0	0.00%	0	0.00%	0	0.00%	0	0.00%
9	256	1	0.01%	0	0.00%	0	0.00%	2	0.03%	0	0.00%	1	0.01%
10	512	0	0.00%	1	0.01%	0	0.00%	0	0.00%	1	0.02%	0	0.00%
11	1024	1	0.01%	1	0.01%	0	0.00%	1	0.02%	1	0.02%	1	0.01%
12	2048	3235	39.45%	3490	43.23%	655	39.25%	2625	39.85%	2302	40.77%	3205	36.58%
13	4096	0	0.00%	0	0.00%	0	0.00%	0	0.00%	0	0.00%	0	0.00%
14	8192	0	0.00%	0	0.00%	0	0.00%	0	0.00%	0	0.00%	0	0.00%
15	16384	6	0.07%	13	0.16%	8	0.48%	15	0.23%	30	0.53%	14	0.16%
16	32768	7	0.09%	1	0.01%	0	0.00%	10	0.15%	5	0.09%	1	0.01%
17	65536	31	0.38%	22	0.27%	0	0.00%	41	0.62%	47	0.83%	39	0.45%
18	131072	29	0.35%	29	0.36%	0	0.00%	44	0.67%	75	1.33%	24	0.27%
19	262144	3	0.04%	0	0.00%	0	0.00%	3	0.05%	1	0.02%	0	0.00%

Table IV-3. Data Error Frequency Distribution Based on 3-Day Data

Flag Type	Flag Code	Northbound						Southbound					
		Lane 1		Lane 2		Lane HOV		Lane 1		Lane 2		Lane HOV	
		Count	Percentage	Count	Percentage	Count	Percentage	Count	Percentage	Count	Percentage	Count	Percentage
1	1	48	0.20%	25	0.11%	1	0.02%	20	0.12%	30	0.21%	8	0.03%
2	2	39	0.16%	47	0.21%	20	0.41%	39	0.24%	60	0.41%	28	0.11%
3	4	13	0.05%	25	0.11%	13	0.27%	22	0.14%	19	0.13%	12	0.05%
4	8	3	0.01%	16	0.07%	0	0.00%	76	0.47%	31	0.21%	23	0.09%
5	16	4516	18.97%	2237	10.19%	739	15.10%	2199	13.51%	1946	13.34%	7464	28.14%
6	32	3	0.01%	16	0.07%	0	0.00%	74	0.45%	32	0.22%	17	0.06%
7	64	9846	41.37%	10092	45.99%	2260	46.19%	7019	43.12%	6135	42.05%	9536	35.95%
8	128	0	0.00%	0	0.00%	1	0.02%	0	0.00%	0	0.00%	0	0.00%
9	256	1	0.00%	3	0.01%	0	0.00%	3	0.02%	0	0.00%	2	0.01%
10	512	0	0.00%	1	0.00%	0	0.00%	0	0.00%	1	0.01%	0	0.00%
11	1024	1	0.00%	2	0.01%	0	0.00%	1	0.01%	1	0.01%	1	0.00%
12	2048	9071	38.11%	9238	42.09%	1785	36.48%	6526	40.09%	5875	40.27%	9226	34.78%
13	4096	0	0.00%	0	0.00%	0	0.00%	0	0.00%	0	0.00%	1	0.00%
14	8192	0	0.00%	0	0.00%	0	0.00%	0	0.00%	0	0.00%	0	0.00%
15	16384	44	0.18%	51	0.23%	34	0.69%	57	0.35%	99	0.68%	48	0.18%
16	32768	9	0.04%	2	0.01%	0	0.00%	15	0.09%	9	0.06%	2	0.01%
17	65536	85	0.36%	93	0.42%	23	0.47%	109	0.67%	126	0.86%	109	0.41%
18	131072	117	0.49%	98	0.45%	16	0.33%	115	0.71%	224	1.54%	50	0.19%
19	262144	4	0.02%	0	0.00%	1	0.02%	4	0.02%	1	0.01%	0	0.00%

APPENDIX V TYPES OF VEHICLES

Motorcycle	Volkswagen Beetle
Small Jeep	Passenger Car
Van/SUV	Small Pickup

Tractor	School Bus
Transit Bus	Dump Truck/Pup Trailer Combination
Car Hauler	

-